

**PRODUCTION AND CHARACTERIZATION OF siRNA  
LOADED MAGNETIC NANOPARTICLES TO BE USED IN  
CANCER TREATMENT**

**KANSER TEDAVİSİNDE KULLANILMAK ÜZERE  
siRNA YÜKLÜ MANYETİK NANOPARTİKÜLLERİN  
ÜRETİMİ VE KARAKTERİZASYONU**

**AMINA SELIMOVIC**

**PROF. DR. EMİR BAKI DENKBAŞ**

**Supervisor**

Submitted to Graduate School of Science and Engineering of Hacettepe University  
as a Partial Fulfilment to the Requirements  
for the Award of the Degree of Master of Science  
in Bioengineering

2017

This work named “**Production and Characterization of siRNA loaded magnetic nanoparticles to be used in cancer treatment**” by AMINA SELIMOVIC has been approved as a thesis for the Degree of **MASTER OF SCIENCE IN BIOENGINEERING** by the below mentioned Examining Committee Members.

Prof. Dr. Saadettin Kılıçkap  
Head



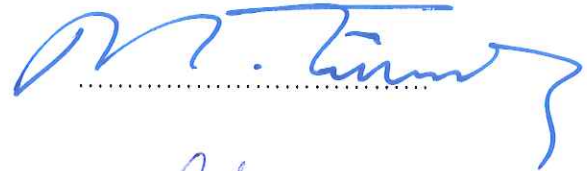
Prof. Dr. Emir Baki Denkbaş  
Supervisor



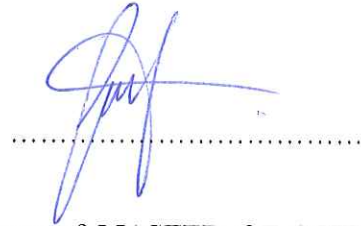
Doç. Dr. Lokman Uzun  
Member



Doç. Dr. Mustafa Türk  
Member



Doç. Dr. Fatih Büyükserin  
Member



This thesis has been approved as a thesis for the Degree of **MASTER OF SCIENCE IN BIOENGINEERING** by Board of the Institute for Graduate School of Science and Engineering.

Prof. Dr. Menemşe GÜMÜŞDERELİOĞLU  
Director of the Institute of  
Graduate School of Science and Engineering

## YAYINLAMA VE FİKRİ MÜLKİYET HAKLARI BEYANI

Enstitü tarafından onaylanan lisansüstü tezimin/raporumun tamamını veya herhangi bir kısmını, basılı (kağıt) ve elektronik formatta arşivleme ve aşağıda verilen koşullarla kullanıma açma iznini Hacettepe üniversitesine verdiğimi bildiririm. Bu izinle Üniversiteye verilen kullanım hakları dışındaki tüm fikri mülkiyet haklarım bende kalacak, tezimin tamamının ya da bir bölümünün gelecekteki çalışmalarda (makale, kitap, lisans ve patent vb.) kullanım hakları bana ait olacaktır.

Tezin kendi orijinal çalışmam olduğunu, başkalarının haklarını ihlal etmediğimi ve tezimin tek yetkili sahibi olduğumu beyan ve taahhüt ederim. Tezimde yer alan telif hakkı bulunan ve sahiplerinden yazılı izin alınarak kullanması zorunlu metinlerin yazılı izin alarak kullandığımı ve istenildiğinde suretlerini Üniversiteye teslim etmeyi taahhüt ederim.

- Tezimin/Raporumun tamamı dünya çapında erişime açılabilir ve bir kısmı veya tamamının fotokopisi alınabilir.**  
(Bu seçenekle teziniz arama motorlarında indekslenebilecek, daha sonra tezinizin erişim statüsünün değiştirilmesini talep etmeniz ve kütüphane bu talebinizi yerine getirirse bile, tezinin arama motorlarının önbelleklerinde kalmaya devam edebilecektir.)
- Tezimin/Raporumun 13.07.2020. tarihine kadar erişime açılmasını ve fotokopi alınmasını (İç Kapak, Özet, İçindekiler ve Kaynakça hariç) istemiyorum.**  
(Bu sürenin sonunda uzatma için başvuruda bulunmadığım takdirde, tezimin/raporumun tamamı her yerden erişime açılabilir, kaynak gösterilmek şartıyla bir kısmı ve ya tamamının fotokopisi alınabilir)
- Tezimin/Raporumun ..... tarihine kadar erişime açılmasını istemiyorum, ancak kaynak gösterilmek şartıyla bir kısmı veya tamamının fotokopisinin alınmasını onaylıyorum.**
- Serbest Seçenek/Yazarın Seçimi**

13 / 07 / 2017

  
Öğrencinin Adı Soyadı

## ETHICS

In this thesis study, prepared in accordance with the spelling rules of Institute of Graduate Studies in Science of Hacettepe University,

I declare that

- all the information and documents have been obtained in the base of the academic rules
- all audio-visual and written information and results have been presented according to the rules of scientific ethics
- in case of using other Works, related studies have been cited in accordance with the scientific standards
- all cited studies have been fully referenced
- I did not do any distortion in the data set
- and any part of this thesis has not been presented as another thesis study at this or any other university.

22\6\2017

*Amina Selimovic*  
AMINA SELIMOVIC

## **ABSTRACT**

# **PRODUCTION AND CHARACTERIZATION OF siRNA LOADED MAGNETIC NANOPARTICLES TO BE USED IN CANCER TREATMENT**

**AMINA SELIMOVIC**

**Master of Science, Bioengineering**

**Supervisor: Prof. Dr. Emir Baki DENKBAŞ**

**June 2017, 73 pages**

Cancer is one of the leading causes of death in economically developed and developing countries and factors such as smoking, physical inactivity and nutritional habits are increasing the possibility of its development. After decades of extensive research of cancer, today it can be described as a genetic disease of the somatic cell. Genetic changes such as rearrangements of chromosomes (deletion, translocation, insertion), point mutation, gene amplification are affecting kinase inhibitors, growth factors, receptors, a cascade of transcription factors and signal transduction members are leading to an impaired balance of cell proliferation and changes in the function of genes that induce apoptosis. These actions are leading to the abnormal growth of the cells called neoplasia. An approach based on nanotechnology provides a great promise in developing strategies for cancer treatment by

helping to improve the safety and efficacy of therapeutic delivery vehicles. Powerful investigational tools with great potential in therapeutics-RNA interference (RNAi) is known as a highly efficient regulatory process in which short double-stranded RNAs are giving rise to sequence-specific posttranscriptional gene silencing. With time it has been proven that specific protein expression can be inhibited. Small interfering RNA (siRNA) as part of RNA interference process has been extensively studied to treat various genetic diseases, cardiovascular diseases and various cancers. However, due to its polyanionic nature siRNAs cannot cross the cellular membrane that is why it needs a carrier to prevent enzymatic degradation and to take siRNA to the specific target inside the cell. Properties such as safety, effectiveness, ease of manufacturing and production are quite important to consider when selecting a proper carrier for siRNA. In this work iron oxide nanoparticles are coated with natural biopolymer gelatin, loaded with mTOR siRNA targeting specific oncogene with the aim to deliver gene silencing complex to colon cancer cells inducing therapeutic effect. For this iron oxide and gelatin coated iron oxide nanoparticles were synthesized, optimized and characterized. Morphological characterization was done using SEM (Scanning Electron Microscopy). Size and surface charge of produced nanoparticles was revealed by Zeta-Sizer (3000 HSA, Malvern, England). To determine the chemical structures of the nanoparticles, molecular bond characterization had been performed using Fourier Transform Infrared Spectroscopy (FTIR) (Nicolet iS10, USA). VSM (vibrating sample magnetometer) and ESR (electro spin resonance) are used to analyse magnetic properties of the prepared particles. siRNA was loaded to gelatin coated iron oxide nanoparticles and its binding efficiency (%) was examined. siRNA loaded nanoparticles were transfected to colon cancer cell line CaCo-2 and mouse fibroblast cell line L929. Cell cytotoxicity test, MTT was performed using different concentrations of siRNA and under different incubation time MTT assay showed that toxic effect in both cell lines was significantly higher when siRNA loaded gelatin coated IONs were used. Also, according to the results obtained, synthesized gelatin coated IONs showed similar anticancer activity as HiperFect which is commercial siRNA carrier. This work showed that gelatin coated iron oxide nanoparticles as cheap and easily synthesized carrier are promising tool for siRNAs delivery.

**Keywords:** nanooncology, iron oxide nanoparticles, gelatin, siRNA

## **ÖZET**

# **KANSER TEDAVİSİNDE KULLANILMAK ÜZERE siRNA YÜKLÜ MANYETİK NANOPARTİKÜLLERİN ÜRETİMİ VE KARAKTERİZASYONU**

**AMİNA SELİMOVİC**

**Yüksek Lisans, Biyomühendislik**

**Tez Danışmanı: Prof. Dr. Emir Baki Denkbaş**

**Haziran 2017, 73 sayfa**

Kanser, gelişmiş ve gelişmekte olan ülkelerde önde gelen ölüm nedenlerinden biridir ve sigara içme, fiziksel hareketsizlik ve beslenme alışkanlıkları gibi faktörler kanserin gelişme olasılığını arttırmaktadır. Kromozomların yeniden düzenlenmesi nokta mutasyonu ve gen amplifikasyonu, kinaz inhibitörleri, büyüme faktörleri, reseptörler, transkripsiyon faktörleri kaskadını ve sinyal iletim elemanlarını etkileyerek hücre proliferasyonunun bozulmasına ve işlev değişikliğine neden olur. Bu eylemler, neoplazi adı verilen hücrelerin anormal büyümesine neden olur. Kanser tedavisinde nanoteknolojiye dayalı yaklaşım, terapötik araçların güvenliğini ve etkinliğini artırarak yeni nesil stratejiler geliştirmede büyük bir avantaj sağlamaktadır. Önemli ölçüde terapötik potansiyele sahip olan RNA interferans

(RNAi) mekanizması, küçük çift sarmallı RNA'ların sekansa spesifik post-transkripsiyonel gen susturulmasına yol açan yüksek etkili regülatör olarak bilinir. Bu mekanizma ile spesifik genlerin ekspresyonlarının inhibe edilebileceği kanıtlanmıştır. RNAi yolağının bir parçası olan küçük interfere edici RNA (siRNA) çeşitli genetik hastalıkların yanı sıra kardiyovasküler hastalıklar ve çeşitli kanserleri tedavi etmek için kapsamlı bir şekilde incelenmiştir. Ancak, siRNA'lar hücrelere verildiğinde polianyonik yapısı nedeniyle hücre zarını etkin bir şekilde geçemez. Bu nedenle siRNA'nın hücre içindeki spesifik hedefe ulaşabilmesi ve enzimatik parçalanmadan korunması için taşıyıcı sistemlere ihtiyaç duyulmaktadır. siRNA için uygun taşıyıcıyı seçmek için biyoyumluluk, terapötik etkinlik, üretim kolaylığı gibi özellikler oldukça önemlidir. Bu çalışmada, demir oksit nanoparçacıkların doğal biyopolimer jelatin ile kaplanması, hücresel proliferasyon yolağında etkin olan mTOR geninin inhibisyonunu sağlayan siRNA'ların bu yapılar ile etkileştirilmesi ve kolon kanseri hücrelerinde terapötik etkinliğin sağlanması hedeflenmektedir. Bu amaçla, demir oksit nanoparçacıkları ve jelatin kaplı demir oksit nanoparçacıkları sentezlenmiş, optimizasyon parametreleri ve karakterizasyonları değerlendirilmiştir. Parçacıkların morfolojik incelemesi SEM (Scanning Electron Microscopy) analiziyle ortaya konmuştur. Üretilen nanoparçacıkların boy-boy dağılımları ve yüzey yükleri Zeta-Sizer kullanılarak elde edilmiştir. Nanoparçacıkların kimyasal yapılarını belirlemek için moleküler bağ karakterizasyonu Fourier Transform Infrared Spectroscopy (FTIR) ölçümleri alınmıştır. Hazırlanan parçacıkların manyetik özellikleri VSM (vibrating sample magnetometer) ve ESR (electro spin resonance) teknikleriyle değerlendirilmiştir. Jelatin kaplı demir oksit nanopartikülüne hedef siRNA'lar yüklenmiş ve (%) bağlanma verimleri elde edilmiştir. siRNA yüklü nanoparçacıkların model kolon kanseri hücre hattı, Caco-2 ve fare fibroblast hücre hattı, L929 hücreleri ile etkileşimleri yapılmıştır. Farklı konsantrasyonlarda yüklenen siRNA'ların ve hücrelerle inkübasyon sürelerinin etkisi incelenerek, hücrelerde sitotoksite çalışmaları MTT analiziyle ortaya konmuştur. MTT testi ile, siRNA-jelatin-demir oksit nanopartiküllerinin her iki hücre hattı üzerinde herhangi bir taşıyıcı kullanılmadan verilen siRNA'lara göre toksik etkisinin önemli derecede fazla olduğu gösterilmiştir. Ayrıca elde edilen sonuçlara göre seztezenen nanopartiküller ticari siRNA taşıyıcısı olarak kullanılan HiperFect ile benzer antikanser etkinlik göstermiştir. Sunulan çalışma ile kolay sentezlenen, ucuz ve biyoyumlu jelatin kaplı demir oksit nanopartiküllerin siRNA taşıyıcısı olarak umut vaad eden sistemler olduğu gösterilmiştir.



**Anahtar Kelimeler:** nanoonkoloji, demir oksit nanoparçacıkları, jelatin, siRNA

## ACKNOWLEDGEMENTS

In the name of Allah, the most gracious and the most merciful. 'But over all those endowed with knowledge is the All-knowing (Allah).' [Qur'an, 12:76] First and for the most, I thank Allah, s.w.t, who always listens and never leaves his worshipers alone.

I would like to thank my supervisor, Prof. Dr. Emir Baki Denkbař for his never-ending support, enthusiasm, immense knowledge and suggestions throughout research development and documentation of this work. I want to express my profound acknowledgment to the driving force behind this work research assistant Ms. Göknur Kara for being available at any time to answer any of my questions, for assistance in the lab while running experiments, for research design, for analysis of experimental results, but above all for unselfish support when the research had hit a wall.

A very special gratitude goes to my friend řükran, her grandmother Hafize, mother Rabiya and whole family Alpdemir for giving me support along the way.

I thank my parents father Jasmin and mother Hatidja, brother Zeid, sister Azra and sister-in-law Hatidja for trusting in me completely, being my indispensable support and whom I aimed to make proud.

I thank fellow labmates in Biopolymeric Systems Research Group (BSRG) who were a joyful part of this long sweet-sour journey; Soheil Malekghasemi, Ebru Erdal, Zeynep Karahaliliođlu, Eda Yalçın, Ebru Kılıçay, Gizem Daban, Serhat Öztürk, Öznur Akbal, Tayfun Vural, Betül Bozdođan Pala, Ekin Çelik and Ali Örs.

Last but not least, I thank Government of Republic of Turkey and Hacettepe University for giving me the opportunity to board their ship and sail the seas of knowledge.

# CONTENT

	<u>Page</u>
ETHICS.....	iii
ABSTRACT.....	iv
ACKNOWLEDGEMENTS.....	viii
CONTENT.....	ix
LIST OF FIGURES.....	xii
LIST OF TABLES.....	xiv
LIST OF ABBREVIATIONS.....	xv
1. INTRODUCTION.....	1
2. GENERAL INFORMATION.....	3
2.1. Gene therapy.....	3
2.2. Gene silencing strategies.....	4
2.2.1. miRNA mechanism.....	5
2.2.2. siRNA mechanism and RNAi.....	5
2.2.2.1. Function of Dicer in silencing.....	7
2.2.3. Design of siRNA.....	8
2.2.4. siRNA and cell interaction.....	8
2.3. Cancer development.....	8
2.3.1. Colon cancer progression.....	12
2.3.1.1. Conventional approach in colon cancer therapy.....	13
2.3.1.2. New generation treatment strategies for colon cancer.....	14
2.4. Nano oncological approaches for cancer treatment.....	16
2.4.1. Liposomes.....	16
2.4.2. Micelles.....	16
2.4.3. Polymeric nanoparticles.....	16
2.4.4. Metal-based nanoparticles.....	17
2.4.2. Iron oxide nanoparticles (IONs).....	18
2.5. Polymers used in delivery vehicle coating.....	18
2.5.1 Gelatin as coating polymer.....	19
2.6. mTOR oncogene.....	22

2.6.1. Expression of mTOR in human cancer.....	23
3. EXPERIMENTAL STUDY.....	24
3.1. Chemicals.....	24
3.2. Synthesis of iron oxide nanoparticles (IONs).....	25
3.3. Coating iron oxide nanoparticles with gelatin.....	26
3.4. Characterization of iron oxide nanoparticles.....	27
3.4.1. Determination of morphology.....	27
3.4.2. Size analysis of nanoparticles.....	28
3.4.3. Charge analysis of nanoparticles .....	28
3.4.4. Determination of chemical structure.....	28
3.4.5. Determination of magnetic properties.....	29
3.5. Loading siRNA to gelatin coated iron oxide nanoparticles.....	29
3.5.1. Binding efficiency of siRNA to gelatin coated iron oxide nanoparticles.....	30
3.6. Preparation of CaCo-2 cell lines.....	31
3.7. Interaction of siRNA loaded nanoparticles with CaCo-2 cancer cells.....	32
3.7.1. Determination of CaCo-2 cells cytotoxicity .....	33
4. EXPERIMENTAL RESULTS AND DISCUSSION.....	33
4.1. Characterization of nanoparticles.....	33
4.1.1. Morphological characterization of nanoparticles.....	34
4.1.2. Size and PDI analysis of iron oxide nanoparticles.....	36
4.1.2.1. Effect of NaOH concentration on size and PDI of iron oxide nanoparticle.....	36
4.1.2.2. Effect of HCl concentration on size and PDI of iron oxide nanoparticles.....	37
4.1.2.3. Effect of atmospheric and N <sub>2</sub> environment on size and PDI of IONs.....	38
4.1.2.4. Effect of distilled water and ethanol on size and PDI of IONs.....	39
4.1.3. Size and PDI analysis of gelatin coated iron oxide nanoparticles (GIONs).....	40
4.1.3.1. Effect of certain amount of iron oxide nanoparticles on size and PDI of gelatin coated iron oxide nanoparticles.....	41
4.1.3.2. Effect of glutaraldehyde concentration on size and PDI of GIONs.....	42
4.1.3.3. Effect of gelatin concentration on size and PDI of GIONs.....	43
4.1.4. Short term stability test for nanoparticles.....	44
4.1.4.1. Short term stability test for iron oxide nanoparticles.....	44
4.1.4.2. Short term stability test for gelatin coated iron oxide nanoparticles.....	46
4.1.5. Chemical structure determination of nanoparticles.....	47
4.1.5.1 FTIR of iron oxide nanoparticles.....	47

4.1.5.2. FTIR of gelatin nanoparticles.....	48
4.1.5.3. FTIR of gelatin coated iron oxide nanoparticles.....	49
4.1.6. Determination of magnetic properties.....	49
4.1.6.1. Results of VSM.....	49
4.1.6.2. Results of ESR.....	51
4.2. Results of binding efficiency of siRNA to gelatin coated iron oxide nanoparticle.....	53
4.3. Determination of CaCo-2 cells cytotoxicity.....	55
5.CONCLUSION.....	59
6, REFERENCES.....	61
CV.....	73

## LIST OF FIGURES

	<u>Page</u>
<b>Figure 2.1.</b> Direct and cell-based delivery in gene therapy.....	3
<b>Figure 2.2.</b> Gene control mechanisms.....	4
<b>Figure 2.3.</b> siRNA-mediated gene silencing process.....	6
<b>Figure 2.4.</b> Schematic representation of Dicer's function.....	7
<b>Figure 2.5.</b> Schematic representation of cell cycle.....	10
<b>Figure 2.6.</b> Influence of environmental factors together with genetic and epigenetic changes on tumour formation.....	11
<b>Figure 2.7.</b> Influence of nanomaterials and physiological compartments in cancer treatment.....	15
<b>Figure 2.8.</b> Available nanoplatforms in clinical trials for cancer treatment.....	17
<b>Figure 2.9.</b> Chemical composition of gelatin.....	19
<b>Figure 2.10.</b> Hydrogen bonding in gelatin chains and bonding between gelatin chains and water molecules.....	21
<b>Figure 2.11.</b> Upstream signalling instructions and regulation points of mTOR pathway...	23
<b>Figure 2.12.</b> Role of mTOR oncogene in digestive tract malignancies.....	24
<b>Figure 3.1.</b> Schematic representation of iron oxide nanoparticles synthesis process.....	26
<b>Figure 3.2.</b> Schematic representation of coating iron oxide nanoparticles with gelatin.....	27
<b>Figure 3.3.</b> Image of CaCo-2 cells of low and high density.....	32
<b>Figure 4.1.</b> Morphological characterization of iron oxide nanoparticles.....	34
<b>Figure 4.2.</b> Morphological characterization of gelatin nanoparticles.....	35
<b>Figure 4.3.</b> Morphological characterization of gelatin coated iron oxide nanoparticles.....	35
<b>Figure 4.4.</b> Concentration of NaOH and its effect on hydrodynamic size of iron oxide nanoparticles.....	36
<b>Figure 4.5.</b> Concentration of HCl and its effect on hydrodynamic size of iron oxide nanoparticles.....	37
<b>Figure 4.6.</b> Effect of air and N <sub>2</sub> atmosphere on hydrodynamic size of iron oxide nanoparticles.....	38
<b>Figure 4.7.</b> Effect of ethanol and distilled water on hydrodynamic size of iron oxide nanoparticles.....	39

<b>Figure 4.8.</b> Amount of iron oxide nanoparticles and its effect on hydrodynamic size of gelatin coated iron oxide nanoparticles.....	41
<b>Figure 4.9.</b> Glutaraldehyde concentration and its effect on hydrodynamic size of gelatin coated iron oxide nanoparticles.....	42
<b>Figure 4.10.</b> Gelatin concentrations and its effect on hydrodynamic size of gelatin coated iron oxide nanoparticles.....	43
<b>Figure 4.11.</b> Hydrodynamic size of iron oxide nanoparticles in span of 30 days.....	45
<b>Figure 4.12.</b> Charge results of gelatin coated iron oxide nanoparticles in span of 30 days..	45
<b>Figure 4.13.</b> Size of gelatin coated iron oxide nanoparticles examined for 30 days.....	46
<b>Figure 4.14.</b> Charge results of gelatin coated iron oxide nanoparticles in span of 20 days..	47
<b>Figure 4.15.</b> FTIR spectra of iron oxide nanoparticles and gelatin nanoparticles.....	48
<b>Figure 4.16.</b> FTIR spectra of gelatin coated iron oxide nanoparticles.....	49
<b>Figure 4.17.</b> VSM results of iron oxide nanoparticles.....	50
<b>Figure 4.18.</b> VSM results of gelatin coated iron oxide nanoparticles.....	51
<b>Figure 4.19.</b> ESR results of iron oxide nanoparticles.....	52
<b>Figure 4.20.</b> ESR results of gelatin coated iron oxide nanoparticles.....	53
<b>Figure 4.21.</b> Calibration curve of RNA standard.....	54
<b>Figure 4.22.</b> The binding efficiency of siRNA to gelatin coated IONs.....	54
<b>Figure 4.23.</b> Results of MTT test for L929 cell lines after 24h incubation.....	55
<b>Figure 4.24.</b> Results of MTT test for CaCo-2 cell lines after 24h incubation.....	56
<b>Figure 4.25.</b> Results of MTT test for L929 cell lines after 48h incubation.....	56
<b>Figure 4.26.</b> Results of MTT test for CaCo-2 cell lines after 48h incubation.....	57
<b>Figure 4.27.</b> The interaction of siRNA loaded iron oxide nanoparticles with L929 and CaCo-2 cell lines for 24h.....	57
<b>Figure 4.28.</b> The interaction of siRNA loaded iron oxide nanoparticles with L929 and CaCo-2 cell lines for 48h.....	58

## LIST OF TABLES

	<u>Page</u>
<b>Table 3.1.</b> Environment of CaCo-2 cell lines.....	31
<b>Table 4.1.</b> Concentration of NaOH and its effect on PDI of iron oxide nanoparticles.....	37
<b>Table 4.2.</b> Concentration of HCl and its effect on PDI of iron oxide nanoparticles.....	38
<b>Table 4.3.</b> Effect of air and N <sub>2</sub> atmosphere on PDI of iron oxide nanoparticles.....	39
<b>Table 4.4.</b> Effect of ethanol and distilled water on PDI of iron oxide nanoparticles.....	40
<b>Table 4.5.</b> Effect of different amounts of IONs on PDI of gelatin coated iron oxide nanoparticles.....	41
<b>Table 4.6.</b> Effect of different GA concentration on PDI of gelatin coated iron oxide nanoparticles.....	43
<b>Table 4.7.</b> Effect of different gelatin concentrations on PDI of gelatin coated iron oxide nanoparticles.....	44
<b>Table 4.8.</b> FTIR spectra peaks for gelatin.....	48
<b>Table 4.9.</b> ESR spectrometer operating conditions.....	51
<b>Table 4.10.</b> ESR spectral parameters.....	52
<b>Table 4.11.</b> RNA standard slope preparation.....	53



## LIST OF ABBREVIATIONS

IONs	Iron oxide nanoparticles
GIONs	Gelatin coated iron oxide nanoparticles
RNA	Ribonucleic acid
mRNA	Messenger RNA
dsRNA	Double-stranded RNA
RNAi	RNA interference
siRNA	Short interference RNA
miRNA	Micro RNA
RISC	RNA-induced silencing complex
Ago-2	Argonaute-2
PTGS	Post-transcriptional gene silencing
mTOR	The mechanistic target of rapamycin
CRC	Colorectal cancer
EPR	Enhanced permeability and retention
RES	Reticuloendothelial system
CIMP	CpG island methylator phenotype
MSI	Microsatellite instability
VSM	Vibrating sample magnetometer
ESR	Electron spin resonance
FTIR	Fourier transform infrared spectroscopy
PDI	Polydispersion index

## 1. INTRODUCTION

Cancer is one of the leading causes of death in economically developed and developing countries. After decades of extensive research today it can be described as a genetic disease of the somatic cell where changes in the sequence of the genome occur. Genetic changes such as rearrangements of chromosomes (deletion, translocation, insertion), point mutation, gene amplifications are affecting kinase inhibitors, growth factors and their receptors, cascade of transcription factors and signal transduction complex members. Today, gene therapy has emerged as one of the promising ways to treat cancer cells. Gene therapy is referring to gene replacement where the right copy (DNA or RNA fragments) of the mutated gene is delivered to the cell without causing toxicity to neighbouring cells and tissues. Gene therapy is providing the possibility to silence the gene that potentially causes hereditary disease. Gene replacement in gene therapy is considered successful if the right delivery vehicle is used to cause gene expression in the target cell. Today, instead of traditional approaches to cancer treatment, great interest is dedicated to targeted therapies because it does not harm healthy cells and have high selectivity. Nanoparticles are having the ability to deliver drugs, vaccines, siRNAs and proteins to different body organs such as lungs, brain, lymphatic system, spleen and lymphatic system for targeting. In this context, a promising approach is RNA interference system where siRNA therapy operates on mRNA level preventing genes from being translated into protein. RNA interference mechanism is a revolutionary process of post transcriptional gene silencing led by double-stranded RNA (dsRNA) who is homologous in the sequence to a target protein inducing sequence-specific degradation of mRNA of interest. Double-stranded RNAs known as siRNA found in the cytoplasm are capable of silencing own complementary mRNA. Dicer is cleaving long dsRNAs into short interfering RNA (siRNA) that is usually RNA double stranded sequence of 21-24 nt in length. Subsequently, obtained siRNAs will be loaded onto activated form of RISC (RNA-induced silencing complex) where protein Ago-2 will cleave dsRNA sequence and release it as ssRNA. Released ssRNA represents guide sequence right toward mRNA of the target with whom it has a high degree of sequence complementarity. All molecular players of RISC complex are yet unknown, however, the susceptibility of siRNA to rapid degradation and its short half-life is an important barrier that restricts therapeutic use.

The efficiency of siRNA delivery in great extent depends on its delivery vehicle and surface modification which gives protection to siRNA complex ones found in the biological environment during circulation.

Basically, in order to avoid systematic elimination of siRNA, chemical modification and selection of nano-sized carrier is crucial. In order to avoid „off-target-effect" and innate immune response there exist several properties in design and synthesis of nanoparticles such as size, shape, surface charge, density, composition, and surface chemistry that gives rise to the amount of efficiency in performing a function. The development and application of nano-oncology have raised as a promising tool for early termination of cancer because coated nanostructures have great potential to carry and deliver oncogene silencing complex to the cells without disturbing its integrity and with no causing damage to healthy tissues. Work of Jiang et al, states that iron metabolism which occurs in the human body through multiple pathways and dextran-coated iron oxide nanoparticles have been clinically tested and approved by the FDA which made it potential drug in cancer treatment but the problem was seen with nanoparticle toxicity and off-target siRNA effects [1, 2]. That is why in order to decrease toxicity biodegradable polymers were used to coat nano carriers to increase results efficiency. In line with a prior study done by of Chen et al, where it is stated that magnetic nanoparticles (IONs) covered with a layer of biodegradable polymer are noted to be effective magnetic drug carrier [3] this study is based on delivering siRNA mTOR to CaCo-2 cell culture by using magnetic nanoparticles covered with a layer of biodegradable polymer gelatin. Gelatin, biological macromolecule except being cheap it is also biodegradable, biocompatible and vastly used in pharmaceutical and nanotechnological approach as drug delivery or vaccine release system. When comparing with other delivery systems, gelatin nanoparticles are a solid delivery system for drug molecules or siRNA they encapsulate. The whole study is composed of three parts where firstly iron nanoparticle synthesis and characterization by the co-precipitation method using iron salts in alkaline medium is done, then same nanoparticles were coated with gelatin. After coating with gelatin, iron oxide nanoparticles were loaded with mTOR siRNA so that interaction and gene silencing performance of produced nano platform could be tested when transfected to CaCO-2 colon cancer cell culture.

## 2.GENERAL INFORMATION

### 2.1. Gene therapy

Twenty years after revealing DNA structure in 1953 by Watson and Crick, DNA restriction enzymes popped out as a new tool in DNA recombinational technology. Recombinant DNA technology provides different ways of DNA usage by DNA recombinant expression in bacteria, expressing recombinant DNAs in transgenic animals or just using DNA recombinant as therapy for replacing or silencing genes causing a specific disease. Right after recombinant technology popped out gene therapy strategies started to be a theme of interest in scientific circles. Gene therapy is referring to gene replacement where the right copy (DNA or RNA fragments) of the mutated gene is delivered to the cell without causing toxicity to neighbouring cells and tissues. Also, gene therapy is providing silencing of the gene that potentially can cause hereditary disease. Gene replacement in gene therapy is considered successful if the right delivery vehicle is used to cause gene expression in the target cell. Delivery to the cell can be made throughout either viral or non-viral method. So far, viral vectors that showed promising results are lentiviral, retroviral, and adeno-associated viral vectors which have the ability to fuse into the human genome. Also, transfection can be done by microinjection, electroporation, ballistic DNA injection or a gene gun, sonoporation or ultrasound, photoporation, magnetofection, jet injection and using many other methods [4, 5].

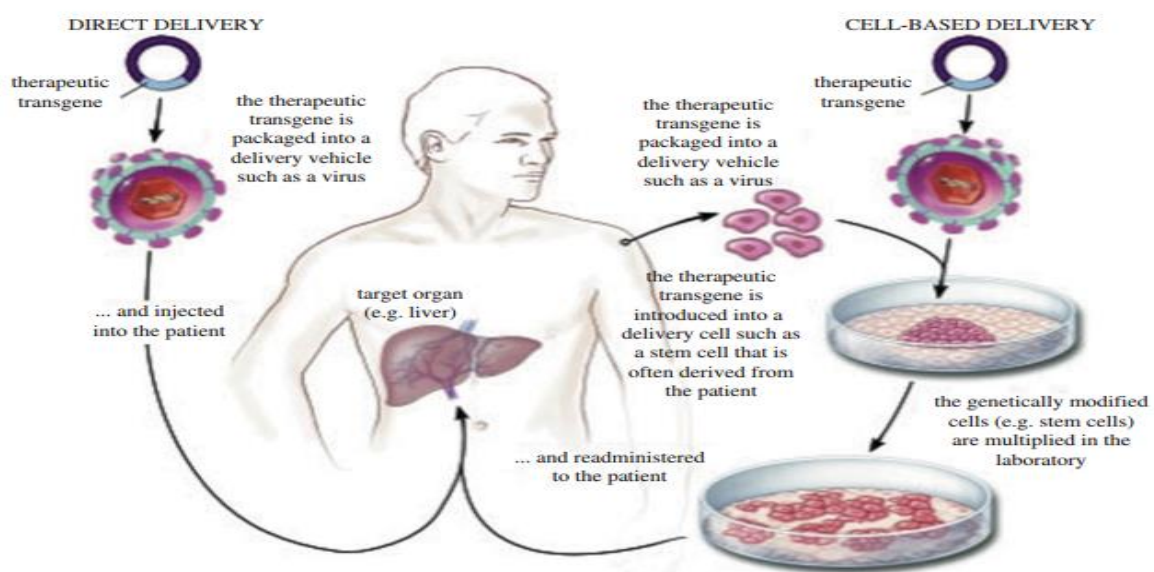


**Figure 2.1.** Direct and cell-based delivery in gene therapy [4].

In so-called cell-based delivery or more known as ex-vivo delivery, cells of interest taken from a patient are genetically modified in the laboratory and packaged with a viral or non-viral delivery vector to be re-transfected to patients. In vivo therapy is relying on delivering vector loaded with genetic material to direct gene modification and permanent silencing of gene expression after entering the cell. In direct delivery or so-called in situ gene therapy, the genetic material after packaging in the delivery vehicle is directly transfected to the target tissue. This method is used in respiratory tract disease treatment using lipids and adenoviruses where the low efficiency of transfection is noted [5]. Gene therapy is reported to have success in treatment primary stages of the disease. To increase the success of therapy proper gene delivery agent has to be chosen to decrease toxicity and increase the cure rate.

## 2.2. Gene silencing strategies

It is reported that small RNAs, miRNAs, siRNAs are involved in sequence-specific inhibition of specific gene. Gene expression is controlled throughout translational repression, chromatin modification and mRNA degradation.

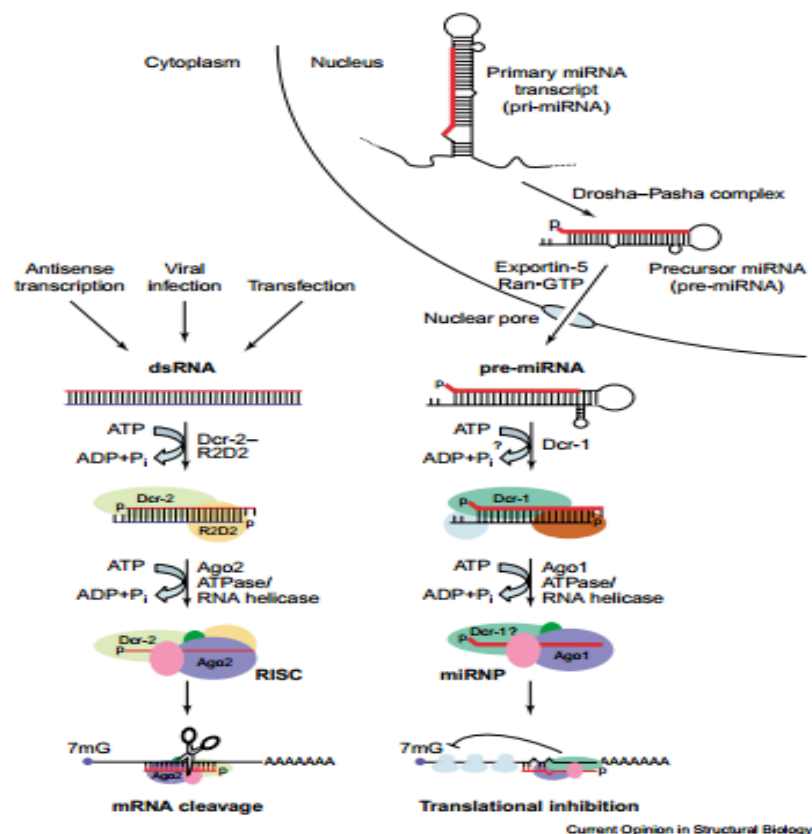


Figure 2.2. Gene control mechanisms [6].

There are two ways how gene control mechanism is taking place; throughout miRNA found in the nucleus or by siRNA found in the cell cytoplasm. miRNA leads to translational inhibition where on the other side siRNA leads to mRNA cleavage after dsRNAs are formed in the cytoplasm or complementary strand is synthetically injected by a viral agent or transfected using different delivery systems [6].

### **2.2.1. miRNA Mechanism**

In the cell nucleus, transcripts of miRNA genes, mostly known as introns are folding into hairpin shape making miRNAs. These miRNAs before leaving nucleus are reaching maturation stage by the help of RNase III family enzymes; Drosha and Dicer making so-called Drosha-Pasha complex. After being processed with Dicer, siRNAs and miRNAs are associated with Argonaut proteins. Like siRNAs, miRNAs are incorporated into RNA-induced silencing complex (RISC) that eventually leads to sequence-specific inhibition of gene expression. With help of exportin-5 pre-miRNA are transported to the cytoplasm. If siRNA is associated complex is known as RISC, but if miRNA is associated miRNPs complex is formed [6].

### **2.2.2. siRNA Mechanism and RNAi**

RNA interference mechanism is a revolutionary process of post transcriptional gene silencing. This mechanism is led by double-stranded RNAs which are homologous in the sequence to a target protein leading to specific degradation of target mRNA. Double-stranded RNAs (dsRNAs) known as siRNAs found in the cytoplasm are capable of silencing own complementary mRNA. siRNAs are part of the non-coding RNAs family (ncRNAs) which is composed of long ncRNAs (lncRNAs) and small ncRNAs. The most well-known small ncRNAs that have a function in transcriptional regulation and post-transcriptional gene silencing are siRNA and miRNA while on the other side long dsRNAs are precursors for siRNAs. Gene silencing mechanism with help of endoribonuclease Dicer is cleaving long dsRNAs into short interfering RNA which are usually RNA double stranded sequences of 21-24 nt in length as shown in Figure 1. Name Dicer (DCR) is coming from the fact it is having the capacity to digest dsRNA into small RNAs of a proper size. As stated in work of Agrawal N. et al, DCR has shown same function and outcome as nucleases of RNAase III family members. It is reported that RNAase III-like enzyme in Drosophila showed the same outcome giving final product of 22nt fragments [7].

Subsequently, obtained siRNAs fragments will be loaded onto activated form of RISC where protein Ago-2 will cleave dsRNA sequence and release it as ssRNA. For proper RISC activation, the passenger strand is removed, while onto Ago-2 guide strand is loaded. Ago-2 cleaves the target mRNA at 5' end between 10 and 11 base of the siRNA antisense strand. Released ssRNA represents guide sequence right toward mRNA of the target with whom it has a high degree of sequence complementarity. All molecular players of RISC complex are yet unknown, so far it is known that Ago2 protein complex has great role in post transcriptional silencing [8].

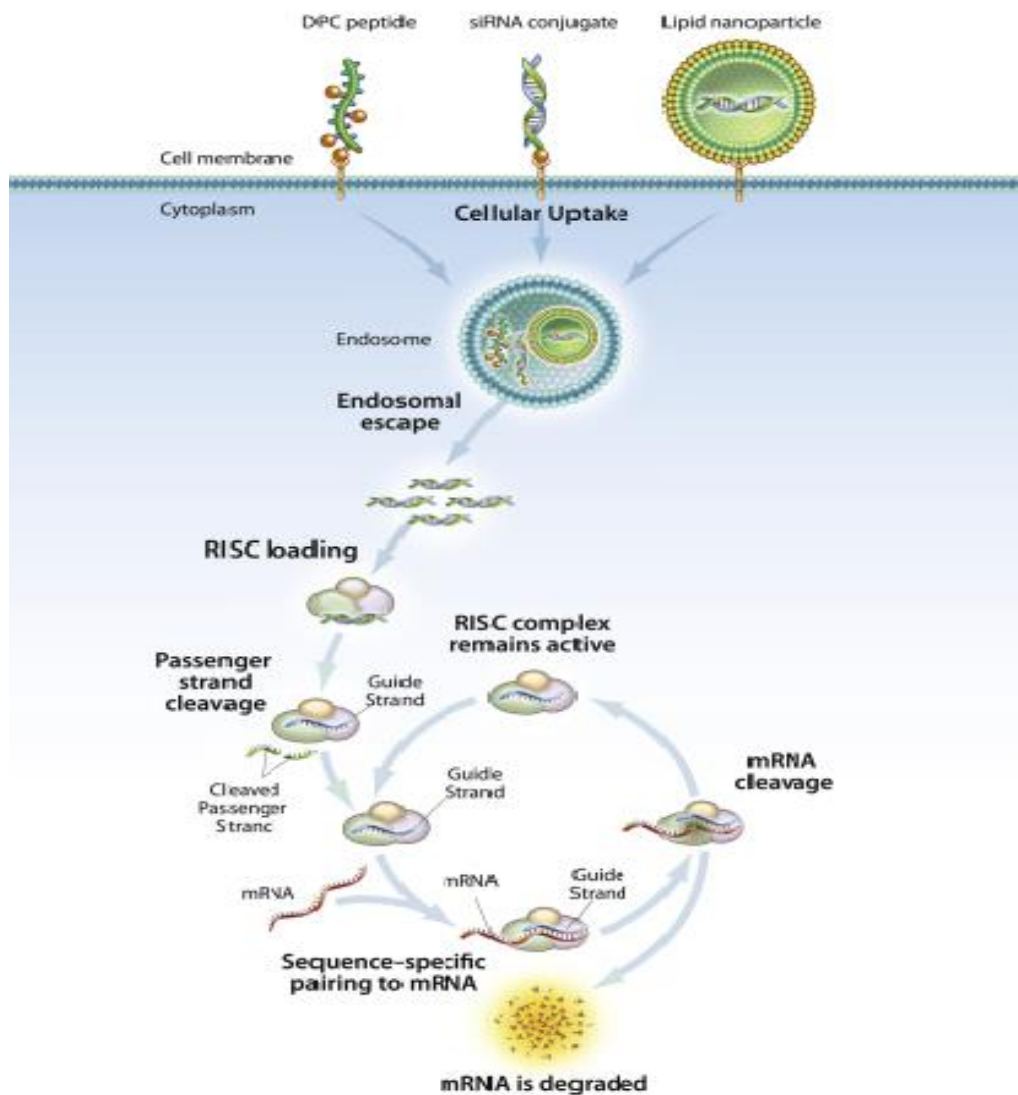


**Figure 2.3.** siRNA mediated gene silencing process [9].

After thermodynamically favourable base pairing of siRNA and mRNA is done mRNA is cleaved and destructed by cellular nucleases. Right after finishing this cycle RISC complex is free to take up additional mRNA molecules of the target.

When it comes to the internalisation process major role play endocytosis enabling molecules internalisation together with cell membrane component. Naked siRNA cannot readily cross anionic cell membrane because of its high molecular weight, large size and negative charge coming from hydrophilic phosphate backbone. It is known that if a carrier is coated with ligands or antibodies specific binding of a carrier to cell membrane enables much easier passage into the cell. In the process of endocytosis, anionic proteoglycans are making interaction with negatively charged siRNAs forming an endocytic vesicle on the cell surface [8]. When RNAi enclosed in endosome is released in cytoplasm it is ready for interaction with RISC. Once RNAi is taken up via endocytosis it is exposed to the degradation by nucleolytic enzymes if successfully avoids it successful delivery is done.

#### 2.2.2.1. Function of Dicer in silencing

Dicer is part of RNase enzyme family composed of PAZ domain, helicase /ATPase, DUF283 domains, a C-terminal dsRBD and two catalytic RNase III domains (RIIIa and RIIIb). Dicer's main role is to process dsRNA to siRNA and to induce cleavage of pre-miRNA to 20-bp miRNA sequences in the cytoplasm. Dicer protein is known to be involved in assembly of RISC complex and close interaction with Argonaute proteins.

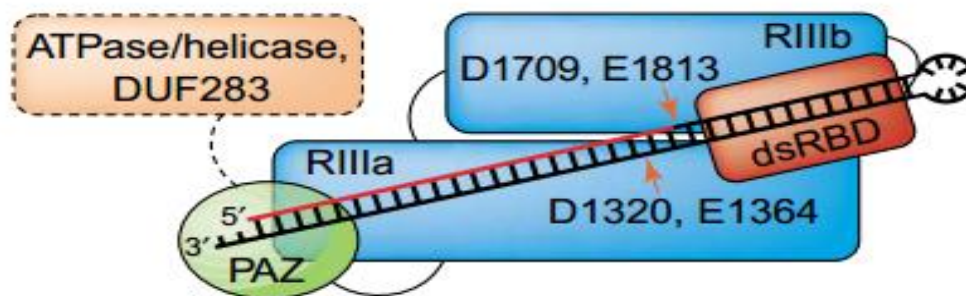


**Figure 2.4.** Schematic representation of Dicer's function [6].



Two catalytic sites RIIIa and RIIIb direct cleavage of dsRNA just 20bp from its terminus. PAZ domain recognises pre-miRNA 3' overhang which is coming from Drosha processing. The function of helicase/ATPase is not fully understood. In RNA silencing Dcr-1 is functioning in the processing of miRNA while on the other side Dcr-2 is involved in RNAi processing [6].

### **2.2.3. Design of siRNA**

When designing siRNAs, basic parameters such as internal bp repeats at specific positions at the sense strand, GC content and siRNA length of around 19–22 bps should be considered. According to Draz et al, substitution of 2'-O-methyl ribosyl group at position 2 in the guide strand could reduce silencing of most off-target transcripts which are complementary to the siRNA guide [10].

### **2.2.4. siRNA and cell interaction**

One of the leading challenges when it comes to delivery of siRNA/nanoparticle complex to the cell is the way because to yield significant effect on a target cell ratio between siRNAs and delivery reagent must be adjusted. Therapeutic use of siRNA is shortened because it is rapidly degraded by nucleases in the cytoplasm and therefore it has a short half-life. For this, it is a great need for the use of effective and suitable carrier system for siRNA to trigger RNAi mechanism. Although effective viral delivery systems have been developed to address this problem risk of virus recombination and strong immunogenicity are limiting its use. The ability of nanoparticles to pass easily through the cell membrane has offered alternative treatment methods by carrying DNA or RNA oligonucleotides. In order to reach the target in the cytoplasm by freely passing through the cell membrane and escaping from the cytoplasmic vesicle; liposomes, peptides, polymer-based, magnetic nanoparticles were offered as an alternative in transfection.

## **2.3. Cancer development**

Cancer is one of the leading causes of death in economically developed and developing countries. After decades of extensive research, cancer can be described as a genetic disease of the somatic cells where certain changes in the sequence of the gene occur. Genetic changes such as rearrangements of chromosomes (deletion, translocation, insertion), point mutation and gene amplification are affecting kinase inhibitors, growth factors, growth factor receptors, a cascade of transcription factors and signal transduction complex members.

Mutations in germ and somatic cells increase the likelihood for cancer-causing random tumour development. The final result increases in tumour cell number which is coming either by stimulation of cell division or dysregulation in cell death program. Impaired balance of cell proliferation and changes in genes that regulate cell death are giving rise to the abnormal growth of the cells. Cells, the simplest building blocks of all living things are taking control of their life cycle. If something goes wrong in cell cycle cells are starting to grow irregularly. Irregular cell growth is giving harm to functions and organs in the body. Cell proliferation is regulated through cell cycle which is comprised of four check phases known as G1 (gap 1), S (DNA synthesis), G2 (gap 2) and M (mitosis). The cell cycle is controlled at two checkpoints at G1 and G2. RB tumour suppressor protein is controlling G1 checkpoint, whereas p53 activation triggers cell cycle arrest at G1 or G2 point once DNA damage or some other abnormal behaviour is sensed. There are three types of genes which are known to be affected by gene alterations. These are tumor-suppressor genes, oncogenes and stability genes (caretakers). Mutations in tumour suppressor and oncogenes are leading to uncontrolled cell growth that is having the potential for constant replication. Stability genes or caretakers promotes tumour development in a way that mistakes in control points of DNA replication are made. These are mismatch repair (MMR), nucleotide-excision repair (NER) and base-excision repair (BER) genes [11]. Normal cells, as part of their life span, are falling into the process of senescence where cells are reaching a critical number of division and stop growing. Although, most tumour cells do not undergo senescence and tend to replicate constantly. Cancer cells are known to have limitless replicative potential, sustained angiogenesis, insensitiveness to anti-growth signals, developed a system to evade apoptosis leading to tissue invasion and metastasis. The metastatic tumour is formed when the malignant cells are gaining the ability to leave the primary tumour and migrating to the circulative system. Tumour cells are settling and gaining the ability to proliferate in new microenvironment [12].

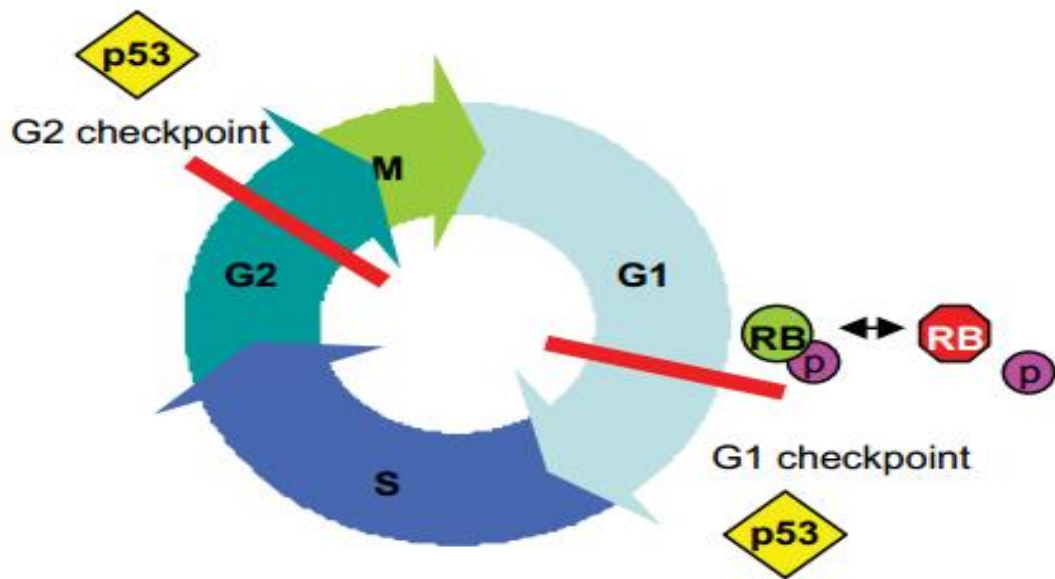


**Figure 2.5.** Schematic representation of cell cycle [12].

In cancer development process, both genetic alterations and epigenetic changes are having influence. These changes are leading to activation or silencing of genes which are in charge of cancer development. Genetic changes such as mutations, polymorphism and translocation are triggering cancer development. Various genetic alterations can be found within one single tumour. Alterations in DNA structure, nucleotide point mutations where specific gene responsible for cancer development is affected, chromosome translocation, chromosome number alterations, amplification or deletions are some of these alterations. On the other side DNA methylation, RNA-mediated silencing and histone modification represent epigenetic changes that are not part of DNA coding part [13]. The best-studied epigenetic mechanism is DNA methylation. DNA methylation refers to the addition of methyl group to cytosine base in CpG island at 5' DNA sequence. DNA hypomethylation promotes tumorigenesis through activation of cellular oncogenes and transposable elements that are increasing genomic instability.

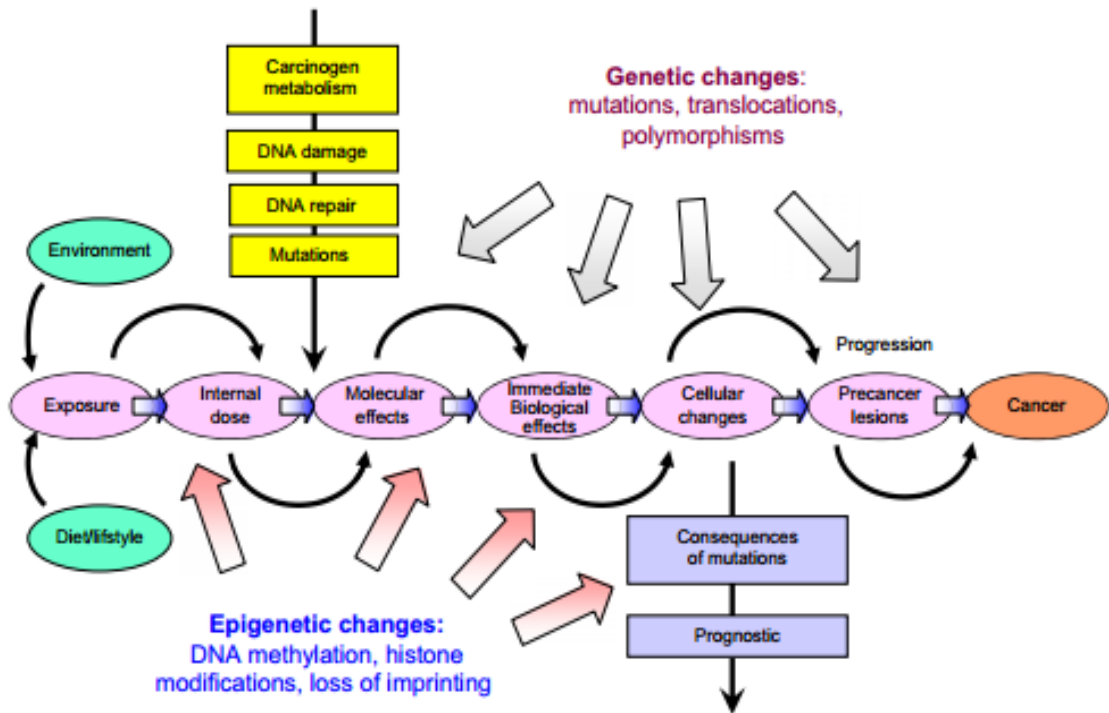


**Figure 2.6.** Influence of environmental factors together with genetic and epigenetic changes on tumor formation [13].

In human cancer there are two forms of DNA methylation found to be cancer-related; loss of methyl group on DNA 5' cytosine in CpG island known as global hypomethylation and CpG island hypermethylation. Hypermethylation promotes tumorigenesis by silencing tumour suppressor genes whereas hypomethylation triggers protooncogene reactivation. CpG island methylator (CIMP) phenotype is found mostly in colon cancer. Histone modifications such as acetylation, phosphorylation, methylation and ubiquitination are having a great role in cell processes. These modifications are being important in DNA repair process, DNA transcription and replication and if there occurs mutation in mechanisms individual is becoming prone to cancer development. Histone acetylation and protein complexes (HATs) are known to be an important part of chromatin modification. This change has been found in certain leukaemias. In contrast to genetic, epigenetic changes are reversible meaning that DNA methylation, histone acetylation represents promising therapeutical targets for cancer prevention and treatment.

### **2.3.1. Colon cancer progression**

Colorectal cancer (CRC) is one of the most prevalent causes of death worldwide. As known throughout the literature, induced transformation of the normal colonic epithelium to the colon adenocarcinoma is the result of a progressive accumulation of epigenetic and genetic alterations. Progression of Colon cancer arises from benign neoplasms called polyps which through multi-step progress transform from normal colonic epithelium to adenoma. Terminally, metastatic and invasive carcinoma with no genomic stability is developed. Genetic instability of colorectal cancer is caused by many different but still overlapping pathways. Extensive molecular analysis of colon cancer cells has proposed chromosomal instability (CIN), CpG island methylator phenotype (CIMP), microsatellite instability (MSI) alterations to be involved in initiation and progression development of colon polyps. The most common one is chromosomal instability (CIN) where 85% cases are assigned to this form of genomic instability. It was diagnosed by examining changes in numbers and structure of chromosomes. Microsatellite unstable (MSI) is giving rise to an app. 15% of total developed CRCs that are identified through diploid karyotype with a set of mutations different from those found in the CIN carcinomas. It is reported the existence of colon cancer that shows both traits of CIN and MSI. CpG Island Methylator Phenotype is manifested as hypermethylation of place containing CpG islands but also whole DNA could be hypomethylated. Normally, all colon cancer cases are having DNA methylation section, but in CIMP app.10-20% have a high portion of abnormally methylated CpG loci. Both, epigenetic and genetic alterations and its specific signalling pathways are important for the research of CRC development. These signalling pathways are either controlling cell proliferation, apoptosis, immortalization, angiogenesis or cell differentiation. Mostly seen signalling pathways in colorectal cancer including WNT, MAPK, PI3K, TGF- $\beta$  and p53 [14]. So far, WNT- $\beta$ -catenin signalling pathway, the epidermal growth factor receptor (EGFR)-MAPK, transforming growth factor  $\beta$  (TGF $\beta$ ) and the phosphatidylinositol 3-kinase (PI3K) signalling pathways are the best-studied cause of colon cancer development. In order to examine which are genetic and epigenetic, it is strongly recommended to examine causes of colon cancer (MSI, CIN, CIMP) to decide effective therapy for developed neoplasm [15, 16].

### **2.3.1.1. Conventional approach in colon cancer therapy**

Colorectal cancer (CRC) is known for being one of a leading cause of cancer subjected deaths worldwide. Besides clinical and pedigree predispositions there are several risk factors known to be the cause of cancer development such as smoking, age, obesity, physical inactivity and heavy alcohol use. Also, having some gastrointestinal diseases such as inflammatory bowel disease (IBD), Crohn's disease and person's previous treatment for cancer disease increase possibility for cancer development. Colorectal cancer screening is a well-known method for early detection of cancer polyps that can be removed before transformation to the cancer cell. Genetic tests are extremely helpful for early colon cancer detection. Patients are tested for development of Lynch syndrome (also known as hereditary non-polyposis colorectal cancer, or HNPCC) and susceptibility of inheritance from family members. Steinke V. et al., raised an issue of Lynch syndrome stating that is a genetic disease caused by a mutation in one of four genes of the DNA mismatch repair system which leads to a hypermutated tumour. MMR (mismatch repair) proteins are part of cascade protein that is maintaining genomic integrity by repairing mismatched bases occurring in DNA replication. In work of Umar A. et al, MSH2, MLH1 and in rare cases MSH6 are reported to be validated MMR proteins in colorectal cancers development [17]. In order to detect alterations typical for Lynch syndrome as well as colon cancer, biopsy sample tumor tissues are tested using immunohistochemistry (IHC) and MSI testing for germline mismatch detection [18]. Flexible sigmoidoscopy and colonoscopy are invasive tests used for colon cancer screening. Thin, flexible tube with a camera is used to examine colon and rectum. Both colonoscopy and sigmoidoscopy are using the same principle for examination just difference is in the fact that colonoscopy is examining overall area of colon whereas sigmoidoscopy covers the only left side of the colon. Found polyps on the colon walls are removed and sent for biopsy to make sure if the tissue is cancerous, non-cancerous or it is a result of inflammation. In practice, computed tomography (CT) is often used where X-ray computer programs are giving a 2D and 3D view of the screened inner part of colon and rectum. Also, patients are deciding to take less invasive tests such as faeces (stool) for cancer detection. If there is still suspicion of cancer development after noninvasive test results colonoscopy is recommended to be done. In clinics, recommended therapy for colon cancer patients is surgical resection combined with chemotherapy. This traditional approach is reported to show good outcomes for patients with early stage carcinoma, but for those with extensive colon development first chemotherapy then liver resection is recommended.

As stated in work of Waisberg J. et al., chemotherapy in colon cancer treatment was having stronger therapeutic effect if new cytotoxic agents and targeted therapies such as bevacizumab, cetuximab, panitumumab were included [19]. Targeted therapies that are used traditionally in CRC treatment are monoclonal antibodies or small molecule drugs. In CRC treatment, bevacizumab drug is monoclonal antibodies targeting VEGF (vascular endothelial growth factor), cetuximab and panitumumab are drugs that target EGFR (epidermal growth factor receptors) [20]. Chemotherapeutical therapies held much promise for CRC treatment but after some time need for an individual approach to each patient was clear.

### **2.3.1.2. New generation treatment strategies for colon cancer**

The biggest limitation of traditional methods for cancer treatment is the unavailability of drugs that are effective for common mutations arising with cancer development. Extensive cancer treatment was making harm to healthy cells. Personalised medicine is a brand-new approach where large-scale tests provide information about genome, exome, transcriptome and epigenome of an individual. For early diagnosis of cancer, there is a need for different molecular assays which are performed using samples with low DNA amount giving a prompt and accurate result. Targeted NGS (next generation sequencing) represents a breakthrough approach for molecular screening test by sequencing DNA samples for detection multiple alterations. What makes NGS superior over traditional methods is its ability to review multiple regions instantaneously leading to identification and understanding effect of chromosomal instability and microsatellite instability pathways as the most common mutations found in CRC patients. In a light of finding a best possible solution for cancer patients interconnection of different cancer members must be examined to obtain a solution. Cancer nanomedicines are not just about loaded nanoparticles, nano drugs or nanotherapeutics it is also about a combination of so far used chemotherapeutic components and its combination with novel nanoscale particles. This also encloses use of medical devices and anti-cancer drugs as therapeutics for personalised medicine improvement [21]. When a nanomaterial enters human body it meets different chemical and biological environment based on reached tissue or organ. Accordingly, on a nanomaterial's surface layer of protein is formed called "protein corona" which makes interaction with other protein in an environment. This layer of proteins is following size, chemical composition and shape of the nanoparticle.

Internalization can be either via passive transport throughout the cell membrane, via clathrin-mediated endocytosis, phagocytosis or macropinocytosis. Shape, size and composition of nanomaterial are key components to consider when designing materials for successful penetration and to degradation avoidance.

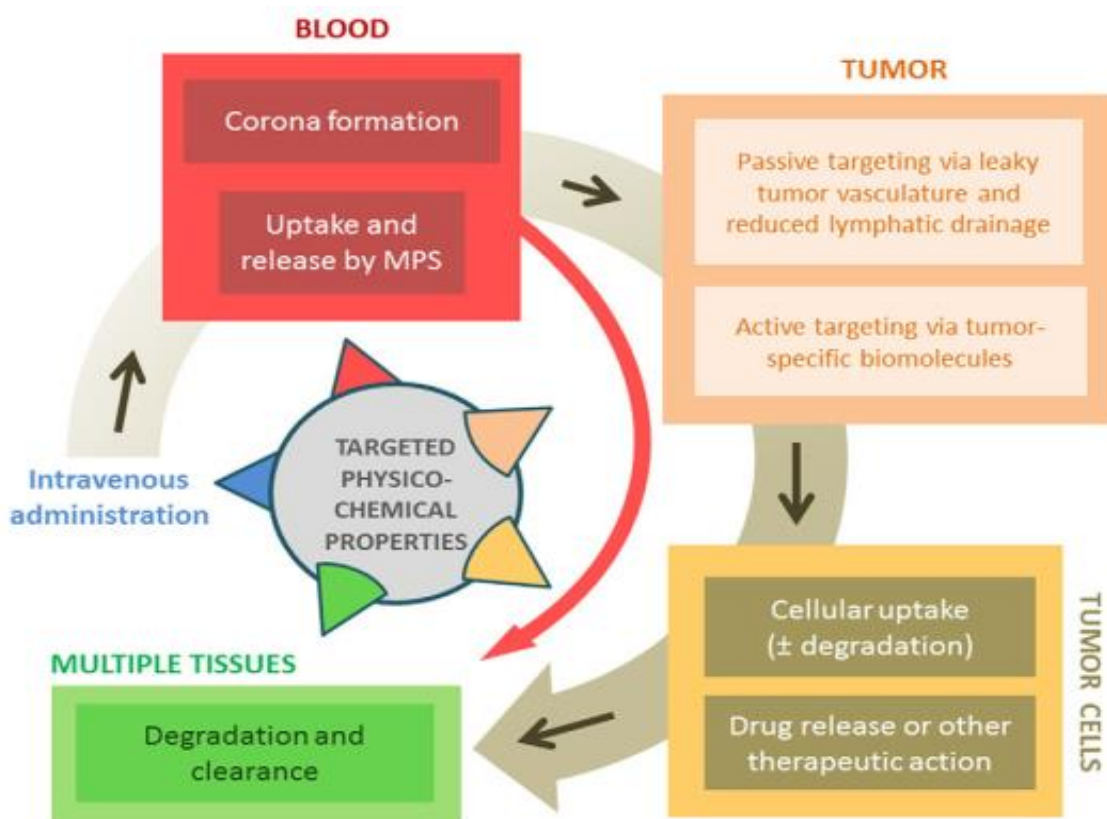


**Figure 2.7.** Influence of nanomaterials and physiological compartments in cancer treatment [21].

In the case of passive intake, it is done via EPR (enhanced permeability and retention) effect because of increased vessel leakiness and impaired lymphatic function that permits the accumulation of nanomaterial at a site. On the other side, active targeting of nanomaterial means assisted penetration and accumulation with the usage of tumor specific and bioactive molecules such as antibodies, folic acid and enzymes.



## **2.4. Nano oncological approaches for cancer treatment**

In research, there are different materials used and approved for cancer treatment. Liposome, a polymer as well as inorganic nanoparticles and micelles are nanoplatfroms that successfully carry and deliver drugs using passive targeting in cancer tissues. The tumour microenvironment is having dense ECM, unevenly distributed vascularization and vessel permeability are obstructing biodistribution of synthesised nanoplatfroms. Also, incomplete understanding of the relationship between diseased organs and nanoparticle interaction are making improvement go slow [21].

### **2.4.1 Liposomes**

First liposomal complex approved by FDA is Doxil. It is anti-cancer drug doxorubicin enveloped with PEGylated liposome to enhance drug accumulation at the target tissue. It is known that liposomes do not possess stability and controlled release of drug to the tumour site. Currently, there are many jobs to be done to get over limitations, to increase stability, to enhance drug loading and release properties of liposomes and also to get approval from FDA to become first-line treatment [21].

### **2.4.2. Micelles**

Similar to liposomes, micelles are particles that composed of amphiphilic molecules that are self-assembled in water to make nanoplatfroms. Micelles are well suited for hydrophobic cargo since its membrane is monolayered making its inner part nonpolar. In breast cancer treatment, Genexol-PM known as micellar nanoparticle releasing paclitaxel drug has gotten FDA approval [21].

### **2.4.3. Polymeric nanoparticles**

In last decades, polymeric nanoparticles have gained attention and were a sphere of interest of many researchers all over the world. Coating of nanoparticles with a polymer such as polyethylene glycol (PEG) is reported to decrease immunogenicity and improve circulation time. Polymeric nanoparticles are known to be used alone and as adjuvant therapeutic agents. In 1994, one of the first tumour targeted polymer coated drug for hepatocellular carcinoma called Zinostatin Stimalamer in Japan was authorised [21, 22].

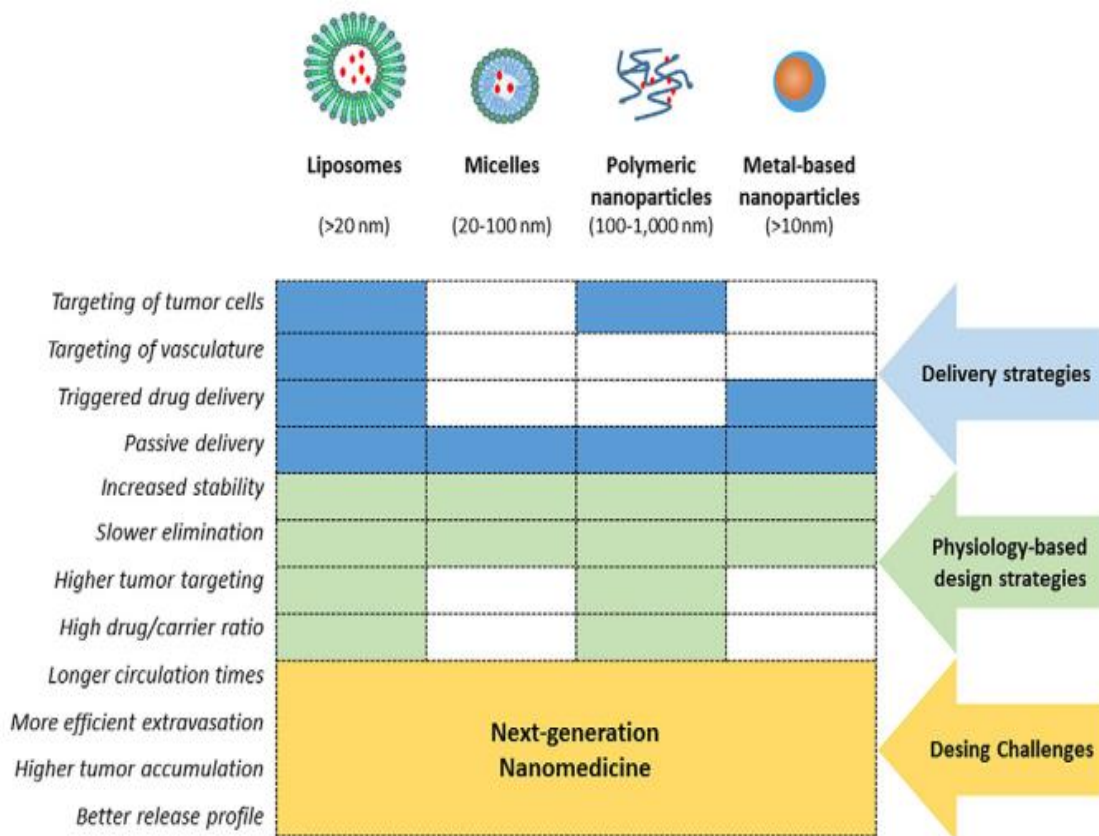


**Figure 2.8.** Available nanoplateforms in clinical trials for cancer treatment [21].

In nanomedicine, extensive research attention is devoted to developing delivery strategies. Micelles and metal-based nanoparticles are mostly being delivered throughout passive whereas polymeric nanoparticles are delivered using active and passive delivery [21].

#### 2.4.4. Metal-based nanoparticles

Metal-based nanoparticles are mostly metal and metal oxide compound of iron (Fe), zinc (Zn), manganese (Mn), aluminium (Al), but also copper (Cu), gold (Au) and silver (Ag). These nanoparticles are able to pass throughout cell membrane but along the way also it can be excreted by liver or kidney. Ag and Cu are nanoparticles that have gained success in avoiding detection by phagocytic defense system [23].

#### **2.4.4.1 Iron oxide nanoparticles (IONs)**

Iron oxide nanoparticles used in therapeutics are typically consisting of three components: an iron oxide nanoparticle core that serves as a carrier for therapeutics and contrast agent for MRI, a coating of iron oxide nanoparticle that promotes favourable interactions between IONs and biological system and a therapeutic payload that performs a function in vivo. In order to promote desired intracellular trafficking, bypass cellular barriers and to enable controlled release of siRNA targeted over mRNA of interest one of the proposed strategies is the use of targeting agents that recognize over-expressed receptors on cancer cells surface to maximise uptake of IONs by cells [24, 25]. As shown in the study Kievit et al., iron oxide NPs with nanocrystalline magnetite cores have great potential for use in oncological medicine. The development and application of Nanotherapeutics have emerged as a promising tool for early and late termination of cancer development because magnetic nanostructures have potential to carry therapeutically active genes to the cells without disturbing its integrity and wit help of external magnetic delivering therapeutics to tumour region with no damage to healthy tissues. It is mostly due to its biocompatibility, biodegradability and ease of synthesis and specific applications. The maghemite ( $\gamma\text{-Fe}_2\text{O}_3$ ) and magnetite ( $\text{Fe}_3\text{O}_4$ ) are the most probed types of iron oxides. The potential application of these nanoparticles includes cell labelling and targeting, drug delivery, hyperthermia and magnetofection [24, 25]. Iron oxide nanoparticles are known to be used as contrast agents for magnetic resonance imaging, as a drug carrier and in treating iron deficiency [50]. According to Chen et al., transfection in the absence of the magnet appeared to be much slower. Iron oxide nanoparticle can be easily combined with negatively charged materials such as anti-cancer drugs and nucleic acids, which contribute greatly to targeted drug delivery and gene transduction [3].

#### **2.5. Polymers used in delivery vehicle coating**

Every taken drug in an organism has a particular half-life that's why in circulation system it is present for short time. Extensive efforts are being made to solve this problem. Some of the solutions would be to increase the dosage of the drug or to increase uptake of drug per a day. In both cases, there is the possibility of reaching toxic response. In the scope of nano oncology, synthesis of nanoparticles coated with biodegradable, nontoxic polymer is used to avoid quick recognition by the immune system, identification by macrophage system and rapid clearance from the body.

In order to get promising results time-specific and special delivery of biodegradable polymeric materials is recommended. Polymeric materials are one of the most suitable materials used in magnetic nanostructures coating. Coating of nanoparticles is performed to stabilize nanoparticle in biological medium. As reported in work of Foox M. et al, because gelatin coated nanoparticles with siRNA led to low toxicity gelatin is considered as an excellent carrier for cancer therapy drug delivery [26].

### 2.5.1. Gelatin as coating polymer

Gelatin is biopolymer found in human body. Its solubility, biodegradability, high biocompatibility, pH-induced surface charge as well as the presence of functional groups makes it a perfect candidate for therapy and interaction with the physiological environment. Gelatin is obtained from collagen denaturation through the process of hydrolyzation. When collagen is heated fibers are starting to lose its primary form and with water interaction bunch of single chains are forming a gel structure. Amino acid composition of gelatin is very similar to collagen with a slight difference in amino acid and molecular composition of gelatin. The complete amino acid composition of gelatin is not known. So far it is known that hydroxyproline, proline and glycine are abundant in mammalian gelatins.

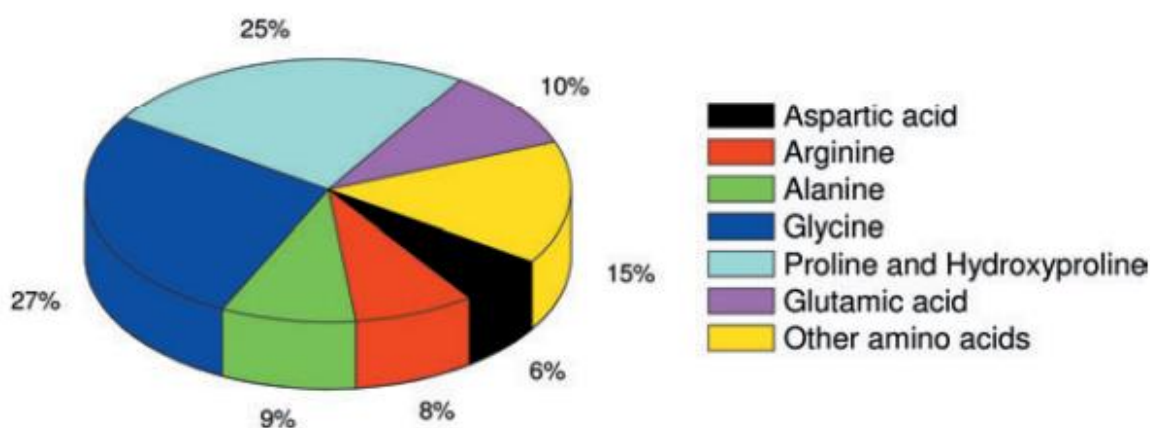


**Figure 2.9.** Chemical composition of gelatin [27].

Due to the presence of large amounts of functional group in the chain of gelatine, such as amine  $-NH_2$  and carboxylic  $-COOH$ , pH charges of gelatin can be negative or positive. The presence of Arg-Gly-Asp (RGD) sequence in gelatin structure makes gelatin more preferable over synthetic polymers lacking this sequence. RGD sequence modifies cell adhesion, improves biological behaviour and cell recognition. Gelatin's high biocompatibility comes from the fact that cell surface and extracellular matrix (ECM) contain many macromolecules including collagen and gelatin [3]. For commercialization purposes, gelatin is mostly extracted from pig skin, cattle bones and bovine hides. It also can be extracted from poultry, vertebrates and fish. It is mostly done by thermal pre-treatment and alkaline or acid baths. In raw materials besides proteins, there are lipids, sugars, ions and small molecular found in both bones and skin. After performing thermal treatment separated proteins from the raw material are deionized, dried and sterilised for further used. If produced from acid pre-treatment it corresponds to type A gelatin and the one produced from alkaline pre-treatment accounts for type B gelatin. In type B gelatin proportion of glutamic acid and aspartic acid is far higher than in type A. It is because of the alkaline process that deaminates asparagine into aspartic acid and glutamine into glutamic acid. As reported in work of Tseng C.L. et al, nanoparticles prepared using type B gelatin were larger and more widely distributed when compared with nanoparticles prepared using type A gelatin. Nanoparticles of type A gelatin were reported to have mostly positive charge whereas those of type B gelatin were having mostly negative surface charge [19]. The stability of gelatin comes from the triple helix structure composed of three polypeptide  $\alpha$ -chains. This structure is mostly composition of  $(Gly-X-Pro)_n$ , where X represents amino acid, mostly lysine, arginine, methionine or valine. Triple helix structures or double strand structures are stabilised by hydrogen bond. These interactions are formed between every three residues of glycine  $\alpha$ -chains. Water molecules are stabilising bonds of the gelatin network. However, exact type and number of formed bonds in gelatin is not defined [28]. Gelatin is interesting polymer not just because of its structure with different functional groups, but also because it offers multiple opportunities for modification using crosslinkers and ligands which represent a useful tool for targeted drug delivery [29]. As reported in work of Foux M. et al., dissolving rate of gelatin in aqueous solutions is extremely high that is why gelatin is not effective for long-term delivery. That is why gelatin needs to be crosslinked to enhance mechanical properties and decrease degradation rate in aqueous solutions.

Most common method is physical crosslinking by hydrothermal treatment, ultraviolet irradiation, microwave energy and chemical crosslinking by chemicals such as formaldehyde, glutaraldehyde and through biological crosslinking by enzymes. Physical crosslinking can be also made using environmental parameters like temperature, pH, ionic strength. For successful crosslinking either physical crosslinking or chemical modification is used.

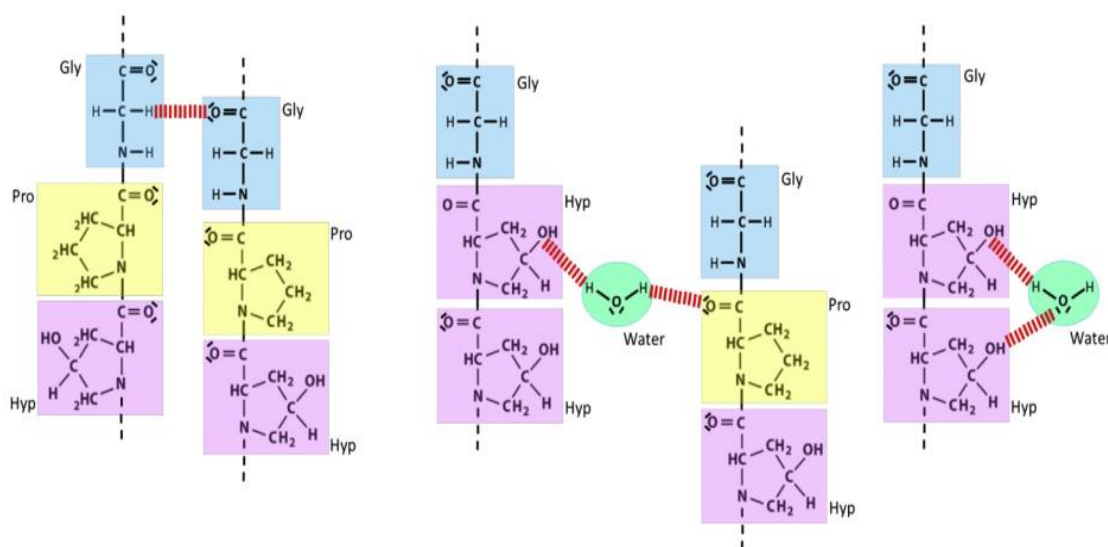


**Figure 2.10.** Hydrogen bonding in gelatin chains (left) and bonding between gelatin chains and water molecules (right) [28].

Gelatin is known as GRAS (generally regarded as safe) material because of its unique properties and extensive use in pharmaceutical, cosmetics and food industry. Moreover, gelatin is known to be drug/vaccine delivery carrier and a matrix for mineralisation in tissue engineering because of its unique properties [30, 27]. For all above-mentioned reasons, synthesised gelatin nanoparticles in cationic form are particularly promising for the release of nucleic acids. Gelatin-coated multifunctional nanostructures have the potential to carry therapeutically active genes to the cells without disturbing its integrity and delivering it to target tumour region.

## 2.6. mTOR oncogene

Genetic malignancies arising from PI3K-mTOR pathway hyperactivation are one of the common disturbances recorded in cancer biology. The mechanistic target of rapamycin (mTOR) pathway is known to play an important role in human cancer development, the progression of obesity and resistance to conventional cancer therapy agents. It represents a junction between signaling pathway, cell proliferation and metabolism. mTOR is a protein kinase that phosphorylates serine/threonine residues triggering activation of the PI3K/Akt pathway. The upstream signal could be ligand binding to EGF receptor, insulin binding to IGF receptor, stress and energy. mTOR has two catalytic, signaling subunits: mTOR complex 1 (mTORC1) and mTOR complex 2 (mTORC2). In both complexes, the existence of DEP domain-containing mTOR-interacting protein (DEPTOR) and mammalian lethal with sec-13 protein 8 (mLST8, also known as GβL) is noticed. Besides these, mTORC1 is comprised of mTOR, regulatory associated protein of mTOR called Raptor and proline-rich Akt substrate 40 kDa, PRAS40. On the other hand, mTORC2 is composed of mTOR, Rictor as regulatory associated protein of mTOR, mammalian stress-activated MAP kinase-interacting protein 1, mSin1 and protein observed with Rictor-1, Proctor. When stimuli come from the upper part mTOR complex 1 then phosphorylates S6K1 (ribosomal protein S6 kinase) and 4E-BP1 (eukaryotic initiation factor 4E) to stimulate protein synthesis and cell growth [31, 32]. Upstream mediators of mTOR complex 2 are not investigated as much as mTOR complex 1, but still it is known that mTORC2 is playing a great role in cell survival and proliferation, cytoskeleton organization and metabolism through phosphorylation of Akt pathway. According to Malley et al, there is an underlying link between obesity, mTOR and cancer development because obesity is known as a leading risk factor for the development of gastrointestinal cancers such as gastric, esophageal, hepatocellular, colorectal and pancreatic. As previously mentioned, insulin is stimulating IGF-1 which can lead to cell proliferation by activating PI3K/Akt, MAPK and STAT3 signaling pathways [31].

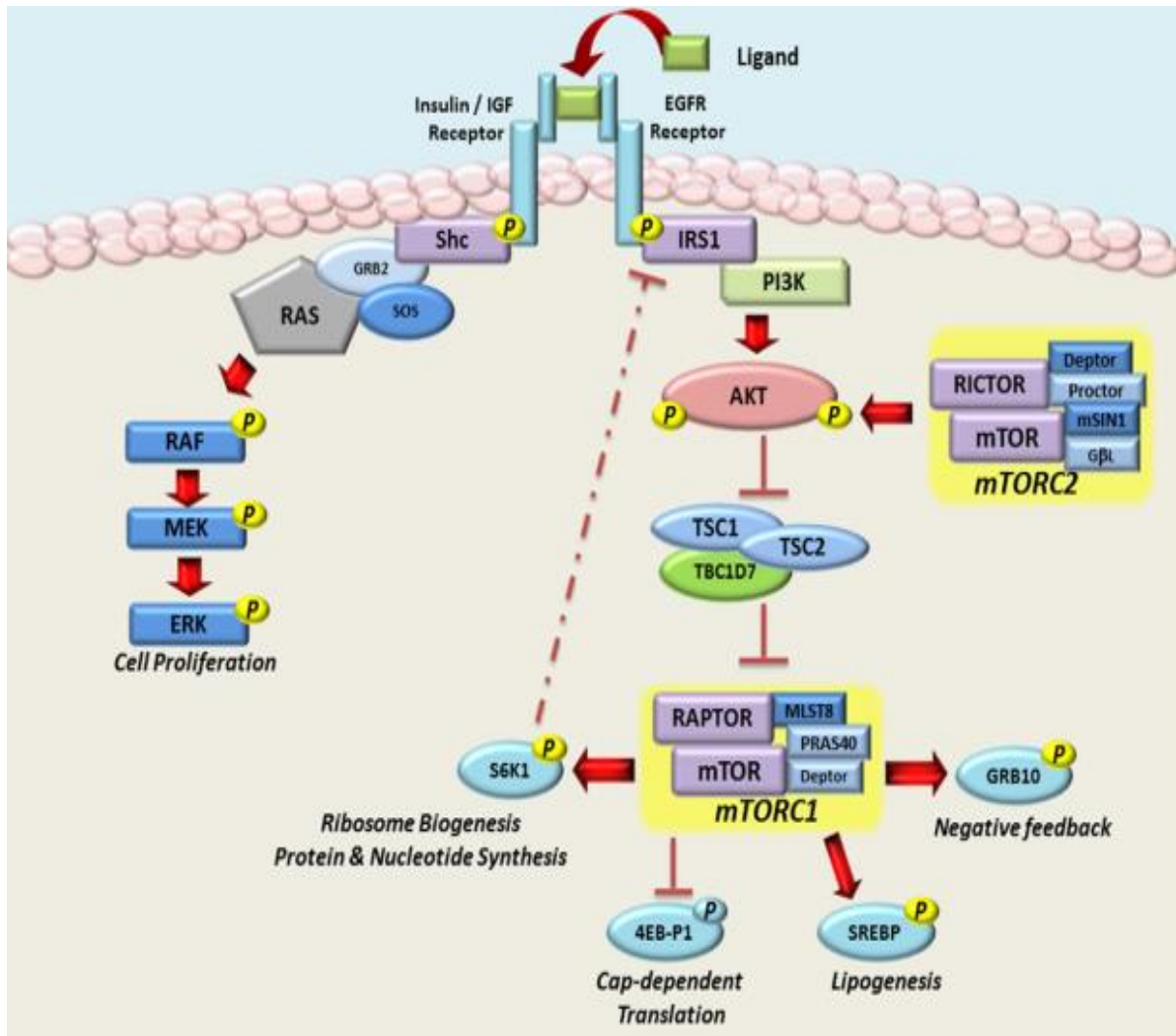


**Figure 2.11.** Upstream signalling instructions and regulation points of mTOR pathway [31].

### 2.6.1. Expression of mTOR in human cancers

In extensive work of Hou et al., it is shown that Esophageal squamous carcinoma (ESCC) xenograft, when treated with mTOR siRNA number of apoptotic cells, was 10-fold more when compared with one in control group. In the same study, it is shown clinical significance when mTOR siRNA complex is used together with a chemotherapeutical medication called cisplatin in sensitivity of cells toward this cancer drug [32].



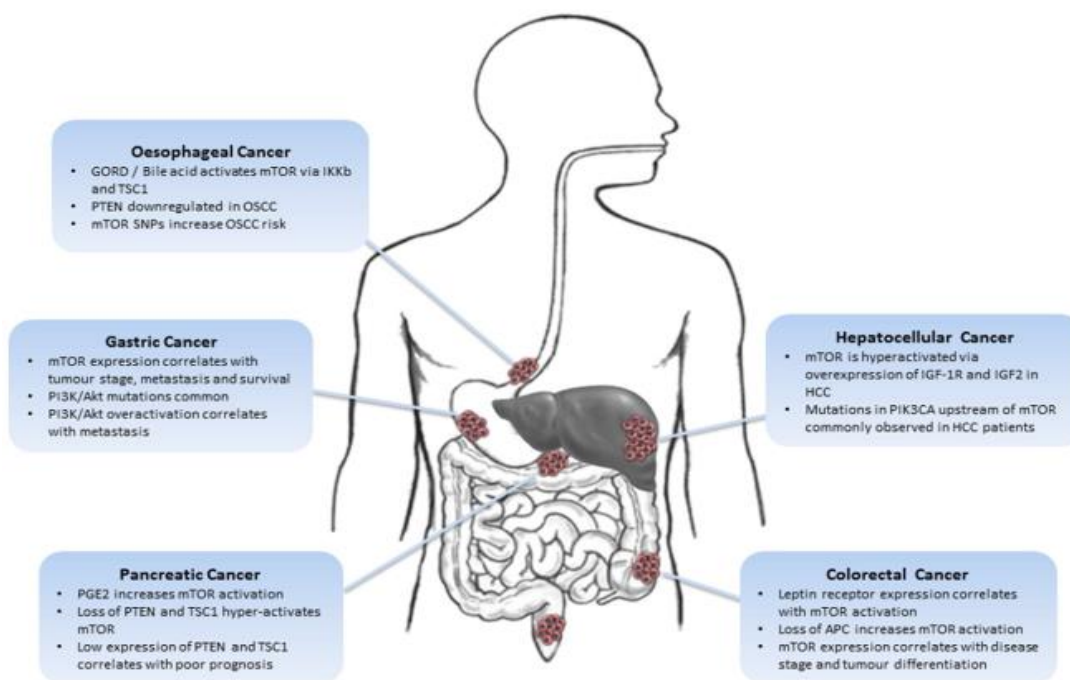


**Figure 2.12.** Role of mTOR oncogene in digestive tract malignacies [31].

### 3.EXPERIMENTAL STUDY

#### 3.1 Chemicals

For synthesis of iron oxide nanoparticle, ferric chloride  $\text{FeCl}_3 \cdot 6\text{H}_2\text{O}$  iron (III) chloride (Merck, Germany), ferrous chloride  $\text{FeCl}_2 \cdot 4\text{H}_2\text{O}$  iron (II) chloride (Merck, Germany), HCl hydrochloric acid (Merck, Germany) and NaOH sodium hydroxide (Sigma-Aldrich, Germany) were used in presence of an inert atmosphere of nitrogen gas. Throughout all steps, distilled water was used. siRNAs used to suppress mTOR gene (sense strand: 5'-GAGUGUUAGAAUAUGCCATT-3', antisense strand: 5' UGGCAUUAUUCUAACACUCCGG-3') were purchased from Qiagen (Germany). For cell culture studies; human colon cancer cell line CaCo-2 was obtained from Şap Entitüsü (Ankara, Turkey) while RPMI- 1640 (Roswell Park Memorial Institute-1640), phosphate buffered saline (PBS), Trypsin-EDTA (Tripin-Ethylenediamine tetraacetic acid), fetal bovine serum (FBS), Trypan blue and pencilin-streptomycin were provided by Pan-Biotech (Germany). trypan blue was used. For cytotoxicity test, tetrazolium salt MTT from Glentham Life Sciences (UK) and isopropyl alcohol from Sigma-Aldrich (Germany) were purchased.

### 3.2. Synthesis of iron oxide nanoparticles

To date, many different methods are used for the preparation of iron oxide nanoparticles such as sol-gel synthesis, laser ablation, thermal decomposition, mechanical grinding, hydrolyzation, chemical co-precipitation, ultrasound irradiation, microemulsions, biological synthesis, etc. After work done by Massart R. et al, co-precipitation procedures became well used because of its simplicity, low-cost production and ease surface treatment with other materials that makes it excellent option for technical and medical application [33]. In this study, iron oxide nanoparticles have been synthesized using a co-precipitation method at a room temperature. It is known that nanoparticles after being present in a single position for too long tend to become unstable leading to aggregation of small NPs into large particles. It leads to a reduction of surface energy and loss of magnetic properties over time when iron oxide nanoparticles are being exposed to oxygen. As the most conventional method, synthesis of the Fe<sub>3</sub>O<sub>4</sub> magnetic nanoparticle is done with FeCl<sub>3</sub>.6H<sub>2</sub>O iron (III) and FeCl<sub>2</sub>.4H<sub>2</sub>O iron (II) salts in the molar ratio 1:2. In this method, Fe<sup>2+</sup> and Fe<sup>3+</sup> ions are precipitated in alkaline solutions of NaOH. During synthesis process, precipitant as a supplier of OH<sup>-</sup> anions when reacted with water is considered to be a main driving force in nanostructure formation of IONs. In order to avoid uncontrollable oxidation of Fe<sup>2+</sup> into Fe<sup>3+</sup> synthesis reaction is performed in an anaerobic condition using inert N<sub>2</sub> gas. In order to neutralize anionic charges on the nanoparticles surface hydrochloric acid (HCl) was used. The synthesis was performed at 60–80°C. Conditions such as mixing methods, stirring rate, digestion time, initial pH and the presence or absence of a magnetic field are having a crucial role on particle size, morphology and magnetic properties [34]. Monitoring pH of the solution in all stages was important to get proper precipitation of Fe<sub>3</sub>O<sub>4</sub>. The overall reaction equation can be shown as follows:  $Fe^{2+} + 2 Fe^{3+} + 8OH^{-} \rightarrow Fe_3O_4 + 4H_2O$  [35]. 5.4 g of FeCl<sub>3</sub>.6H<sub>2</sub>O, iron (III) together with 2 g of FeCl<sub>2</sub>.4H<sub>2</sub>O iron(II) was precipitated with 60 mL of 0.16 M HCl. It is left stirring for 1.5 h. Afterwards, 100 mL of 1.0 M NaOH solution was added dropwise under vigorous stirring, N<sub>2</sub> gas and starting temperature of 65°C.

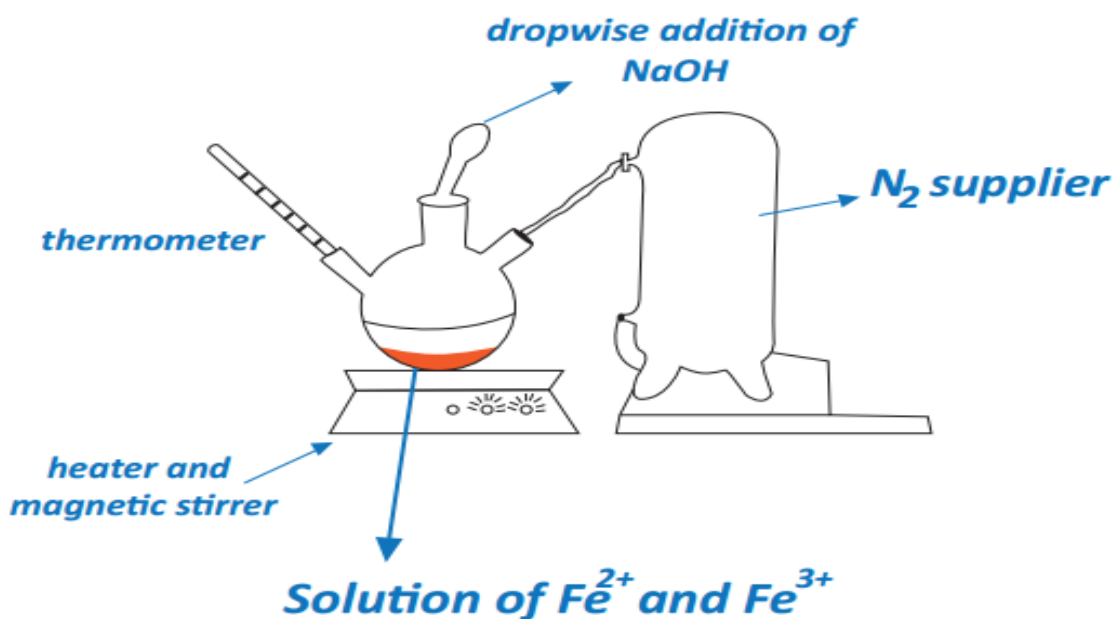


**Figure 3.1.** Schematic representation of iron oxide nanoparticles synthesis process

The iron solution was purged with N<sub>2</sub> gas for 30 seconds just before dropwise addition of NaOH to the solution. Well mixed solution was kept heated up to 85 °C under a nitrogen atmosphere and left one hour at vigorous stirring. The precipitation process occurs immediately promoting color change of solution from light brown to dark black. Dark black is characteristic for magnetite while dark brown color implies that side products of magnetite have formed [36]. pH level of the solution was reduced from approximately 12.75 to 10.25 by a washing with distilled water.

### 3.3. Coating iron oxide nanoparticles with gelatin

Nanoparticles when coated exhibit higher biocompatibility and lower agglomeration tendency which leads to avoidance of rapid elimination by macrophages. In the study done by Gaihre B. et al, desolvation/cross-linking technique was used in coating iron oxide nanoparticles with gelatin to stabilize solution and to reduce the size of a obtained complex.

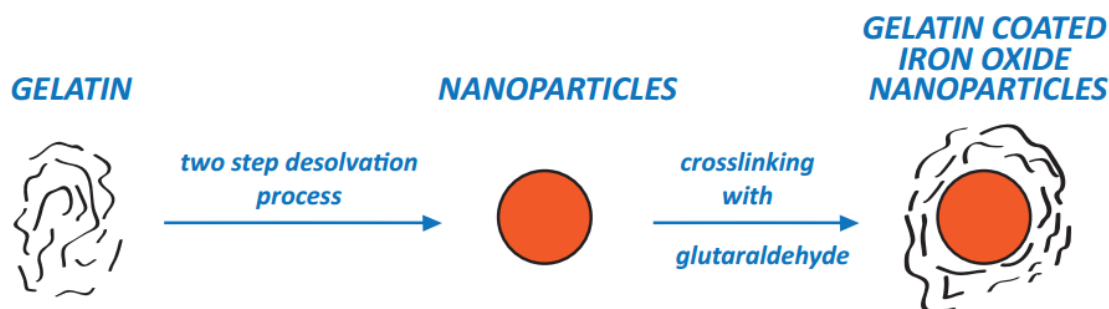


**Figure 3.2.** Schematic representation of coating iron oxide nanoparticles with gelatin

After synthesizing iron oxide nanoparticles by co-precipitation method obtained first-rate nanoparticles were coated with gelatin type A (Sigma-Aldrich, USA) using desolvation/cross-linking technique. Firstly, 1.250 mL acetone and 1.250 mL H<sub>2</sub>O together with 0.005 g. IONs were sonicated for 1h. Afterwards, 0.05 g of gelatin mixed with 125  $\mu$ L H<sub>2</sub>O (0.625% gelatin) was heated for 3-5 minutes at 37°C at a maximum stirring rate in order to get a completely dissolved mixture. The mixture is transferred to a stirrer where 2 mL acetone was added. Once when the pellet is formed acetone leftover was discarded and again 125  $\mu$ L H<sub>2</sub>O is added. In order to gelatin pellet mixed with water dissolves completely it is heated again for 3-5 min. at 37°C at a maximum stirring rate. On completely dissolved mixture 1 drop of 1M NaOH was added to adjust 12-13 pH. Previously sonicated IONs with acetone and water is dropwise to a mixture making stirred rate 7 constant. Lastly, 12  $\mu$ L 8% glutaraldehyde was added to a mixture to cross-link with gelatin's functional groups to decrease hydrodynamic size of ferrofluids. Proper ratio adjustment of acetone as a desolvation agent and glutaraldehyde as a cross-linker results in the fact that ferrofluid solution had better stability [37].

### 3.4. Characterization of iron oxide nanoparticles

#### 3.4.1 Determination of morphology

SEM, scanning electron microscopy, was used to determine morphology, geometry, surface and cross-sectional structure of attained iron oxide nanoparticles. From obtained images clearly it could be seen whether nanoparticles are aggregated or having well dispersed, monodispersed morphology of size. If IONs are agglomerated, it is assumed to be due to Van der Waals attraction force that occurs between particles [38].

### **3.4.2. Size analysis of nanoparticles**

Zeta Sizer (3000 HAS, Malvern, England) is used to determine molecular weight, hydrodynamic size, surface charge and diffusion coefficient of the nanoparticles without destroying it. Stable, colloidal solution of nanoparticles is required to quantify the size of nanoparticles. The main principle of work is based on dynamics of electrophoretic light scattering. In order to get an effective characterization of nanoparticles its viscosity, a temperature of solution and refractive index must be followed accordingly. Size distribution disclosed as the polydispersity index (PDI) and hydrodynamic size are obtained from diffusion coefficients. Particles in the suspension are exposed to the emulsions and Brownian molecule motion. This motion is driven by the thermal energy of the self-initiative molecules that are causing molecular bombardment. When particles or molecules are illuminated by a laser, scattered intensity of light in relation to the size of the particles is waved. The quite small particles are pushed by solvent molecules and they move much faster. The final measurement is obtained by passing laser light through the solution. Obtained data is given as an average of the volume, intensity and size of nanoparticles in solution. Prepared iron oxide nanoparticles of approximately 1 mL were placed in a polystyrene tub so that size of particle is determined after passing a laser beam through the solution.

### **3.4.3. Charge analysis of nanoparticles**

A Zeta-Sizer device (3000 HAS, Malvern, England) was used for surface charge analysis of prepared iron oxide nanoparticles. Zeta potential ( $\zeta$ ) value is obtained by charged particle's movement calculation in regard to applied electric field. Results of zeta potential are giving a possibility to make an estimation about storage stability of IONs colloid dispersion. In the solution of charged particles (high zeta potential) aggregation of particles is less likely to occur due to the electric repulsion. But this rule is not fully valid for systems containing steric stabilizers because adsorption of steric stabilizers is decreasing zeta potential.

### **3.4.4. Determination of chemical structure**

Chemical structures and molecular bond characterization of iron oxide nanoparticles were done using Fourier Transform Infrared Spectroscopy (FTIR) (Nicolet iS10, USA). Obtained FTIR spectra is giving information of the functional groups and state of bonds in the structure of synthesized samples. Basically, it is examined if the planned chemical structure is obtained or not.

### **3.4.5. Determination of magnetic properties**

VSM (vibrating sample magnetometer) is used to determine magnetic properties of prepared nanoparticles. Magnetic properties of particles in the magnetic field are expressed in units of magnetic force (emu). In VSM measurement magnetic field of constant frequency is applied on dried sample. If the sample is possessing magnetic properties it will act as a magnet due to a transient magnetic flow that creates a potential difference in the conductive rod. Vibrating magnetometer determines magnitude of potential difference giving out magnetization curve peaks. According to Eivari et.al, sample hysteresis curves of -7000 to 7000 and -50 to 50 Oersted at 300 K is implication that wanted magnetization level is reached [38]. ESR (electron spin resonance) is analyzing magnetic properties of molecules with unpaired electrons. Since molecules with unpaired electrons exhibit magnetic properties using this type of characterization it can be determined whether the materials have a magnetic properties or not.

### **3.5. Loading siRNA to gelatin coated iron oxide nanoparticles**

After iron oxide nanoparticles are coated with gelatin and its optimization is done, siRNA of different concentration is added. In 3.3. section iron oxide coating with gelatin is explained in detail. Firstly, 1.250 mL acetone and 1.250 mL H<sub>2</sub>O together with 0.005 g. IONs were sonicated for 1h. 0.05g. of gelatin mixed with 125  $\mu$ L H<sub>2</sub>O (0.625% gelatin) was heated for 3-5 min. at 37°C at a maximum stirring rate and then 2 mL acetone was added. Once when the pellet is formed acetone leftover was discarded and 125  $\mu$ L H<sub>2</sub>O is added. In order to gelatin pellet mixed with water dissolves completely it is heated again for 3-5 min. at 37°C at a maximum stirring rate. 1 M NaOH was added to adjust 12-13 pH. siRNA solution of different concentrations (2.5, 5, 10 and 20  $\mu$ L which is equal to 0.7125, 1.425, 2.85, 5.7  $\mu$ g siRNA, respectively) was added to solution and incubated for 10min. Previously sonicated 0.005 g of IONs with acetone and water is dropwise to a mixture. Lastly, 12  $\mu$ L 8% glutaraldehyde was added to a mixture to cross-link with gelatin's functional groups to decrease hydrodynamic size of ferrofluids. Solution is covered with with alumium folie. After 12 hours of incubation two times centrifugation of 15 min./12000 rpm was done and supernatant was collected.

### 3.5.1. Binding efficiency of siRNA to gelatin coated iron oxide nanoparticles

In literature, gelatin coated iron oxide nanoparticles were not found as a carrier for siRNAs.. In order to get high binding efficiency between siRNAs and nanoparticles of different siRNA concentration were used. To qualitatively determine siRNA loading efficiency to gelatin coated iron oxide nanoparticles Quant-iT™ RiboGreen® RNA kit was used. The use of Ribogreen kit helps to create a spectrophotometric slope of standard ribosomal RNAs kit isolated from the E. coli strain to be compared with iron oxide nanoparticles siRNA loading efficiency. The fluorometric intensities of these solutions were measured by spectrophotometer (AquaFluor, USA). Stock buffer of 15 mL was prepared using 200 mM, Tris-HCl, 20 mM EDTA together with RNA-free water (20XTE buffer) maintaining pH 7.5. Then, 750 µL of 20XTE buffer is diluted in 14.25 mL of RNA-free water. Quant-iT RiboGreen RNA dye was dissolved in 1mL DMSO. 50 µl of dye was taken from the stock and diluted in 9.950µL 20XTE buffer. RNA solutions were prepared at 4 different concentrations to generate standard slope:

1. 5 µL of E. coli RNA + 995 µL of buffer
2. 15 µL of E. coli RNA + 985 µL of buffer
3. 20 µL of E. coli RNA + 980 µL of buffer
4. 25 µL of E. coli RNA + 975µL of buffer

All different concentrations of RNA solution (1 mL) were interacted with 1 mL dye solution. The fluorometric intensities of these solutions were measured by spectrophotometer (AquaFluor, USA). Maximum intensity of Ribogreen dye interaction with RNA was expressed in 500 nm (excitation) and the maximum emission wavelength was 525 nm (emission) in regard to Ribogreen Kit standard measurements. The fluorometric intensity of standard RNAs and obtained different calibrations were represented on a chart. Using equation of calibration graph, the amount of siRNA in samples was calculated by substituting the fluorometric intensity equation given by the nanoparticle-siRNA (supernatant) samples. The result is the amount of siRNA which is not bound to nanoparticles. The unbound amount was subtracted from the starting siRNA amount to achieve % binding efficiency.

### 3.6. Preparation of CaCo-2 cell lines

All prepared nanoparticles and siRNA-loaded particles were transfected to CaCo-2 cancer cells to see their effect on cell viability. Additionally, biocompatibility tests of the same groups are performed healthy cells called L929 mouse fibroblast cells.

CaCo-2 colon cancer cells were grown in complete medium which is composed of RPMI supplement containing 20% Fetal Bovine Serum (FBS), 100 µg /mL streptomycin, 100 U/mL penicillin and 2 mM L-Glutamic acid. Placing into 96-cell well plates cells were incubated for 24 h at 37°C, in 5% CO<sub>2</sub> incubator Medium was microscopically analyzed every 24 hours to follow cell's growth cells and to make sure there are no fungal or bacterial contaminations. When cells reach 80-90% confluency 1/4 passage was done and cells were transferred to new flask. Upon cell multiplication, cell culture was treated with trypsin enzyme to de-touch from bottom of flask siRNAs prepared by dilution with RNase-free water and serum-free medium after loading to gelatin coated iron oxide nanoparticle were transfected into cancer cells. All biological analyzes were performed according to this transfection procedure.

Cell type	Colon from human, Caucasian colon adenocarcinoma (CaCo-2)
Petri dish	25 cm <sup>2</sup> polystyrene flask (T25), suitable for surface cell attachment
Cultural Property	Adherent
Routine subculture	1/4
Features of culture	Monolayer
Total volume	5 mL
pH	7.2-7.5
Temperature	37±0,5°C
Incubation medium	5 % CO <sub>2</sub> , incubator

**Table 3.1.** Environment of CaCo-2 cell lines



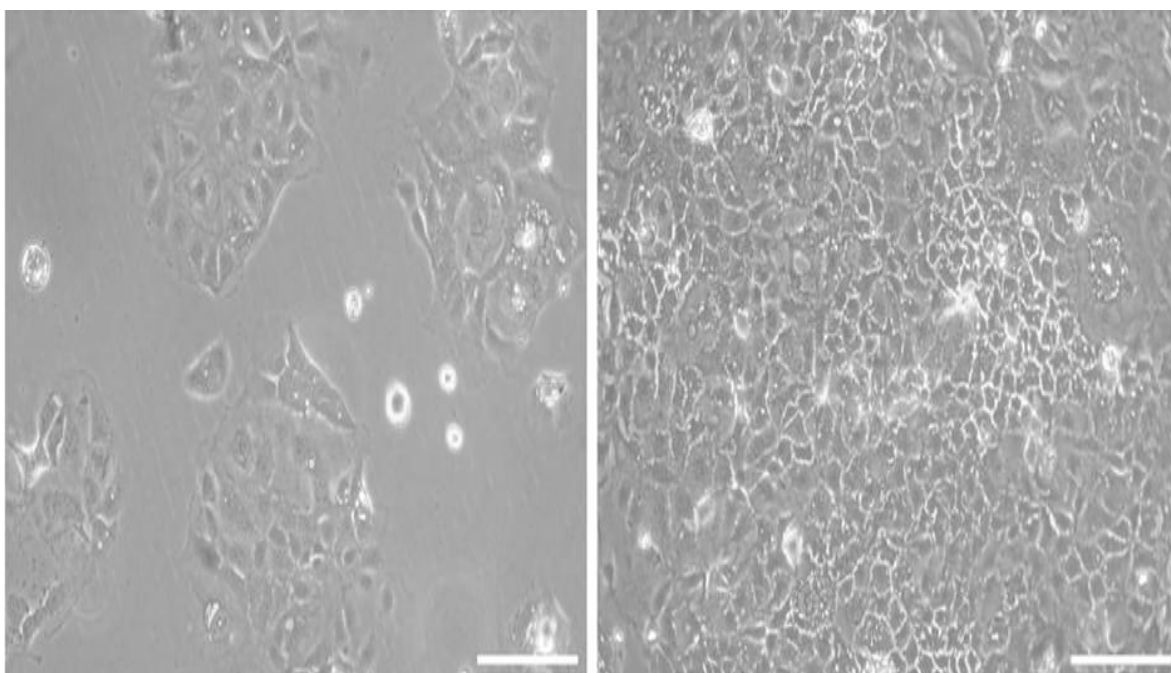


**Figure 3.3.** Image of CaCo-2 cells of low (left) and high density (right)

### **3.7. Interaction of siRNA loaded nanoparticles with CaCo-2 cancer cells**

To evaluate the cellular interaction of particles, both cancerous and non-cancerous cells, Caco-2 (human colorectal adenocarcinoma cells) and L929 (mouse fibroblast cells) were used. Prior to transfection, m-TOR siRNA was prepared according to manufacturer's instructions. Freeze-dried siRNA was diluted with 1 mL RNase-free water so that 20  $\mu\text{M}$  of stock siRNA solution was obtained. Further dilutions were carried out with serum-free RPMI. The cells ( $5 \times 10^3$  cells per well) were seeded in 96-well plates and left overnight in incubator for cell attachment. Next day, all experimental groups were ready for transfection. Bare magnetic gelatin nanoparticles at various concentrations (62,5 – 125- 250- 500  $\mu\text{g/mL}$ ) were prepared using completed cell medium. Naked siRNA and siRNA loaded nanoparticles were prepared at different amounts of siRNA; 0.7125-1.425-2.85-5.7  $\mu\text{g}$ . As a positive control, a liposomal nanocarrier HiperFect (Qiagen, Germany) was used. 0,75  $\mu\text{L}$  of HiperFect and siRNAs in serum free medium were incubated for complexation reaction and left in a rotor for 30 min. at room temperature. For siRNA transfections, firstly 40  $\mu\text{L}$  of solution with siRNA was added onto cells. After 1 hour of incubation time, 50  $\mu\text{L}$  of serum free RPMI was added.

Finally, after 2 hours 10  $\mu$ l of FBS was added reaching the final volume of per well to 100  $\mu$ L. The plates for both Caco-2 and L929 cells were left in incubator for 24 h and 48h for further cytotoxicity analysis.

### **3.7.1. Determination of CaCo-2 cells cytotoxicity**

The toxicity of bare nanoparticles, siRNA loaded nanoparticles, naked siRNA and Hiperfect-siRNA formulations on Caco-2 and L929 cells was examined using colorimetric test MTT.

Yellow MTT is reduced to purple formazan by mitochondrial dehydrogenase in the cell. Dye passes throughout the membrane of dead cells so they will appear purple due to the MTT formazan crystal formation. After 24 and 48 h of incubation time periods, the media in each well was removed and 90  $\mu$ L of fresh RPMI and 10  $\mu$ L MTT agent (5 mg/mL, diluted with PBS) were added onto cells. The plates were cover with foil and incubated for 4 hours at 37°C and 5 % CO<sub>2</sub> humidified atmosphere conditions. Next, the MTT solution was replaced with 100  $\mu$ L of acidic isopropanol (0,04 M HCl included isopropanol). To dissolve the formazyl crystals with isopropanol, the foil-covered plates were left for additional 30 min. at room temperature. The absorbance measurements were conducted via ELISA microplate reader at 570 nm. . The MTT test was run in 5 replicates for each test group and control group. Unlike uncoated iron oxide nanoparticles, gelatin coated IONs are expected to be internalized to the cell without damaging cell morphology and maintaining cell viability.

## **4. EXPERIMENTAL RESULTS AND DISCUSSION**

Within the scope of this work, gelatin coated iron oxide nanoparticles were synthesized and characterized to be used in siRNA therapy. Gelatin because of its solubility, biodegradability, high biocompatibility and presence of functional groups in its structure have been chosen as a perfect candidate for cancer therapy [2]. After work was done by Massart R. et al, co-precipitation procedures became well used because of its simplicity, low-cost production and ease surface treatment with other materials. Iron oxide nanoparticles were synthesized using co-precipitation of FeCl<sub>2</sub>·4H<sub>2</sub>O and FeCl<sub>3</sub>·6H<sub>2</sub>O in the ratio of 1 : 2 together with precipitant sodium hydroxide. In order to get the best possible size and charge of nanoparticles, different parameters were examined.

#### 4.1. Characterization of iron oxide nanoparticles

For prepared iron oxide nanoparticles; size distribution, surface charge and morphology were examined and characterized.

##### 4.1.1. Morphological characterization of nanoparticles

SEM, scanning electron microscopy, was used to see morphology, geometry, surface and cross-sectional structure of obtained iron oxide nanoparticles. From obtained images clearly it could be seen whether nanoparticles are aggregated or having well dispersed, monodispersed morphology of size. If IONs are agglomerated, it is assumed to be due to the Van der Waals attraction force that occurs between particles [38].

Obtained SEM images showed that predominant particle morphology is containing clusters where each cluster of iron oxide nanoparticles is having a size around 60 nm, a cluster of gelatin coated iron oxide nanoparticles is having size around 75 nm and clusters of gelatin nanoparticles were having size of approximately 120 nm.

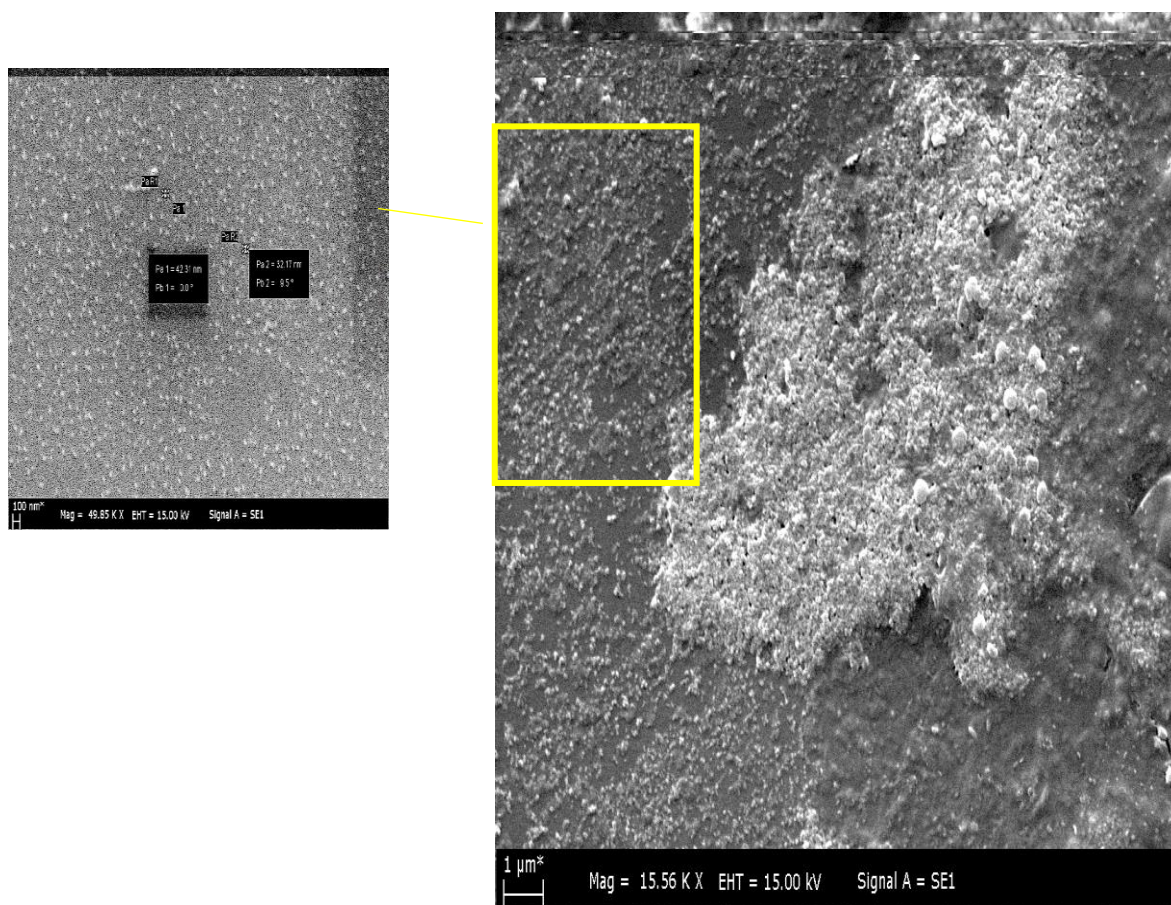


**Figure 4.1.** Morphological characterization of iron oxide nanoparticles



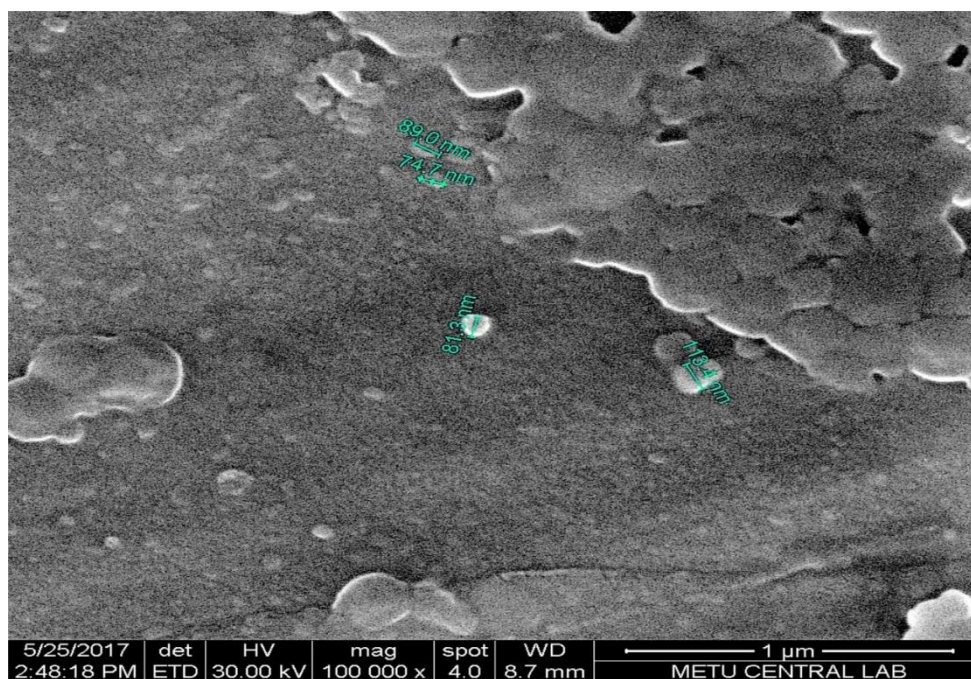


**Figure 4.2.** Morphological characterization of gelatin nanoparticles

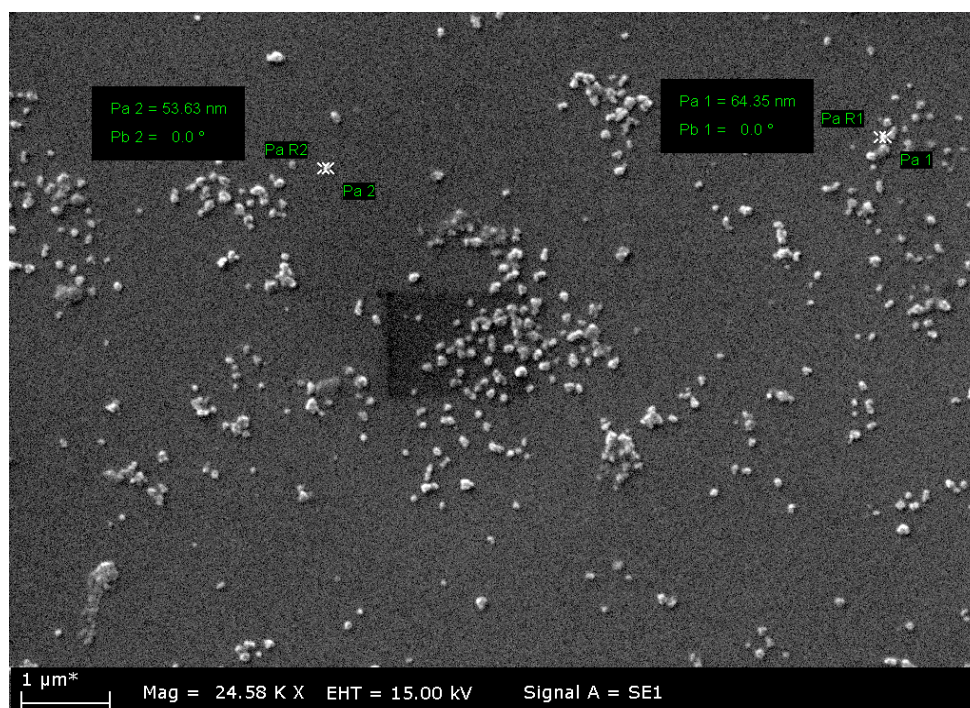


**Figure 4.3.** Morphological characterization of gelatin coated iron oxide nanoparticles

#### 4.1.2. Size and PDI analysis of iron oxide nanoparticles

As previously mentioned ferrous and ferric salt were precipitated with 1 M of NaOH. Together with iron salts 0.16 M of HCl was used to gettin as a final result nanoparticles of an around 60 nm. In order to getting preferred size of iron oxide nanoparticles, different concentration of NaOH and HCl were examined. Influence of ethanol and distilled water in washing outs, as well as influence of air and N<sub>2</sub> atmosphere on a hydrodynamic size and PDI of the colloidal dispersions, were examined.

##### 4.1.2.1. Effect of NaOH concentration on size and PDI of iron oxide nanoparticle

As mentioned before, NaOH was used as a source of anion solution. The concentration of NaOH in following manner 0.9, 1, 1.1, 1.2, 1.3, 1.4, 1.5 M was tested to see its effect on the hydrodynamic size of iron oxide nanoparticles When in interaction with a cationic solution of iron salts the concentration of 1M NaOH was shown to give an optimal size of approximately 60 nm..

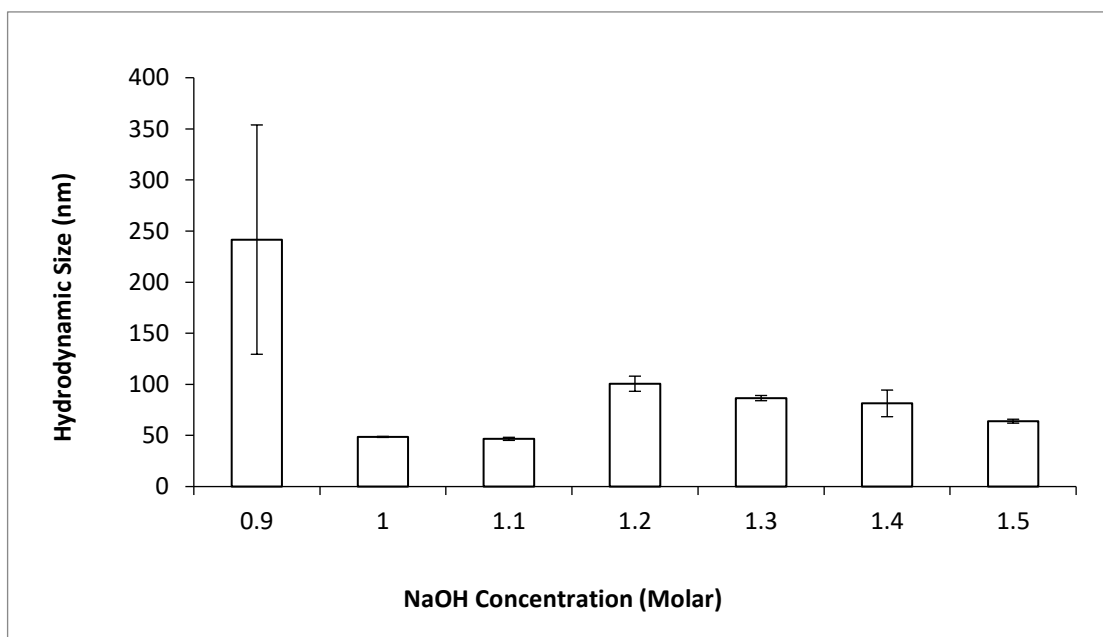


**Figure 4.4.** Concentration of NaOH and its effect on hydrodynamic size of iron oxide nanoparticles

Also, different concentrations of NaOH 0.9, 1, 1.1, 1.2, 1.3, 1.4, 1.5 M were tested to see its effect on PDI (polydispersion index) of iron oxide nanoparticles.

Both, hydrodynamic size and PDI are preferable when 1M NaOH is used in iron oxide nanoparticles synthesis. When compared with PDI of other NaOH concentrations PDI of 0.190 obtained when using 1M NaOH was shown as the best result.

NaOH conc. (M)	0.9	1	1.1	1.2	1.3	1.4	1.5
PDI	0.9123 ± 0.1518	0.1903 ± 0.0045	0.2603 ± 0.0432	0.2693 ± 0.0720	0.3693 ± 0.0825	0.3073 ± 0.0645	0.3117 ± 0.0295

**Table 4.1.** Concentration of NaOH and its effect on PDI of iron oxide nanoparticles

#### 4.1.2.2. Effect of HCl concentration on size and PDI of iron oxide nanoparticles

In order to get the a preferable result, 0.08, 0.16 and 0.32 M HCl concentrations were tested to see its effect on the hydrodynamic size and PDI of iron oxide nanoparticles. Obtained results confirm that optimal size of iron oxide nanoparticle is gained using 0.16 M HCl when all other protocol parameters were being fixed as stated before. The size of 48.57 nm was obtained using 0.16 M HCl when compared with the size of 60.22 nm using 0.08M HCl or size of 5591.33 nm vwhen using 0.32M HCl was remarkable and much more preferable.

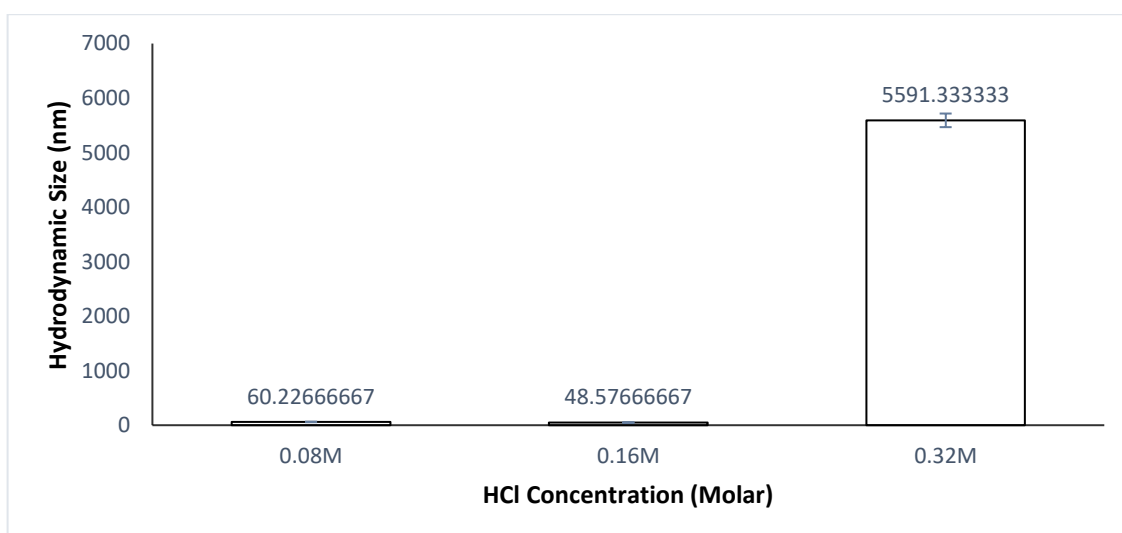


**Figure 4.5.** Concentration of HCl and its effect on hydrodynamic size of iron oxide nanoparticles

In the same way, 0.08, 0.16 and 0.32 M HCl concentrations were tested to see its effect on PDI of iron oxide nanoparticles. Obtained results confirm that optimal size of iron oxide nanoparticle is gained using 0.16 M HCl when all other protocol parameters were being fixed as stated before. When compared with PDI of 0.2573 using 0.08 M HCl or PDI of 1 when using 0.32 M HCl, PDI of 0.1903 obtained using 0.16 M HCl was remarkable and much more preferable.

HCl concen. (M)	<b>0.008</b>	<b>0.16</b>	<b>0.32</b>
PDI	0.2573+0.0850	0.1903+0.0045	1+0

**Table 4.2.** Concentration of HCl and its effect on PDI of iron oxide nanoparticles

#### 4.1.2.3. Effect of atmospheric and N<sub>2</sub> environment on size and PDI of iron oxide nanoparticles

Massart's method proposes adding a base to FeCl<sub>2</sub>·4H<sub>2</sub>O and FeCl<sub>3</sub>·6H<sub>2</sub>O solution in the ratio of 1 : 2 in an inert atmosphere of nitrogen gas to get an acceptable result [60]. As it is shown in Figure 4.6, iron oxide nanoparticles synthesised in air atmosphere are bigger in size when compared with those obtained under N<sub>2</sub> gas. The size of 266.59 nm is obtained when iron oxide synthesis is performed without N<sub>2</sub> gas while on the other side size of 48.57 nm was obtained when using N<sub>2</sub> gas. This is a strong indicator that iron oxide nanoparticles tend to aggregate when N<sub>2</sub> gas is absent.

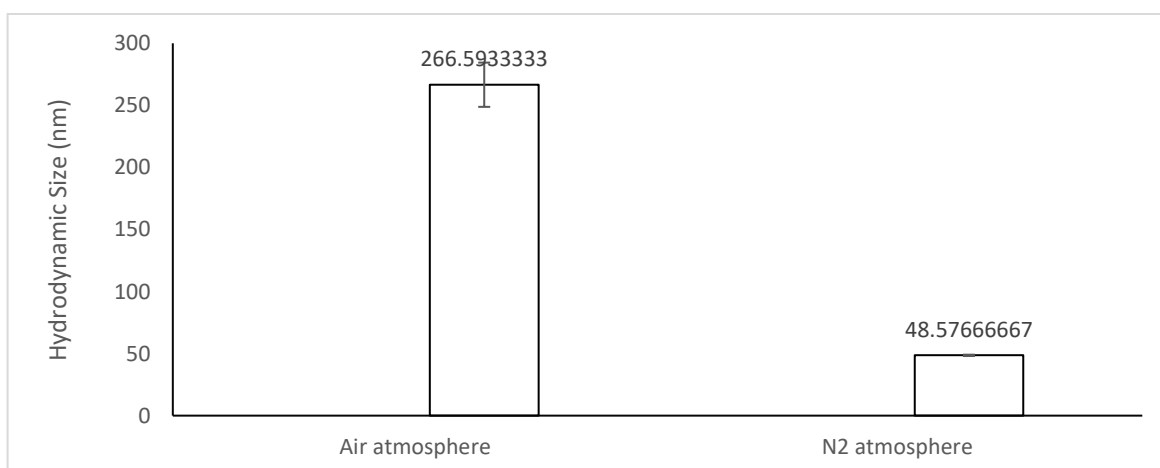


**Figure 4.6.** Effect of air and N<sub>2</sub> atmosphere on hydrodynamic size of iron oxide nanoparticles

Also, iron oxide nanoparticles when synthesised in air atmosphere are having larger PDI when compared with those obtained under N<sub>2</sub> gas. PDI of 0.94 is obtained when iron oxide synthesis is performed without N<sub>2</sub> gas while on the other side PDI of 0.1903 was obtained when using N<sub>2</sub> gas. This is a strong indicator that iron oxide nanoparticles tend to aggregate and cluster when N<sub>2</sub> gas is absent.

	Atmosphere	N <sub>2</sub> gas
PDI	0.94 ± 0.0549	0.1903±0.00450

**Table 4.3.** Effect of air and N<sub>2</sub> atmosphere on PDI of iron oxide nanoparticles

#### 4.1.2.4. Effect of distilled water and ethanol on size and PDI of iron oxide nanoparticles

After completing synthesis reaction and leaving iron oxide solution under N<sub>2</sub> gas on a magnetic stirrer at maximum stirring rate and temperature of 85 °C for one-hour washing out of iron oxide nanoparticles was performed. In two separate experiments washing out was performed with distilled water and with ethanol to see the effect on a size of nanoparticles. In ethanol washing outs nanoparticles of approximately 173 nm were yielded where on the other side washing outs with distilled water gave a size of nanoparticles around 49 nm. From that moment on every next experiment is performed with distilled water washing outs.

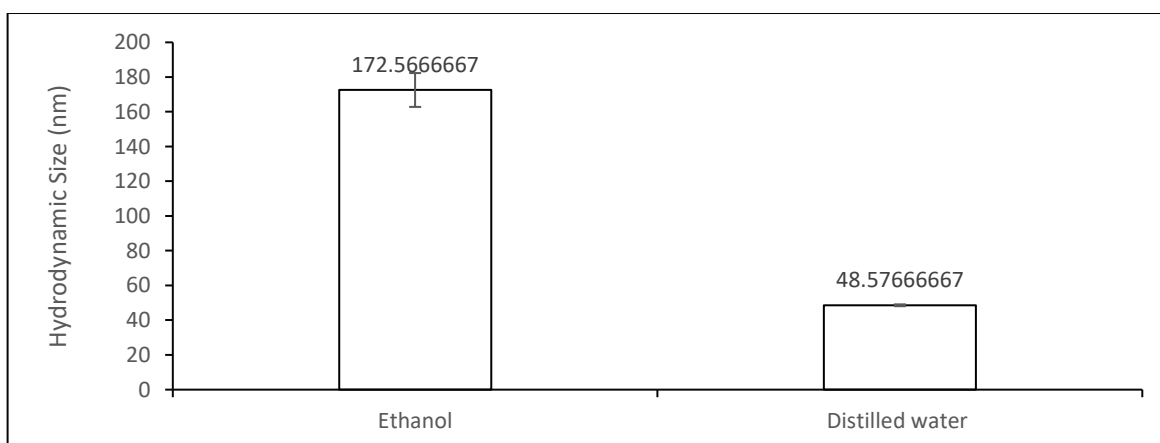


**Figure 4.7.** Effect of ethanol and distilled water on hydrodynamic size of iron oxide nanoparticles



In washing outs using ethanol nanoparticles of approximately 0.278 PDI were yielded where on the other side with distilled water PDI of nanoparticles were around 0.1903.

	<b>Ethanol</b>	<b>Distilled water</b>
<b>PDI</b>	0.278 ± 0.0282	0.1903 ± 0.00450

**Table 4.4.** Effect of ethanol and distilled water on PDI of iron oxide nanoparticles

#### **4.1.3. Size and PDI analysis of gelatin coated iron oxide nanoparticles (GIONs)**

After optimizing iron oxide nanoparticles and obtaining best possible result coating of synthesized iron oxide nanoparticles with gelatin was done using desalvation process. The coating is performed to stabilize solution and to reduce a size of a obtained nanoparticles complex. Parameters such as iron oxide nanoparticles amount, glutaraldehyde concentration and gelatin concentration were slightly changed in order to get the smaller hydrodynamic size and acceptable PDI value of gelatin coated iron oxide nanoparticles. 199.43 nm is noted as most preferable hydrodynamic size result. It is obtained when 1.250 mL acetone and 1.250 mL H<sub>2</sub>O together with 0.005 g IONs were sonicated for 1h. Then, 0.05 g of gelatin was mixed with 125 μL H<sub>2</sub>O (0.625% gelatin) and heated for 3-5 min. at 37°C at a maximum stirring rate in order to get a completely dissolved mixture. The mixture is transferred to a stirrer to add 2 mL of acetone. When the pellet is formed acetone leftover was discarded and again 125 μL H<sub>2</sub>O is added. In order to gelatin pellet mixed completely dissolves, it was heated for about 3-5 min. at 37°C. 1 drop of 1M NaOH was added to adjust 12-13 pH. Previously sonicated IONs with acetone and water was dropwise to a mixture while being stirred at rate 7. Lastly, 12 μL 8% glutaraldehyde was added to a mixture in order to crosslink and decrease a hydrodynamic size of ferrofluids.

#### 4.1.3.1. Effect of certain amount of iron oxide nanoparticles on size and PDI of gelatin coated iron oxide nanoparticles

Synthesized iron oxide nanoparticles were lyophilized in order to continue with a coating. IONs of 0.0025, 0.0015, 0.05 and 0.01 g were examined in order to see which one will give smallest hydrodynamic size when all other parameters were stable. Among all used amount of IONs, the minimum size of 319.91 nm was obtained when 0.05 g iron oxide nanoparticles were used. According to this result, in following experiments 0.05 g of iron oxide nanoparticles were used to get an even smaller size of nanoparticles.

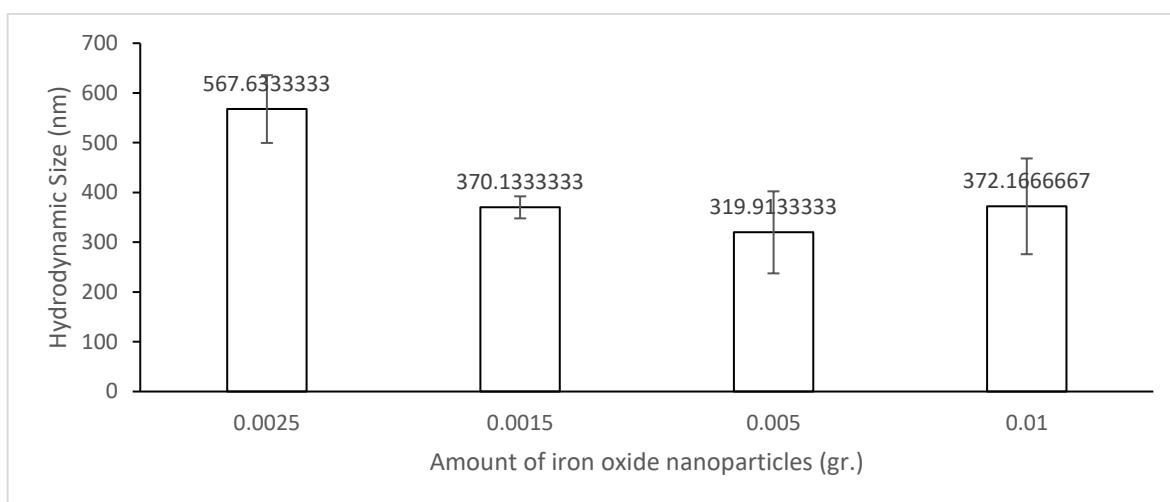


**Figure 4.8.** Amount of iron oxide nanoparticles and its effect on hydrodynamic size of gelatin coated iron oxide nanoparticles

In same manner, PDI value of synthesized iron oxide nanoparticles was examined when different amount of IONs were used. As shown in Table 4.5. a preferable PDI of 0.244 obtained when 0.005 g of IONs were used.

IONs (g)	0.0015	0.0025	0.005	0.01
PDI	0.484 ± 0.014	0.508 ± 0.418	0.244 ± 0.011	0.477 ± 0.138

**Table 4.5.** Effect of different amounts of IONs on PDI of gelatin coated iron oxide nanoparticles

#### 4.1.3.2. Effect of glutaraldehyde concentration on size and PDI of gelatin coated iron oxide nanoparticles size

Proper ratio adjustment of acetone as a desolvation agent and glutaraldehyde as a crosslinker resulted in better stability of obtained ferrofluid solution. In the following graph, different concentration of 2, 4, 6 and 8% glutaraldehyde were examined to be able to yield gelatin coated iron oxide nanoparticles with smallest hydrodynamic size. Glutaraldehyde of 8% was showing an acceptable hydrodynamic size of 255.26 nm when compared with other where results were above 300 nm [37]. In order to decrease a hydrodynamic size of ferrofluids 8% glutaraldehyde was used.

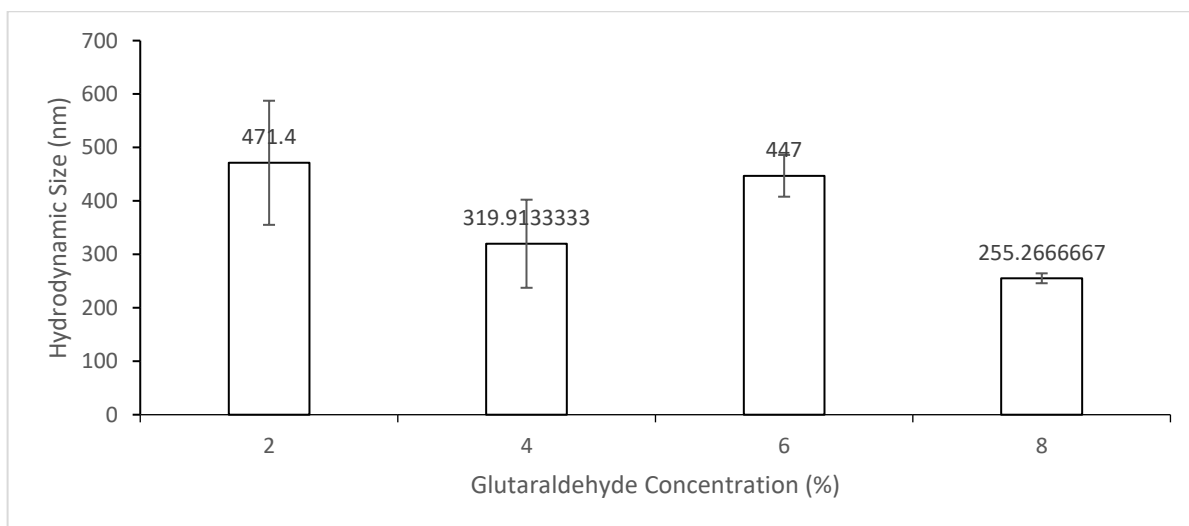


**Figure 4.9.** Glutaraldehyde concentration and its effect on hydrodynamic size of gelatin coated iron oxide nanoparticles

As for the size, also for PDI 2, 4, 6, 8% of glutaraldehyde were examined to see which one will give the best result. PDI of 0.244 was obtained when using 8% glutaraldehyde which is when compared with other glutaraldehyde concentrations the most acceptable one for protocol proceeding.

<b>GA concen.(%)</b>	<b>2</b>	<b>4</b>	<b>6</b>	<b>8</b>
<b>PDI</b>	0.297 ± 0.116	0.518 ± 0.045	0.368 ± 0.070	0.244 ± 0.011

**Table 4.6.** Effect of different GA concentrations on PDI of gelatin coated iron oxide nanoparticles

#### 4.1.3.3. Effect of gelatin concentration on size and PDI of gelatin coated iron oxide nanoparticles

When aiming to decrease the hydrodynamic size of ferrofluids 0.625% gelatin concentration was used. In the following graph, different concentration of 5, 2.5, 1.25 and 0.625% gelatin were examined to be able to yield gelatin coated iron oxide nanoparticles with smallest hydrodynamic size. Gelatin concentration of 0.625% was showing the acceptable hydrodynamic size of 199.43 nm when compared with other gelatin concentrations.

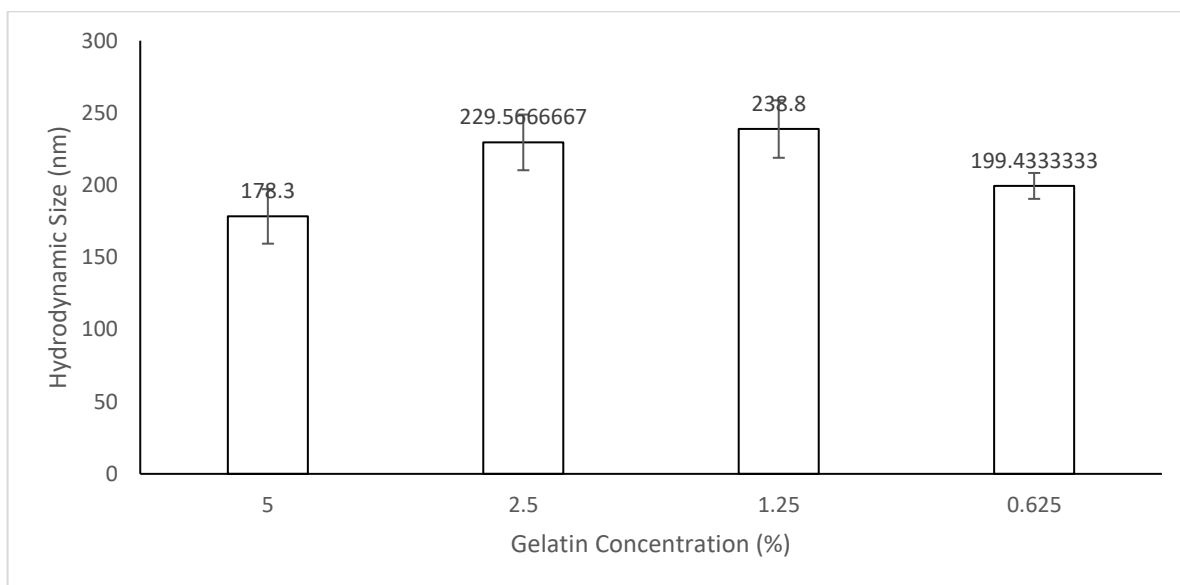


**Figure 4.10.** Gelatin concentration and its effect on hydrodynamic size of gelatin coated iron oxide nanoparticles

In the same way, 5, 2.5, 1.25 and 0.625% gelatin concentrations were tested to see its effect on PDI of gelatin coated iron oxide nanoparticles. Obtained results confirm that optimal size of gelatin coated iron oxide nanoparticle is gained using 0.625% gelatin concentration when all other protocol parameters were being fixed as stated before. When compared with PDI of 0.709 using 5% gelatin or PDI of 0.247 when using 1.25% gelatin, PDI of 0.213 obtained using 0.625% gelatin concentration was remarkable and much more preferable.

<b>Gelatin con.%)</b>	<b>5</b>	<b>2.5</b>	<b>1.25</b>	<b>0.625</b>
<b>PDI</b>	0.709 ± 0.055	0.295 ± 0.054	0.247 ± 0.010	0.213 ± 0.013

**Table 4.7.** Effect of different gelatin concentrations on PDI of gelatin coated iron oxide nanoparticles

#### **4.1.4. Short term stability test for nanoparticles**

After optimizining iron oxide nanoparticles and gelatin coated iron oxide nanoparticles size and charge were examined for 30 days to see if the major change in size and charge will occur. After 30 days it is seen that major change has happened in size of iron oxide nanoparticle when compared with the size of gelatin coated iron oxide nanoparticles.

##### **4.1.4.1. Short term stability test for iron oxide nanoparticles**

After 30 days IONs best possible size of 48.57 nm was increased size over 300 nm. It indicates that naked iron oxide nanoparticles are unstable and prone to aggregation if not coated.

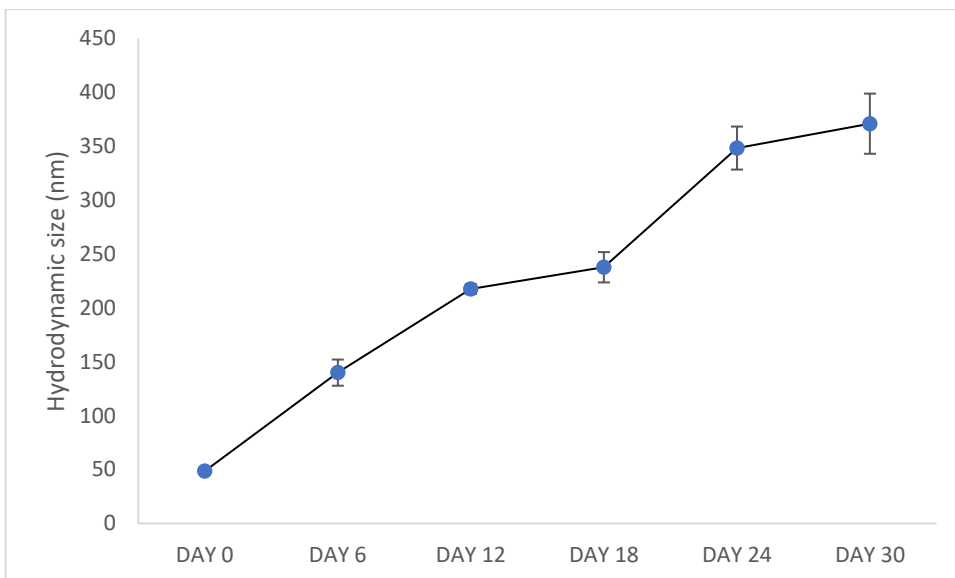


**Figure 4.11.** Hydrodynamic size of iron oxide nanoparticles in span of 30 days

After 30 days of examination charge of iron oxide nanoparticles have slightly decreased from -30.86 mV to 21.76 mV. It indicates that naked iron oxide nanoparticles are unstable and prone to aggregation if not coated.

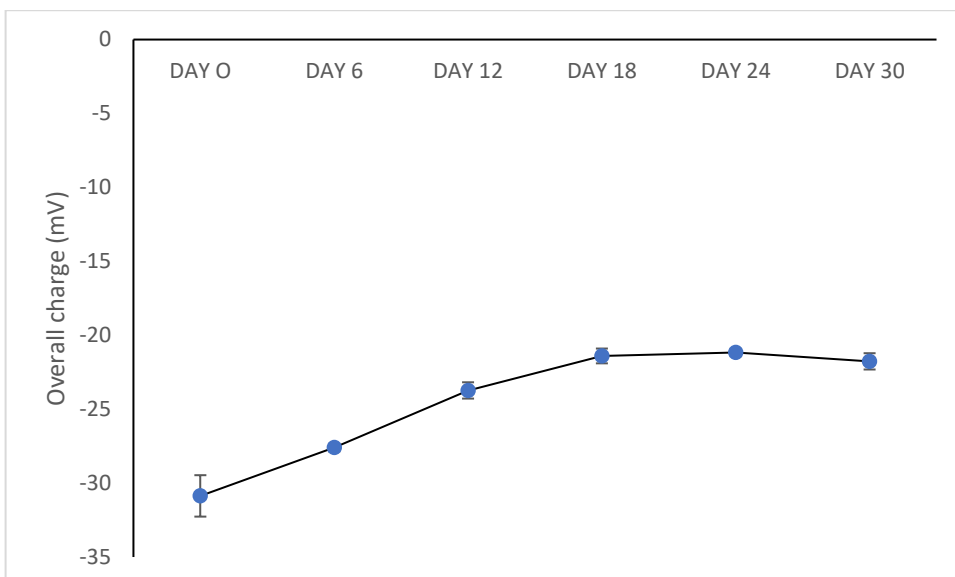


**Figure 4.12.** Charge result of iron oxide nanoparticles in span of 30 days

#### 4.1.4.2. Short term stability test for gelatin coated iron oxide nanoparticles

To increase and improve the stability of iron oxide nanoparticles it was coated with a biological polymer, gelatin. After 30 days best possible size result of iron oxide nanoparticles of 174.13 nm has slightly increased to over 200 nm. It indicates that coated iron oxide nanoparticles are being more stable and less prone to aggregation when compared with naked iron oxide nanoparticles.

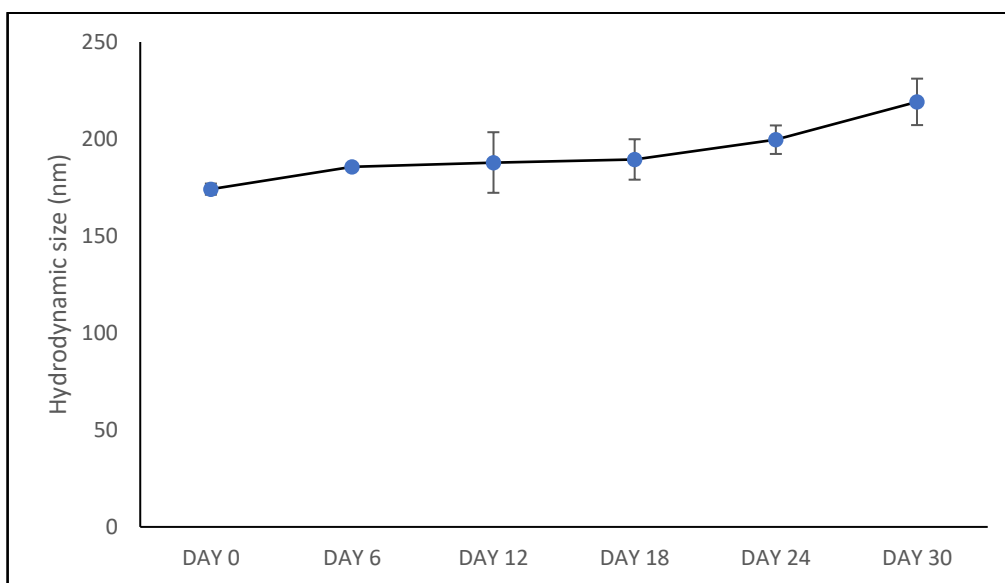


**Figure 4.13.** Size of gelatin coated iron oxide nanoparticles examined for 30 days

After 30 days of examination charge of gelatin coated iron oxide nanoparticles have increased from -2.22 mV to 1.44 mV. It indicates that coated iron oxide nanoparticles are much more stable and tend not to aggregate when compared with naked IONs.

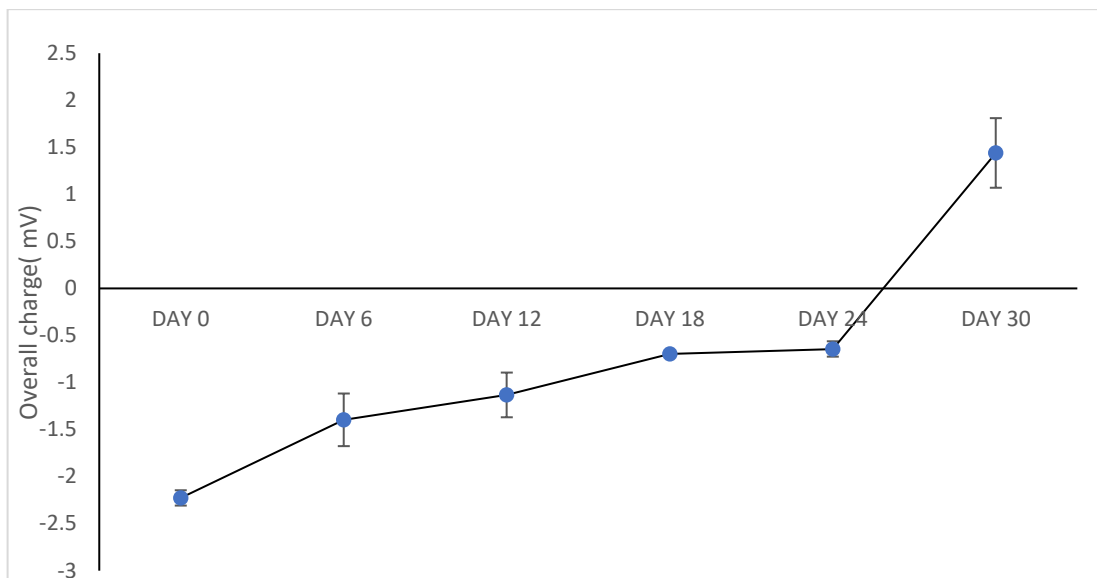


**Figure 4.14.** Charge result of gelatin coated iron oxide nanoparticles in span of 30 days

#### 4.1.5. Chemical structure determination of nanoparticles

Fourier Transform Infrared Spectroscopy (FTIR) (Nicolet iS10, USA) is used to determine molecular bond characterization and functional group analysis of the sample for compound comparison. FTIR characterization has been performed for iron oxide nanoparticles, gelatin nanoparticles and gelatin coated iron oxide nanoparticles. Obtained FT-IR spectrum peaks have proven existence of gelatin polymer on the surface of iron oxide nanoparticles.

##### 4.1.5.1 FTIR of iron oxide nanoparticles

In obtained FTIR spectra for iron oxide nanoparticles, a peak of around  $650\text{ cm}^{-1}$  indicates magnetite composite followed with a sharp peak which matches to the Fe-O chemical bond of the nanoparticles [39]. Similarly, in the study of Gaihre B., et al., it is stated that characteristic FTIR peaks for iron oxide nanoparticles are positions at  $580$  and  $400\text{ cm}^{-1}$  [40].



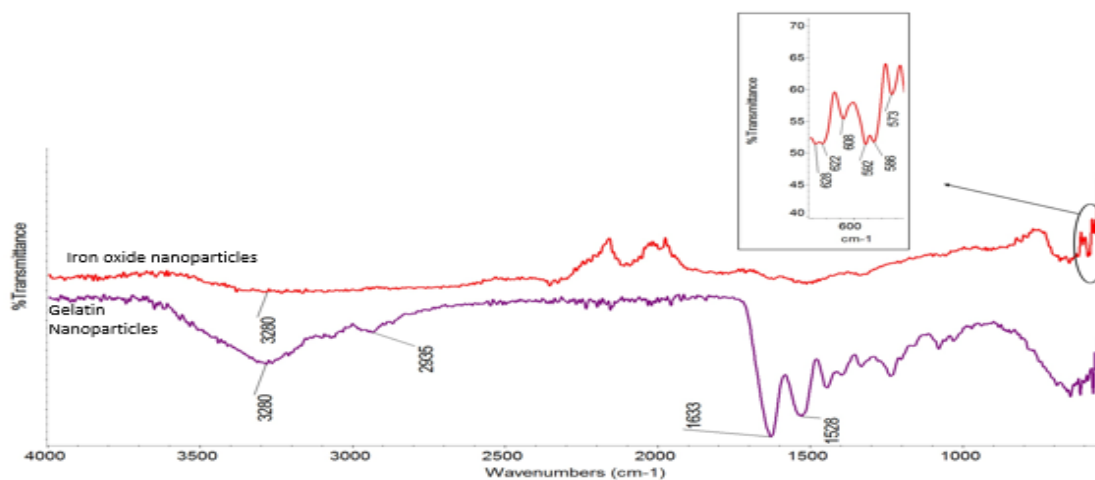


**Figure 4.15.** FTIR spectra of iron oxide nanoparticles and gelatin nanoparticles

#### 4.1.5.2. FTIR of gelatin nanoparticles

Gelatin nanoparticles are having few peaks which are matching with Amide A, Amide B, Amide I, Amide II and Amide III. Gelatin nanoparticles are composed of almost five C=O stretchings. N-H deformation of Amide III is part of C=O stretching of Amide I. As shown in Table 4.5. Amide II assigning N-H deformation is seen at  $1560\text{ cm}^{-1}$ , while Amide I is representing C=O stretching and is found at  $1670\text{ cm}^{-1}$  [39]. As shown in the study of Gaihre B., et al., FT-IR spectrum speaks at  $3200\text{--}3600\text{ cm}^{-1}$  are showing N-H and O-H bonding [23].

Gelatin peaks		Peaks for gelatin $\text{cm}^{-1}$
Amide A	N-H stretching	3300–3500
Amide B	C-H stretching	3064
Amide I	C=O stretching	1670
Amide II	N-H deformation	1560
Amide III	C-N stretching	1020–1220
	N-H deformation	2400–3200

**Table 4.8.** FTIR spectra peaks for gelatin [39].

#### 4.1.5.3. FTIR of gelatin coated iron oxide nanoparticles

In line with study Gaihre B., et al., FT-IR spectrum peaks of gelatin nanoparticles for amide I at  $1670\text{ cm}^{-1}$  and amide II at  $1560\text{ cm}^{-1}$  were shifted after interacting with iron oxide nanoparticles. After interaction peak for amide I is noticed at  $1643\text{ cm}^{-1}$  and peak for amide II was seen at  $1517\text{ cm}^{-1}$ . In obtained FT-IR spectrum of gelatin coated iron oxide nanoparticles peaks seen at  $602\text{ cm}^{-1}$  and  $591\text{ cm}^{-1}$  are assigned to iron oxide nanoparticles [40].

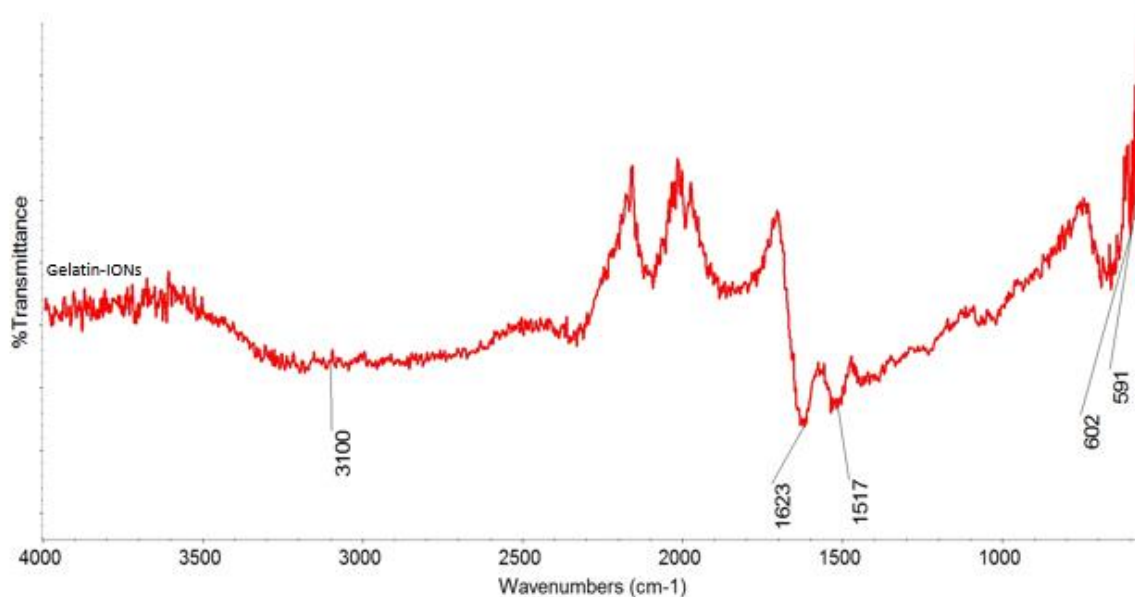


**Figure 4.16.** FTIR spectra of gelatin coated iron oxide nanoparticles

#### 4.1.6. Determination of magnetic properties

To determine magnetic properties of prepared iron oxide nanoparticles and gelatin coated iron oxide nanoparticles VSM (vibrating sample magnetometer) and ESR (electron spin resonance) characterization has been performed. The magnetic properties of the particles in the magnetic field are expressed in units of magnetic force (emu).

##### 4.1.6.1. Results of VSM

In vibrating sample magnetometer (VSM) magnetic saturation curve of iron oxide nanoparticles against the magnetic field is shown. All of the magnetic moments in magnetic particle are directed in the applied field direction. VSM curves were made using Origin 9.0 drawing program.

For both samples, mass normalization was done, for gelatin coated iron oxide nanoparticles 1 g and for iron oxide nanoparticles 3.1 g. In order to fully understand magnetic properties samples were examined in magnetic field scale of 20000 – 20000 Oe. VSM characterization results revealed super paramagnetic properties.

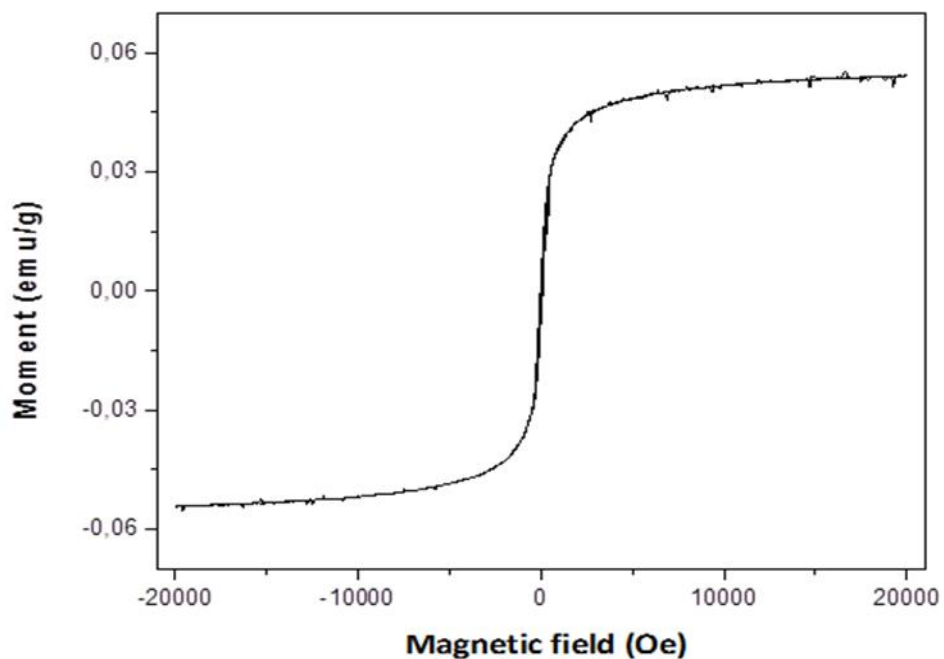


**Figure 4.17.** VSM results of iron oxide nanoparticles

As iron oxide nanoparticles were coated with gelatin, magnetic saturation decreased as a polymeric layer entered between the magnetic units.

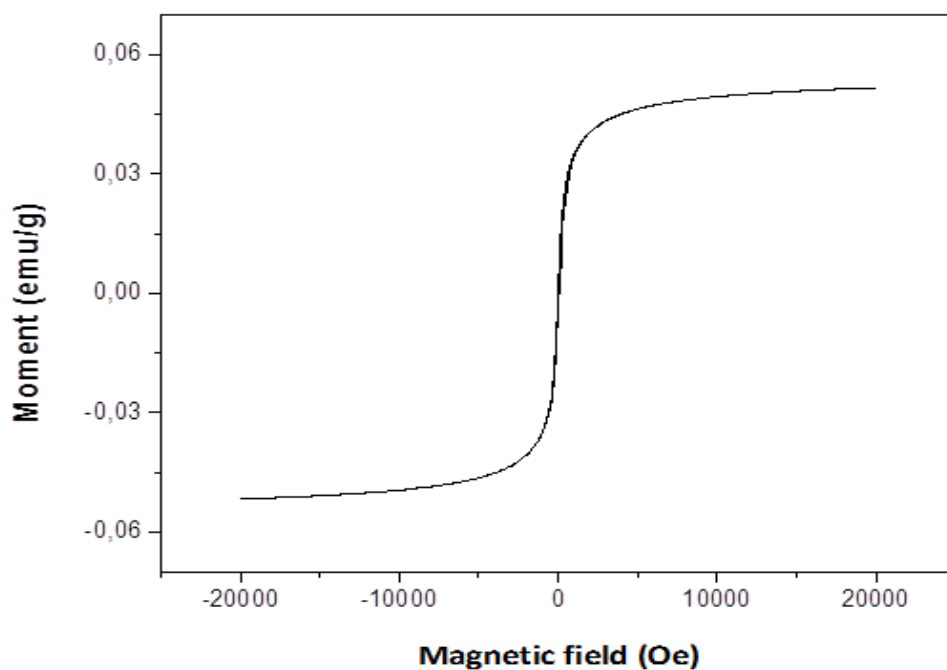


**Figure 4.18.** VSM results of gelatin coated iron oxide nanoparticles

#### 4.1.6.2. Results of ESR

The ESR spectrum peak of Fe<sub>3</sub>O<sub>4</sub> and Fe<sub>3</sub>O<sub>4</sub> gelatin coated nanoparticles is asymmetric resonance curve.

Central Area	270 mT
Sweeping Area	500 mT
Microwave Frequency	9.78 GHz
Microwave Power	0.1 mW
Modulation Frequency	100 kHz
Modulation Amplitude	1 G
Sweep Time	83.89 s
Fixed Time	81.92 s
Time of Conversion	163.84
Temperature	Room Temperature

**Table 4.9.** ESR spectrometer operating conditions

	Spectroscopic splitting factor (g)	Top-to-top line width ( $\Delta H_{pp}$ )
Iron oxide nanoparticles	$g = 2.592$	$\Delta H_{pp} \cong 113 \text{ mT}$
Gelatin coated IONs	$g = 2.409$	$\Delta H_{pp} \cong 125 \text{ mT}$

**Table 4.10.** ESR spectral parameters

According to g-value in obtained ESR results it can be said that samples are having super paramagnetic properties containing  $\text{Fe}^{+3}$  complex in its structure.

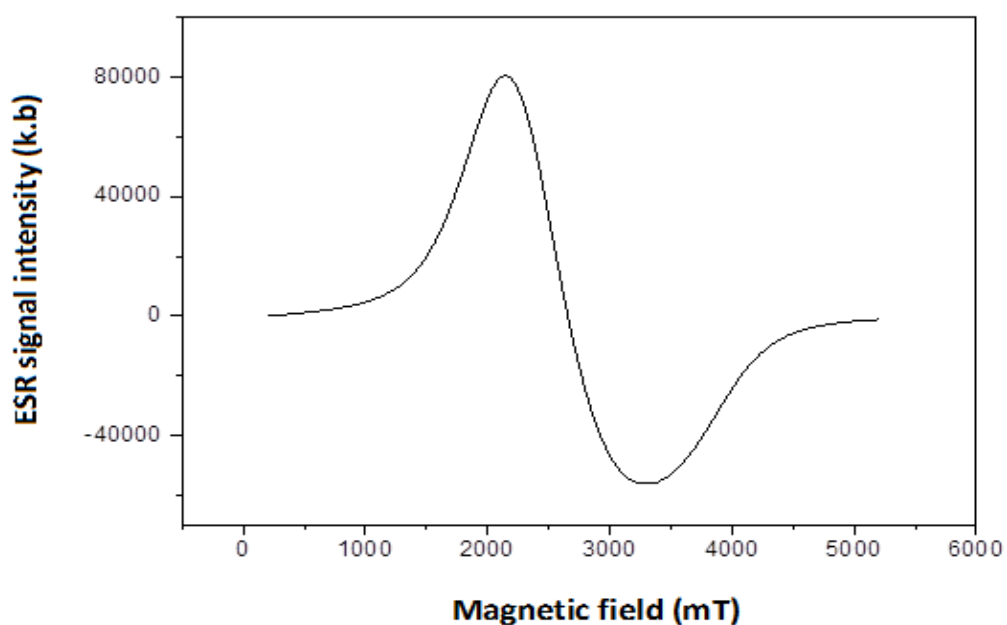


**Figure 4.19.** ESR results of iron oxide nanoparticles

ESR signal of iron oxide nanoparticles is having 10 times higher intensity than ESR signal of gelatin coated iron oxide nanoparticles. This difference can be assigned to fact that coating with the dimagnetic material is decreasing magnetic properties.

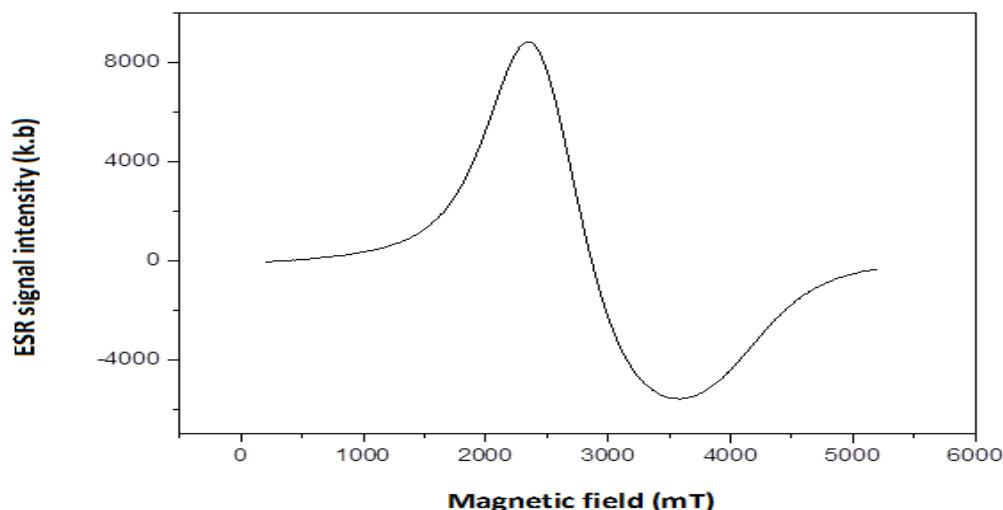


**Figure 4.20.** ESR results of gelatin coated iron oxide nanoparticles

#### 4.2. Results of binding efficiency of siRNA to gelatin coated iron oxide nanoparticles

Coating iron oxide nanoparticles with gelatin by two desolvation process, loading of siRNA to nano platform have to be confirmed with spectrophlometer. Beside our samples, for binding efficiency test Ribogreen kit standards were prepared in following manner:

Sample	Binding Efficiency (%)
Gelatin IONs + siRNA (2,5µL= 0,625 µg)	18,45 ± 1,34
Gelatin IONs + siRNA (5 µL =1,25 µg)	22,08 ± 1,67
Gelatin IONs + siRNA (10 µL = 2,5 µg)	33,77 ± 1,39
Gelatin IONs + siRNA (20 µL = 5 µg)	41,50 ± 1,05

**Table 4.11.** The biniding efficiency (%) of gelatin coated IONs with different siRNA amounts

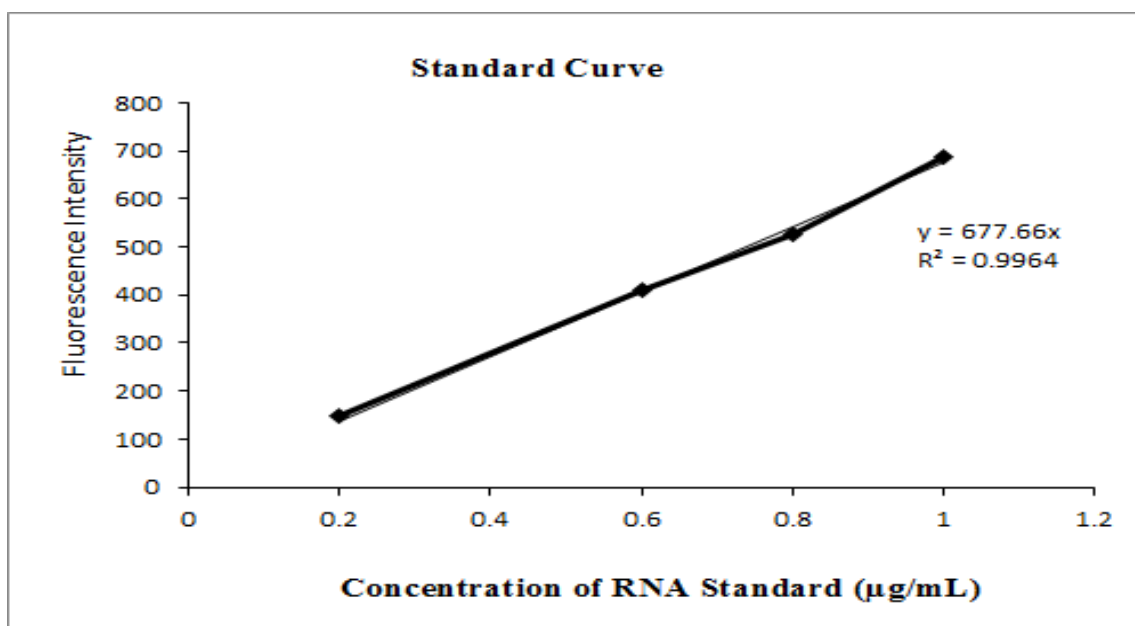


**Figure 4.21.** Calibration curve of RNA standard

Maximum intensity of Ribogreen dye interaction with RNA was expressed in 500 nm (excitation) and the maximum emission wavelength was 525 nm (emission) in regard to Ribogreen Kit standard measurements. The fluorometric intensity of standard RNAs and obtained different calibrations were represented on a charts. According to standard curve the concentration of unbounded siRNA was calculated. The highest binding efficiency 41% was obtained when 5 µg siRNA was used.

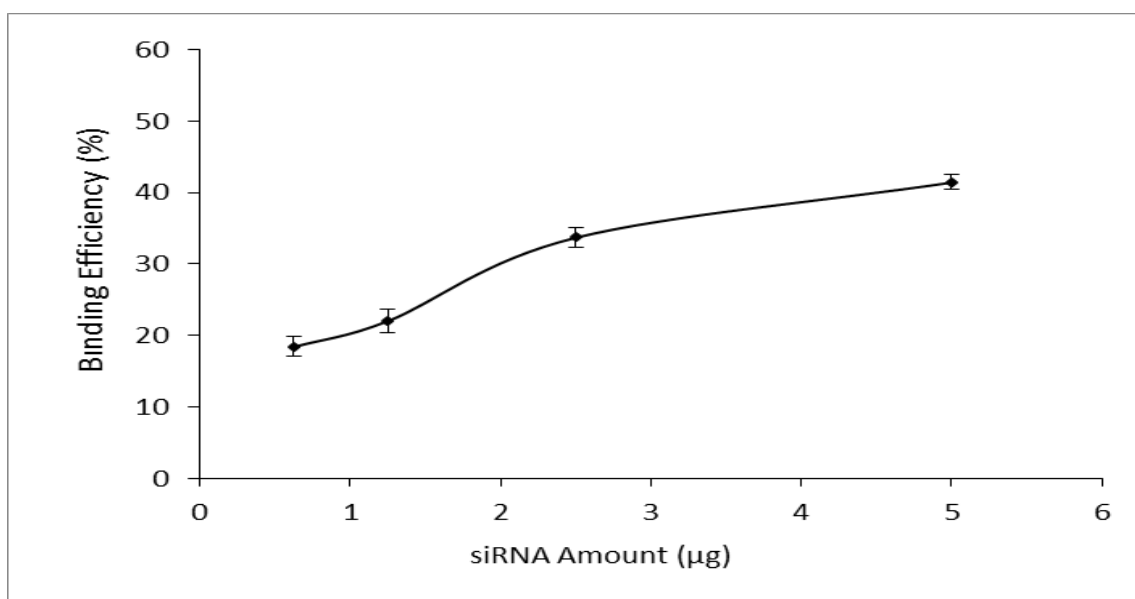


**Figure 4.22.** The binding efficiency (%) of siRNA to gelatin coated iron oxide nanoparticles

### 4.3. Determination of CaCo-2 cell cytotoxicity

To examine the effect on cell viability, prepared siRNA loaded gelatin coated iron oxide nanoparticles were transfected to CaCo-2 colon cancer cell and L929 mouse fibroblast healthy cells.

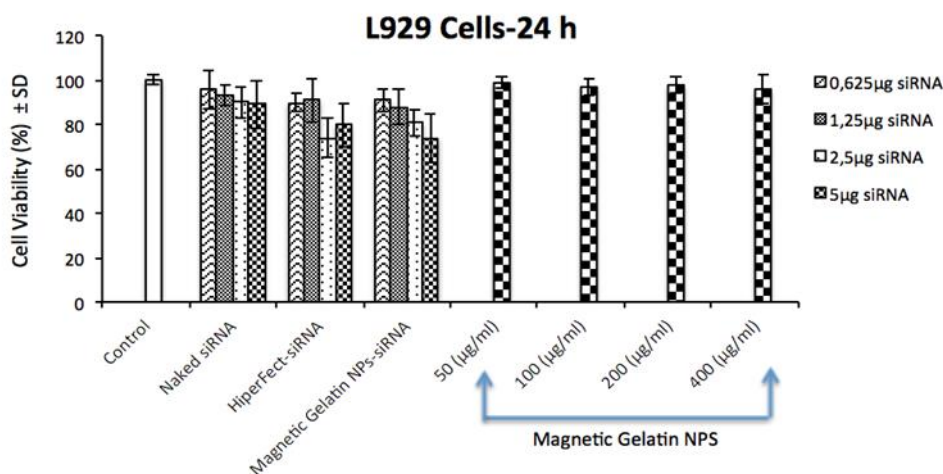


**Figure 4.23.** Results of MTT test for L929 cell lines after 24 h incubation

As seen in Figure 4.23 and Figure 4.24, bare magnetic gelatin nanoparticles with various concentration has almost no toxicity for both cell lines, for 24 h incubation time. When siRNA molecules were interacted with cells via gelatin-IONs, a significant decrease in cell viability for both cell lines were observed. Moreover, siRNA-HiperFect and siRNA-gelatin-ION formulations demonstrated nearly parallel results for the toxicity of cells.



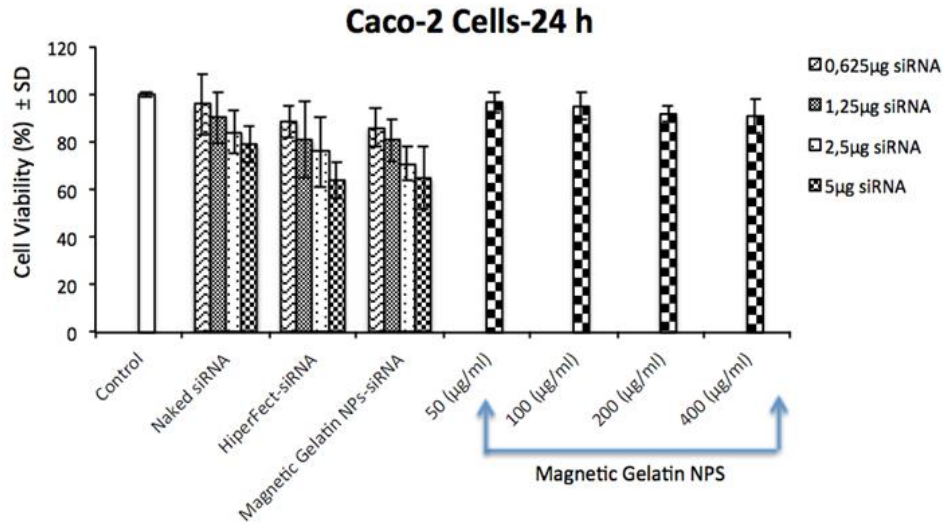


**Figure 4.24.** Results of MTT test for CaCo-2 cell lines after 24 h incubation

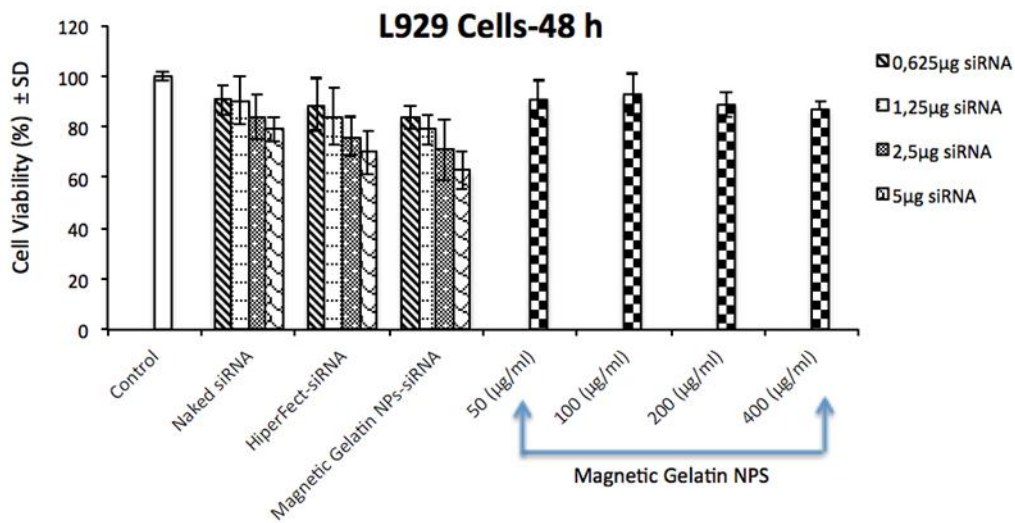


**Figure 4.25.** Results of MTT test for L929 cell lines after 48 h incubation

For 48 h cellular interaction, Figure 4.25 and Figure 4.26 show that the viability of cells decreased in time depended manner compared to 24 h interaction. Similar to the results for 24 h, the toxicity of siRNA loaded gelatin coated iron oxide nanoparticles in both cell lines increased when using increasing amount of siRNA.

The viability values (%) of  $43,76 \pm 5,97$  and  $62,76 \pm 7,31$  were calculated for Caco-2 and L929 cells, respectively, after transfecting the cells with  $5 \mu\text{g}$  siRNA loaded gelatin coated iron oxide formulation.

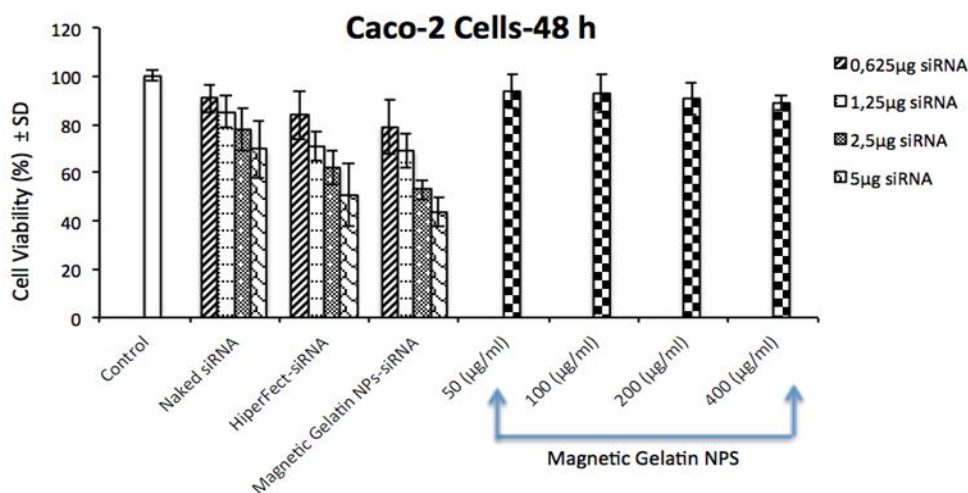


**Figure 4.26.** Results of MTT test for CaCo-2 cell lines after 48 h incubation

When comparing the toxicity of siRNA loaded gelatin coated iron oxide nanoparticles on cancerous and non-cancerous cell types, it can be seen that the nanoparticles with different concentrations of siRNA are more effective against Caco-2 cells (Figure 4.27 and Figure 4.28).

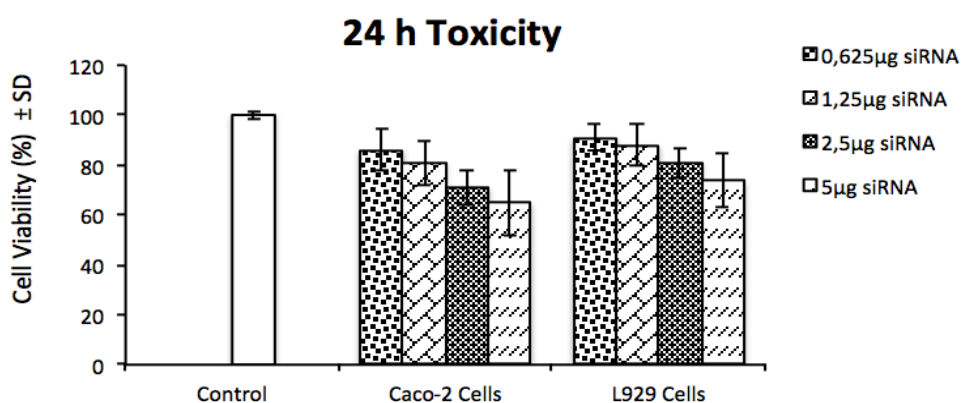


**Figure 4.27.** The interaction of siRNA loaded iron oxide nanoparticles L929 and CaCo-2 cell lines for 24 h

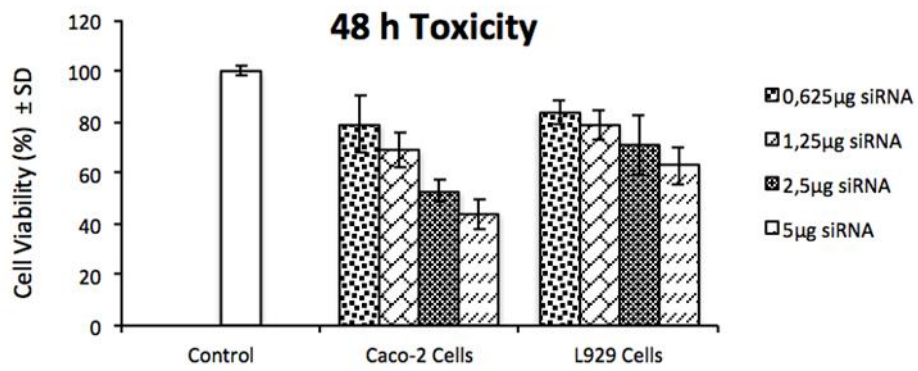


**Figure 4.28.** The interaction of siRNA loaded iron oxide nanoparticles with L929 and CaCo-2 for 48 h

## 5. CONCLUSION

- Firstly, optimization of iron oxide nanoparticles synthesis was performed. It is showed that  $\text{FeCl}_3 \cdot 6\text{H}_2\text{O}$  iron (III) and  $\text{FeCl}_2 \cdot 4\text{H}_2\text{O}$  iron (II) salts must be in molar ratio 1:2. In order to neutralize the anionic charges on the nanoparticles surface hydrochloric acid (HCl) was used. In this method,  $\text{Fe}^{2+}$  and  $\text{Fe}^{3+}$  ions are precipitated in alkaline solutions of 1 M NaOH. In order to avoid uncontrollable oxidation of  $\text{Fe}^{2+}$  into  $\text{Fe}^{3+}$  synthesis reaction is performed in an anaerobic condition using inert  $\text{N}_2$  gas. Obtained size of iron oxide nanoparticles was 48-60 nm.
- Secondly, optimization of gelatin coating of iron oxide nanoparticles was performed. Desolvation/cross-linking technique was used in iron oxide nanoparticles coating with gelatin to stabilize solution and to reduce the size of a obtained complex. Proper ratio adjustment of acetone as a desolvator and glutaraldehyde as a cross-linker results in that obtained ferrofluid solution had better stability. Size of nanoparticles after coating was around 120-180 nm.
- Performing short term stability test (30 days) for iron oxide nanoparticles and gelatin coated iron oxide nanoparticles it is seen that size of iron oxide nanoparticle have increased when compared with size of gelatin coated iron oxide nanoparticles where no significant increase in size have noticed. This is strong indicator that iron oxide nanoparticles without coating are unstable and tend to aggregate. Proper coating with gelatin have ensured long term stability and makes IONs biocompatible.
- Morphological characterization of both, iron oxide nanoparticles and gelatin coated iron oxide nanoparticles was done using SEM. Obtained SEM images showed that predominant particle morphology is containing clusters where each cluster of iron oxide nanoparticles is having size around 60 nm, cluster of gelatin coated iron oxide nanoparticles is having size around 120 nm.
- FTIR is used to determine molecular bond characterization and functional group analysis of the sample for compound comparison.

Characteristical FTIR peaks for iron oxide nanoparticles are positions at 580 and 400  $\text{cm}^{-1}$ . After interaction with iron oxide nanoparticles, FT-IR spectrum peaks of gelatin nanoparticles for amide I at 1670  $\text{cm}^{-1}$  and amide II at 1560  $\text{cm}^{-1}$  were shifted at 1642  $\text{cm}^{-1}$  and 1533  $\text{cm}^{-1}$ , respectively. In obtained FT-IR spectrum of gelatin coated iron oxide nanoparticles peaks seen at 427  $\text{cm}^{-1}$  and 578  $\text{cm}^{-1}$  are assigned to iron oxide nanoparticles. Obtained FT-IR spectrum peaks have proven existence of gelatin polymer on surface of iron oxide nanoparticles.

- VSM and ESR characterization results were revealed super paramagnetic properties of both IONs and gelatin coated IONs.
- Coating iron oxide nanoparticles with gelatin by two desolvation process, loading of siRNA to nano platform have to be confirmed with spectrofluorometer. Maximum intensity of Ribogreen dye interaction with RNA was expressed in 500 nm (excitation) and the maximum emission wavelength was 525 nm (emission) in regard to Ribogreen Kit standard measurements. Loaded siRNAs to nano complex showed proportional binding efficiency in regard to siRNA concentration increase. Binding efficiency of siRNA to gelatin coated IONs was confirmed with spectrofluorometer using Ribogreen kit as control- The highest binding efficiency of 41% was obtained when 5  $\mu\text{g}$  siRNA was used.
- MTT cytotoxicity assay revealed that the bare gelatin-IONs with different amounts are safe and biocompatible for both Caco-2 and L929 cells. Silencing mTOR gene via delivering target siRNA molecules into cells with a carrier (HiperFect or gelatin-IONs) exhibited significant toxic effect especially in the case of higher siRNA amounts in contrast to naked siRNAs. Furthermore, the siRNA-gelatin-IONs systems were found to be more effective on toxicity of Caco-2 cells than L929 cells.
- The results of this work suggest that the synthesised cost-effective and safe gelatin-IONs are promising candidates as siRNA delivery tools for cancer treatment. The results of this work suggest that the synthesized cost-effective and safe gelatin coated IONs are promising theranostic candidate for cancer treatment and diagnosis.

## 6, REFERENCES

- [1] Jiang S., Ahmed A.E., Kevin L., Lipidoid-coated Iron Oxide Nanoparticles for Efficient DNA and siRNA delivery, *National Institute of Health*, 1059–1064, **2013**.
  
- [2] Young S., Stenzel M., Yang J., Nanoparticle-siRNA: A potential cancer therapy?, *Critical, Reviews in Oncology/Hematology*, 98, 159–169, **2016**.
  
- [3] Chen, et al., Superparamagnetic iron oxide nanoparticles mediated <sup>131</sup>I-hVEGF siRNA inhibits hepatocellular carcinoma tumor growth in nude mice, *BMC Cancer*, 14:114, **2014**.
  
- [4] Collins M., Thrasher A., Gene therapy: progress and predictions. *Proc. R. Soc. B*, 282, **2015**.
  
- [5] Agi E., Mosaferi Z., et al., Different strategies of gene delivery for treatment of cancer and other disorders, *Journal of Solid Tumors*, Vol. 6, No. 2., **2016**.
  
- [6] Filipowicz W., Jaskiewicz L., et al, Post-transcriptional gene silencing by siRNAs and miRNAs, *Current Opinion in Structural Biology*, 15:331–341, **2005**.
  
- [7] Agrawal N., Dasaradhi P.V.N., et al., RNA Interference: Biology, Mechanism, and Applications, *Microbiology and Molecular Biology Reviews*, 657–685, Vol. 67, No. 4, **2003**.
  
- [8] Wang J., Lu Z., et al., Delivery of siRNA Therapeutics: Barriers and Carriers, *The AAPS Journal*, Vol. 12, No. 4, Review article, **2010**.

- [9] Gish R.G., Yuen M.F., et al, Synthetic RNAi triggers and their use in chronic hepatitis B therapies with curative intent, Review, *Antiviral Research*, 121, 97–108, **2015**.
- [10] Draz M.S., Fang B.A., et al., Nanoparticle-Mediated Systemic Delivery of siRNA for Treatment of Cancers and Viral Infections, *Theranostics*, Vol. 4, Issue 9, Review, **2014**.
- [11] Vogelstein B., Kinzler W. K., Cancer genes and the pathways they control, *Nature Medicine*, Vol. 10 No. 8, **2004**.
- [12] Strahm B., Capra M., Insights into the molecular basis of cancer development, *Current Paediatrics*, 15, 333–338, **2005**.
- [13] Herceg Z., Hainaut P., Genetic and epigenetic alterations as biomarkers for cancer detection, diagnosis and prognosis, *Molecular oncology*, 1, 26–41, Review, **2007**.
- [14] Ciombor K.K., et al, How Can Next-Generation Sequencing (Genomics) Help Us in Treating Colorectal Cancer?, *Curr Colorectal Cancer Rep.*, 10(4): 372–379, **2014**.
- [15] Kheirelseid E. A. H., et al, Molecular biology of colorectal cancer, *American Journal of Molecular Biology*, 3, 72-80, **2013**.
- [16] Grady M.W., et al, The molecular pathogenesis of colorectal cancer and its potential application to colorectal cancer screening, *Dig Dis Sci.*, 60(3), 762–772, **2015**.

- [17] Umar A., et al, Revised Bethesda Guidelines for Hereditary Nonpolyposis Colorectal Cancer (Lynch Syndrome) and Microsatellite Instability, *J Natl Cancer Inst.*, 18, 96(4), 261–268, **2004**.
- [18] Steinke V., et al., Hereditary nonpolyposis colorectal cancer (HNPCC) / Lynch syndrome, *Dtsch Arztebl Int*, 110(3), 32–8, **2013**.
- [19] Waisberg J., et al., Liver-first approach of colorectal cancer with synchronous hepatic metastases: A reverse strategy, *World Journal of Hepatology*, 18, 7(11), 1444-1449, **2015**.
- [20] Fontanges Q., et al, Clinical Application of Targeted Next Generation Sequencing for Colorectal Cancers, *International Journal of Molecular Sciences, Review*, 17, 2117, **2016**.
- [21] Bregoli L., Movia D., et al, Nanomedicine applied to translational oncology: A future perspective on cancer treatment, *Nanomedicine: Nanotechnology, Biology, and Medicine* 12, 81–103, **2016**.
- [22] Suk S.J., Xu Q., et al., PEGylation as a strategy for improving nanoparticle-based drug and gene delivery, *Advanced Drug Delivery Reviews*, 99, 28–51, **2016**.
- [23] Schrand A.M., Rahman F.M., et al., Metal-based nanoparticles and their toxicity assessment, *WIREs Nanomedicine and Nanobiotechnology*, Volume 2, Advanced Review, **2010**.
- [24] Kievit F.M., Zhang M., Surface Engineering of Iron Oxide Nanoparticles for Targeted Cancer Therapy, *Accounts of chemical research*, Vol. 44, No. 10, 853–862, **2011**.



- [25] Sadhasivam S., Savitha S., et al., Carbon encapsulated iron oxide nanoparticles surface engineered with polyethylene glycol-folic acid to induce selective hyperthermia in folate over expressed cancer cells, *International Journal of Pharmaceutics*, 480, 8–14, **2015**.
- [26] Foox M., Zilberman M., Drug delivery from gelatin-based systems, Review, *Expert Opin. Drug Deliv.*, 12(9), 1547-1563, **2015**.
- [27] Kommareddy S., Shenoy D.B., Gelatin Nanoparticles and Their Biofunctionalization In Biofunctionalization of Nanomaterials edited by Edited by Challa S. S. R. Kumar, *Nanotechnologies for the Life Sciences* Vol. 1, **2005**.
- [28] Duconseille A., et al., Gelatin structure and composition linked to hard capsule dissolution: A review, *Food Hydrocolloids*, 43, 360-376, **2015**.
- [29] Sahoo N., Ranjan K., Biswas N., et al., Recent advancement of gelatin nanoparticles in drug and vaccine delivery, *International Journal of Biological Macromolecules*, 81, 317–331, **2015**.
- [30] Lee S.J., et al., Biocompatible gelatin nanoparticles for tumor-targeted delivery of polymerized siRNA in tumor-bearing mice, *Journal of Controlled Release*, 172, 358–366, **2013**.
- [31] Malley C.O., Pidgeon G.P., The mTOR pathway in obesity driven gastrointestinal cancers: Potential targets and clinical trials, *BBA Clinical* 5 29–40, **2016**.

- [32] Hou G., Yang S., Zhou Y., et al, Targeted Inhibition of mTOR Signaling Improves Sensitivity of Esophageal Squamous Cell Carcinoma Cells to Cisplatin, *Journal of Immunology Research*, 9 pages, Research Article, **2014**.
- [33] Massart R., Preparation of aqueous magnetic liquids in alkaline and acidic media, *IEEE Trans. Magn.* 17, 1247, **1981**.
- [34] Mascolo C.M., Pei Y., Ring T.A., Room temperature co-precipitation synthesis of magnetite nanoparticles in a large pH window with different bases, *Materials*, 6, 5549-5567, **2013**.
- [35] Kazemzadeh H., Ataie A., Rashchi F., Synthesis of magnetite nano-particles by reverse coprecipitation, *International Journal of Modern Physics*, Conference Series Vol. 5, 160–167, **2012**.
- [36] Andrade A.L., Souza D.M., et al., pH effect on the synthesis of magnetite nanoparticles by the chemical reduction precipitation method, *Quim. Nova*, Vol. 33, No. 3, 524-527, **2010**.
- [37] Gaihre B., Khil M.S., et al, Techniques of controlling hydrodynamic size of ferrofluid of gelatin-coated magnetic iron oxide nanoparticles, *J Mater Sci*, 43, 6881–6889, **2008**.
- [38] Eivari H.A., Rahdar A., et al., Preparation of Super Paramagnetic Iron Oxide Nanoparticles and Investigation their Magnetic Properties, *International Journal of Science and Engineering Investigations*, Vol. 1, issue 3, **2012**.

- [39] Parikh N., Parekh N., Technique to optimize magnetic response of gelatin coated magnetic nanoparticles, *J Mater Sci: Mater Med*, 26:202, **2015**.
- [40] Gaihre B., Aryal S., et al., Gelatin stabilized iron oxide nanoparticles as a three dimensional template for the hydroxyapatite crystal nucleation and growth, *Materials Science and Engineering C* 28, 1297–1303, **2008**.
- [41] Babita G., Khil M., et al., Gelatin-coated magnetic iron oxide nanoparticles as carrier system: Drug loading and *in vitro* drug release study, *International Journal of Pharmaceutics*, 365, 180–189, **2009**.
- [42] Richard A. Revia and Miqin Zhang, Magnetite nanoparticles for cancer diagnosis and treatment monitoring: recent advances, *Materials Today*, Volume 19, Research, **2016**.
- [43] Yang S., Zhang S., et al., In situ preparation of magnetic Fe<sub>3</sub>O<sub>4</sub> nanoparticles inside nanoporous poly (l-glutamic acid)/chitosan microcapsules for drug delivery, *Colloids and Surfaces B: Biointerfaces*, 113, 302–311, **2014**.
- [44] Kim E., Jung Y., et al., Prostate cancer cell death produced by the co-delivery of Bcl-xL shRNA and doxorubicin using an aptamer-conjugated polyplex, *Biomaterials*, 31, 4592-4599, **2010**.
- [45] Park K., Lee M.Y., et al., Target specific tumor treatment by VEGF siRNA complexed with reducible polyethyleneimine hyaluronic acid conjugate, *Biomaterials*, 31, 5258-5265, **2010**.
- [46] Hasan W., Chu K., et al., Delivery of Multiple siRNAs Using Lipid-Coated PLGA Nanoparticles for Treatment of Prostate Cancer, *Nano Lett.*, 287–292, **2012**.

- [47] Lee S.H., Huh M.S., et al., Tumor-Homing Poly-siRNA/Glycol Chitosan Self-Cross-Linked Nanoparticles for Systemic siRNA Delivery in Cancer Treatment, *Angew. Chem. Int. Ed.*, 51, 7203–7207, **2012**.
- [48] Long L., Wang W., et al., PinX1-siRNA/mPEG-PEI-SPION combined with doxorubicin enhances the inhibition of glioma growth, *Experimental and therapeutic medicine*, 7, 1170-1176, **2014**.
- [49] Bae H.K., Lee K., et al., Surface functionalized hollow manganese oxide nanoparticles for cancer targeted siRNA delivery and magnetic resonance imaging, *Biomaterials*, 32, 176-184, **2011**.
- [50] Chen M. A., Zhang M., et al., Co-delivery of Doxorubicin and Bcl-2 siRNA by Mesoporous Silica Nanoparticles Enhances the Efficacy of Chemotherapy in Multidrug-Resistant Cancer Cells, *Small*, 5, No. 23, 2673–2677, **2009**.
- [51] Xiao Y., Jaskula-Sztul R., et al., Co-delivery of doxorubicin and siRNA using octreotide-conjugated gold nanorods for targeted neuroendocrine cancer therapy, *Nanoscale*, 4, 7185–7193, **2012**.
- [52] Kievit F.M., Veiseh O., et al., PEI-PEG-Chitosan-Copolymer-Coated Iron Oxide Nanoparticles for Safe Gene Delivery: Synthesis, Complexation, and Transfection, *Adv. Funct. Mater.*, 19, 2244–2251, **2009**.
- [53] Kievit F.M., Wang Y.F., et al., Doxorubicin loaded iron oxide nanoparticles overcome multidrug resistance in cancer in vitro, *Journal of Controlled Release*, 152, 76–83, **2011**.

- [54] Wang J., Lu Z., et al., Delivery of siRNA Therapeutics: Barriers and Carriers, *The AAPS Journal*, Vol. 12, No. 4, Review Article, **2010**.
- [55] Li S.D., Chen Y.C., et al., Tumor-targeted Delivery of siRNA by Self-assembled Nanoparticles, *Molecular Therapy*, Vol. 16 No. 1, 163–169, **2008**.
- [56] Xu C.F., Wang J., Delivery systems for siRNA drug development in cancer therapy, *Asian Journal of pharmaceutical sciences*, 10, 1-12, **2015**.
- [57] Uludağ H., Landry B., et al., Current attempts to implement siRNA-based RNAi in leukemia models, *Drug Discovery Today*, Volume 00, Number 00, Reviews, **2016**.
- [58] Jiang J., Yang S.J., et al., Sequential treatment of drug-resistant tumors with RGD-modified liposomes containing siRNA or doxorubicin, *European Journal of Pharmaceutics and Biopharmaceutics*, 76, 170–178, Research paper, **2010**.
- [59] Jere D., Jiang H.L., et al., Chitosan-graft-polyethylenimine for Akt1 siRNA delivery to lung cancer cells, *International Journal of Pharmaceutics*, 378, 194–200, **2009**.
- [60] Pitella F., Miyata K., et al., Pancreatic cancer therapy by systemic administration of VEGF siRNA contained in calcium phosphate/charge-conversional polymer hybrid nanoparticles, *Journal of Controlled Release*, 161, 868–874, **2012**.
- [61] Li J., Yang Y., Calcium phosphate nanoparticles with an asymmetric lipid bilayer coating for siRNA delivery to the tumor, *Journal of Controlled Release*, 158, 108–114, **2012**.

- [62] Augustin E., Czubek B., et al., Improved cytotoxicity and preserved level of cell death induced in colon cancer cells by doxorubicin after its conjugation with iron-oxide magnetic nanoparticles, *Toxicology in Vitro*, 33, 45–53, **2016**.
- [63] Rosenberger I., Strauss A., et al., Targeted diagnostic magnetic nanoparticles for medical imaging of pancreatic cancer, *Journal of Controlled Release*, 214, 76–84, **2015**.
- [64] Lee S.Y., Yang C.Y., A theranostic micelleplex co-delivering SN-38 and VEGF siRNA for colorectal cancer therapy, *Biomaterials*, 86, 92-105, **2016**.
- [65] Wei W., Lv P.P., Codelivery of mTERT siRNA and paclitaxel by chitosan-based nanoparticles promoted synergistic tumor suppression, *Biomaterials*, 34, 3912-3923, **2013**.
- [66] Li X., Chen Y., A mesoporous silica nanoparticle e PEI e Fusogenic peptide system for siRNA delivery in cancer therapy, *Biomaterials*, 34, 1391-1401, **2013**.
- [67] Veisheh O., Kievit K.M., et al., Cell transcytosing poly-arginine coated magnetic nanovector for safe and effective siRNA delivery, *Biomaterials*, 32, 5717-5725, **2011**.
- [68] Gao J., Liu W., et al., The promotion of siRNA delivery to breast cancer overexpressing epidermal growth factor receptor through anti-EGFR antibody conjugation by immunoliposomes, *Biomaterials*, 32, 3459-3470, **2011**.
- [69] Yen S.K., Padmanabhan P., et al., Multifunctional Iron Oxide Nanoparticles for Diagnostics, Therapy and Macromolecule Delivery, *Theranostics*, Vol. 3, Issue 12, Review, **2013**.

- [70] Lee S.J., Yhee Y.Y., Biocompatible gelatin nanoparticles for tumor-targeted delivery of polymerized siRNA in tumor-bearing mice, *Journal of Controlled Release* 172, 358–366, **2013**.
- [71] Chen S., Yang K., et al., Targeting tumor microenvironment with PEG-based amphiphilic nanoparticles to overcome chemoresistance, *Nanomedicine: Nanotechnology, Biology, and Medicine*, 12, 269–286, Review Article, **2016**.
- [72] Mok H., Veisheh O., et al., pH-Sensitive siRNA Nanovector for Targeted Gene Silencing and Cytotoxic Effect in Cancer Cells, *Molecular Pharmaceutics* Vol. 7, No. 6, 1930–1939, **2010**.
- [73] Mao C.K., Du J.Z., et al., A biodegradable amphiphilic and cationic triblock copolymer for the delivery of siRNA targeting the acid ceramidase gene for cancer therapy, *Biomaterials*, 32, 3124-3133, **2011**.
- [74] Deng X., Cao M., et al., Hyaluronic acid-chitosan nanoparticles for co-delivery of MiR-34a and doxorubicin in therapy against triple negative breast cancer, *Biomaterials*, 35, 4333-4344, **2014**.
- [75] Malmo J., Sjørgård H., et al., siRNA delivery with chitosan nanoparticles: Molecular properties favoring efficient gene silencing, *Journal of Controlled Release* 158, 261–268, **2012**.
- [76] Wang Z., et al., Survivin-targeted nanoparticles for pancreatic tumor imaging in mouse model, *Nanomedicine: Nanotechnology, Biology, and Medicine*, 12, 1651–1661, **2016**.
- [77] Li J., Chen Y.C., Biodegradable calcium phosphate nanoparticle with lipid coating for systemic siRNA delivery, *Journal of Controlled Release*, 142, 416–421, **2010**.

- [78] Mahajan U. M., Teller S., et al., Tumour-specific delivery of siRNA-coupled superparamagnetic iron oxide nanoparticles, targeted against PLK1, stops progression of pancreatic cancer, *Gut*, 0:1–12, **2016**.
- [79] Nawroth I., Alsner J., et al., Intraperitoneal administration of chitosan/DsiRNA nanoparticles targeting TNF $\alpha$  prevents radiation-induced fibrosis, *Radiotherapy and Oncology*, 97, 143–148, **2010**.
- [80] Xu J., Sun J., et al., Application of Iron Magnetic Nanoparticles in Protein Immobilization, *Molecules*, 19, Review, **2014**.
- [81] Scwertmann U., Cornell R.M., Iron Oxide in the Laboratory Preparation and Characterization, Second, Completely Revised and Extended Edition, Wiley-VCH, A book, **2000**.
- [82] Zanganeh S., Hutter G., Spitler R., et al., Iron oxide nanoparticles inhibit tumour growth by inducing pro-inflammatory macrophage polarization in tumour tissues, *Nature Nanotechnology*, Articles, **2016**.
- [83] Laurent S., Forge D., et al., Magnetic Iron Oxide Nanoparticles: Synthesis, Stabilization, Vectorization, Physicochemical Characterizations, and Biological Applications, *Chem. Rev.*, 108, 2064–2110, **2008**.
- [84] Chin A.B., Yaacob I. I., et al., Synthesis and characterization of magnetic iron oxide nanoparticles via w/o microemulsion and Massart's procedure, *Journal of Materials Processing Technology*, 191, 235–237, **2007**.
- [85] Mahmoudi M., Sant S., Wang B., et al., Superparamagnetic iron oxide nanoparticles (SPIONs): Development, surface modification and applications in chemotherapy, *Advanced Drug Delivery*, Reviews 63, 24–46, **2011**.



- [86] Silva V.A.J., Andrade P.L., et al., Synthesis and characterization of Fe<sub>3</sub>O<sub>4</sub> nanoparticles coated with fucan polysaccharides, *Journal of Magnetism and Magnetic Materials*, 343, 138–143, **2013**.
- [87] Morel M., Martinez F., et al., Synthesis and characterization of magnetite nanoparticles from mineral magnetite, *Journal of Magnetism and Magnetic Materials*, 343, 76–81, **2013**.
- [88] Leng Y., Sato K., Li J.H. et al., Iron nanoparticles dispersible in both ethanol and water for direct silica coating, *Powder Technology*, 196, 80–84, **2009**.
- [89] Wilson C.R., Doudna A.J., Molecular Mechanisms of RNA Interference, *Annu. Rev. Biophys.*, 42:217-239, **2013**.
- [90] Johnson B., Cooke L., Mahadevan D., Next generation sequencing identifies ‘interactome’ signatures in relapsed and refractory metastatic colorectal cancer, *Journal of Gastrointestinal Oncology*, Original Article, 8(1), 20-31, **2017**.
- [91] Lee S.D., et al, Dose-Dependent Targeted Suppression of P-glycoprotein Expression and Function in Caco-2 Cells, *Mol. Pharmaceutics* 10, 2323-2330, **2013**.
- [92] Raja, M. A. G., Katas, H., Wen, T. J., “Stability, Intracellular Delivery, and Release of siRNA from Chitosan Nanoparticles Using Different Cross-Linkers”, *Plos One*, 1-19, **2015**.

## **CURRICULUM VITAE**

### **Credentials**

Name, Surname : Amina Selimovic

Place of birth : 29.09.1991.

Marital Status : Single

E-mail : aminaselimovic@hotmail.com

Adress : Vakuf 20a, 72270 Travnik, Bosnia and Herzegovina

### **Education**

**BSc** : International Univesity of Sarajevo-Biological Sciences and Bioengineering (2010-2014)

**Foreign Languages** : English

Turkish

**Work experience** :

**Ares of Experiences** : Cancer therapy, siRNA mechanism

**Projects and Budgets:**

**Publications :**

**Oral and Poster Presentations :**



HACETTEPE UNIVERSITY  
GRADUATE SCHOOL OF SCIENCE AND ENGINEERING  
THESIS/DISSERTATION ORIGINALITY REPORT

HACETTEPE UNIVERSITY  
GRADUATE SCHOOL OF SCIENCE AND ENGINEERING  
TO THE DEPARTMENT OF BIOENGINEERING

Date: 12/07/2017

Thesis Title / Topic: **PRODUCTION AND CHARACTERIZATION OF siRNA LOADED MAGNETIC NANOPARTICLES TO BE USED IN CANCER TREATMENT**

According to the originality report obtained by myself/my thesis advisor by using the *Turnitin* plagiarism detection software and by applying the filtering options stated below on 11/07/2017 for the total of 59 pages including the a) Title Page, b) Introduction, c) Main Chapters, d) Conclusion sections of my thesis entitled as above, the similarity index of my thesis is 9 %.

Filtering options applied:

1. Bibliography/Works Cited excluded
2. Quotes excluded / included
3. Match size up to 5 words excluded

I declare that I have carefully read Hacettepe University Graduate School of Science and Engineering Guidelines for Obtaining and Using Thesis Originality Reports; that according to the maximum similarity index values specified in the Guidelines, my thesis does not include any form of plagiarism; that in any future detection of possible infringement of the regulations I accept all legal responsibility; and that all the information I have provided is correct to the best of my knowledge.

I respectfully submit this for approval.

*Amina Selimovic*  
12/07/2017

Name Surname: AMINA SELIMOVIC

Student No: N14125676

Department: BIOENGINEERING

Program: BIOENGINEERING

Status:  Masters  Ph.D.  Integrated Ph.D.

**ADVISOR APPROVAL**

APPROVED

*E. Baki Denkbaş*  
PROF. DR. EMIR BAKI DENKBAŞ

(Title, Name Surname, Signature)